

# Phenomenological investigation of the interplay among Quantum and Gravity at LNGS, an overview

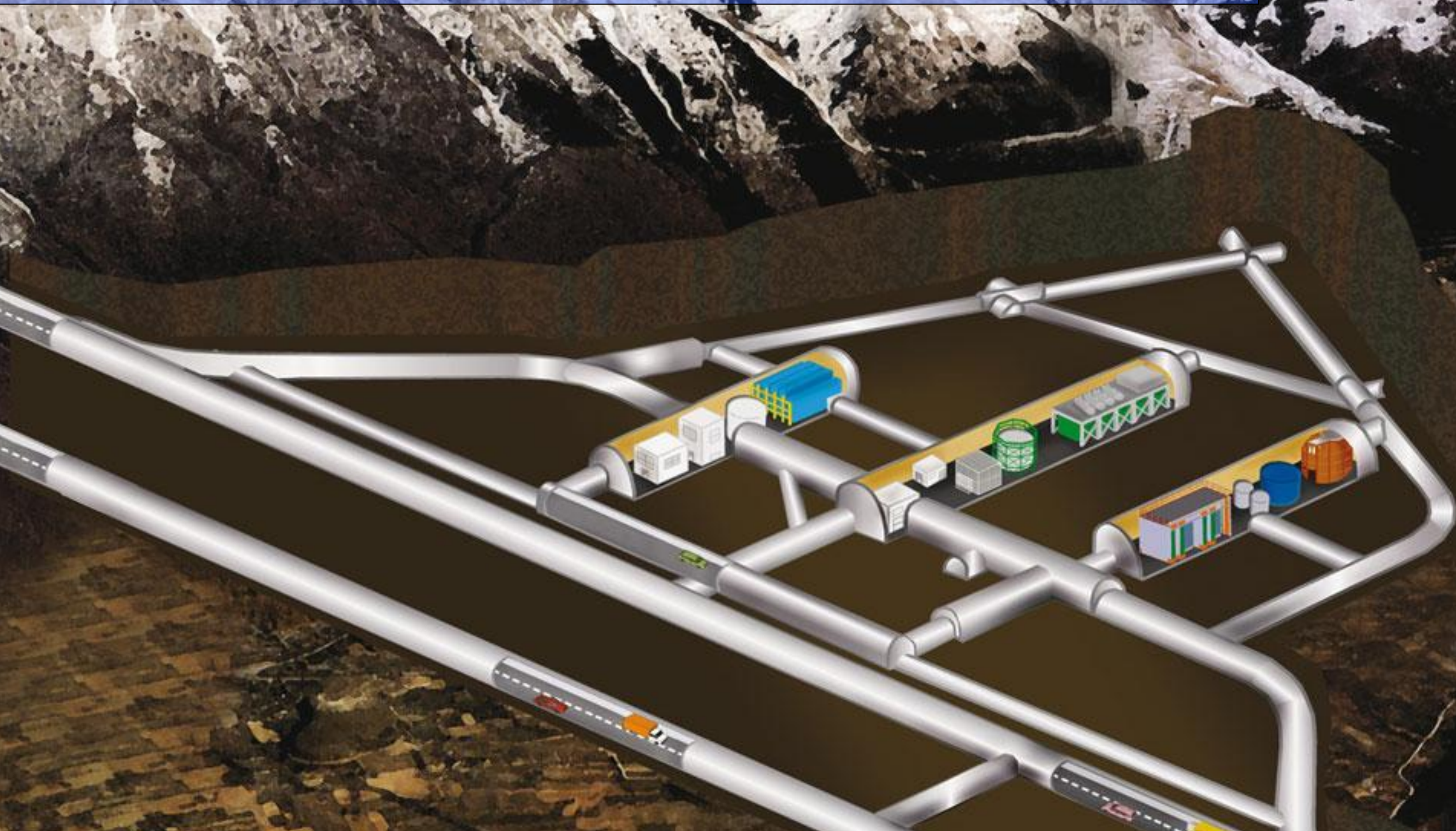
**K. Piscicchia**

Centro Ricerche Enrico Fermi, LNF (INFN)

on behalf of the VIP collaboration

A Modern Odyssey: Quantum Gravity meets Quantum Collapse at Atomic and  
Nuclear physics energy scales in the Cosmic Silence  
ECT\* Trento, 3 – 7 June 2024

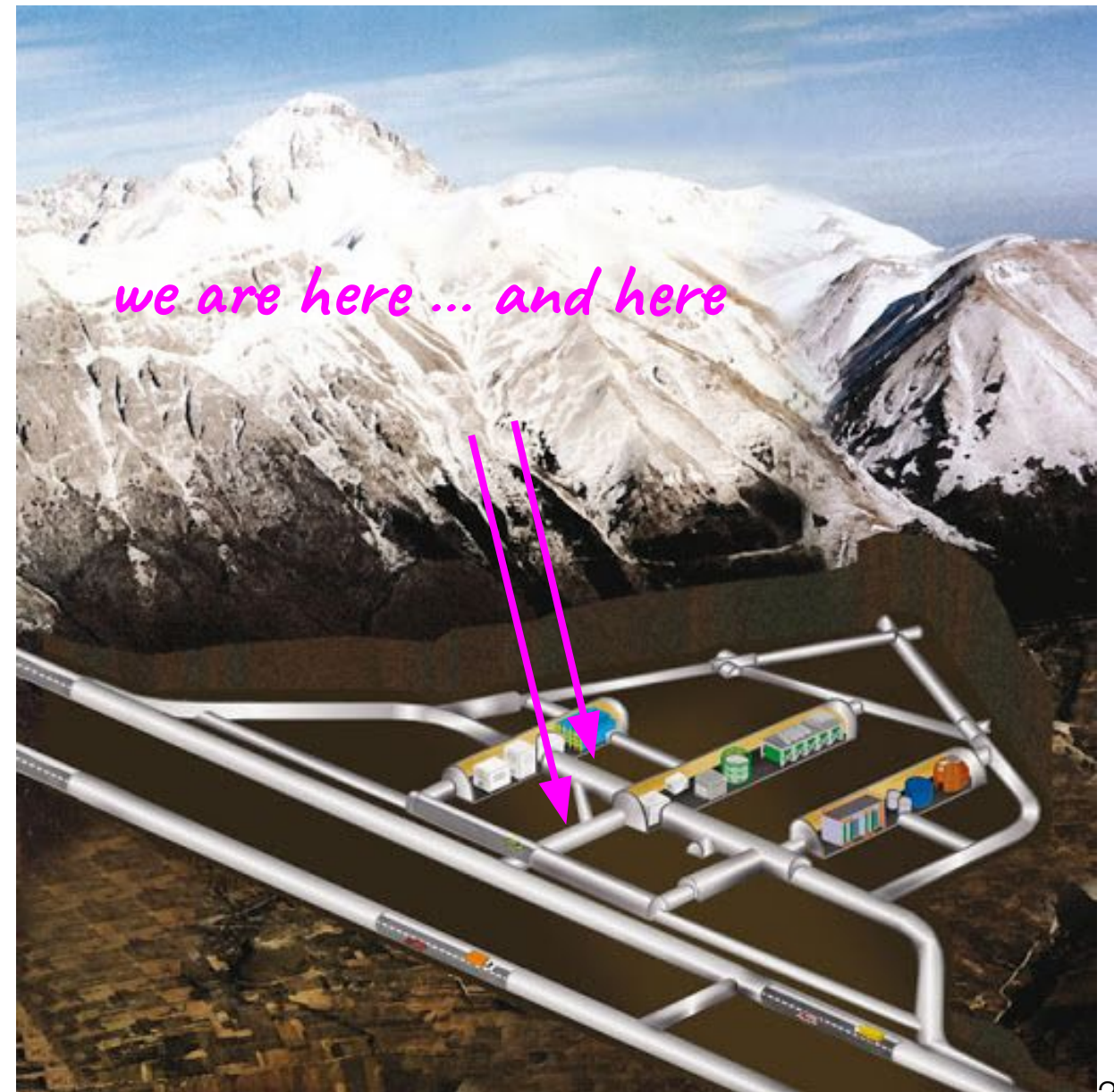
VIP is performing Quantum Mechanics tests:  
- Pauli Exclusion Principle Violation  
- Collapse Models  
by applying atomic physics techniques

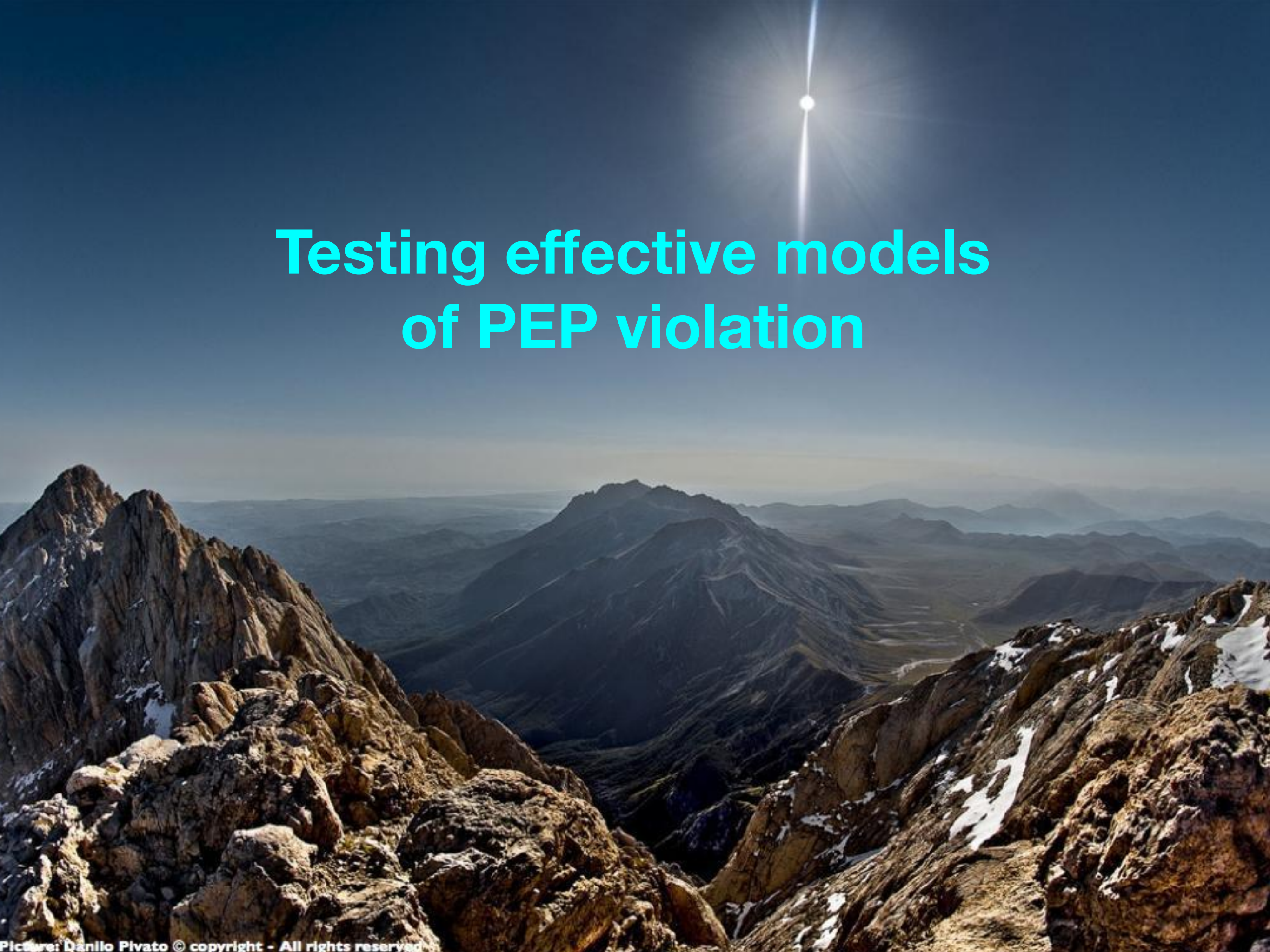


# Where? At The LNGS

The experiments are performed in the low-background environment of the underground *Gran Sasso National Laboratory of INFN*:

- overburden corresponding to a minimum thickness of 3100 m w.e.
- the muon flux is reduced by almost six orders of magnitude, to a flux of three oom.
- the main background source consists of  $\gamma$ -radiation produced by long-lived  $\gamma$ -emitting primordial isotopes and their decay products.





# Testing effective models of PEP violation

## Spin statistics theorem (Fierz 1939, Pauli 1940, Schwinger, Lüders, Zumino...)

Postulates: inhomogeneous Lorentz group, locality, microcausality, vacuum is the state of lowest energy, Hilbert space metric positive definite, vacuum is not identically annihilated by a field  $\rightarrow$

(pseudo)scalar fields commute and spinor fields anticommute

### Models of PEP violation:

- Pioneering work of Fermi, Gentile, Green ...
- Ignatiev and Kuzmin [A.Y. Ignatiev, V.A. Kuzmin, Proceedings of the Seminar, Tbilisi, USSR, 15-17 April 1986] (deformation of the standard Fermi oscillator)

$$\begin{array}{ll} a^+|0\rangle = |1\rangle & a|0\rangle = 0 \\ a^+|1\rangle = \beta|2\rangle & a|1\rangle = |0\rangle \\ a^+|2\rangle = 0 & a|2\rangle = \beta|1\rangle \end{array}$$

- **Rahal and Campa** [V. Rahal, A. Campa, Thermodynamical implications of a violation of the Pauli principle. Phys. Rev. A 38(7), 3728–3731 (1988)] **global w.f. of the electrons is not exactly antisymmetric, PEP holds as long as the number of wrongly entangled pairs is small.**

O. W. Greenberg (AIP Conf. Proc. 545): 113-127, 2004 “Possible external motivations for violation of statistics include: (a) violation of CPT, (b) violation of locality, (c) violation of Lorentz invariance, (d) extra space dimensions, (e) discrete space end or time and (f) non commutative spacetime”



**Two classes of PEP violation models:**

Static deformation of comm/anticomm relations ([Particle properties](#)) - **Greenberg & Mohapatra, quon model** [O.W. Greenberg, R.N. Mohapatra, Phys. Rev. Lett. 59(22), 2507–2510 (1987)]

$$a_k a_l^\dagger - q a_l^\dagger a_k = \delta_{k,l}$$

is subject to the **M-G Superselection Rule** -> can be only tested with **open systems**.

Space-time properties - Antonino Marcianò, Addazzi, Balachandran, Illuminati, Mavromatos, Bosso, Petruzzello ... **unrestricted by M-G Superselection Rule** -> can be tested with **closed systems**.

# From theory to Open Systems experiments

In standard QFT it is difficult to violate the statistics of identical particles;

SUPERSELECTION RULE : Messiah, Greenberg, Amado and Primakoff:

The  $\mathcal{H}$  must be totally symmetric in the dynamical variables of the identical particles;  $\mathcal{H}$  cannot change the permutation symmetry type of the wave function.

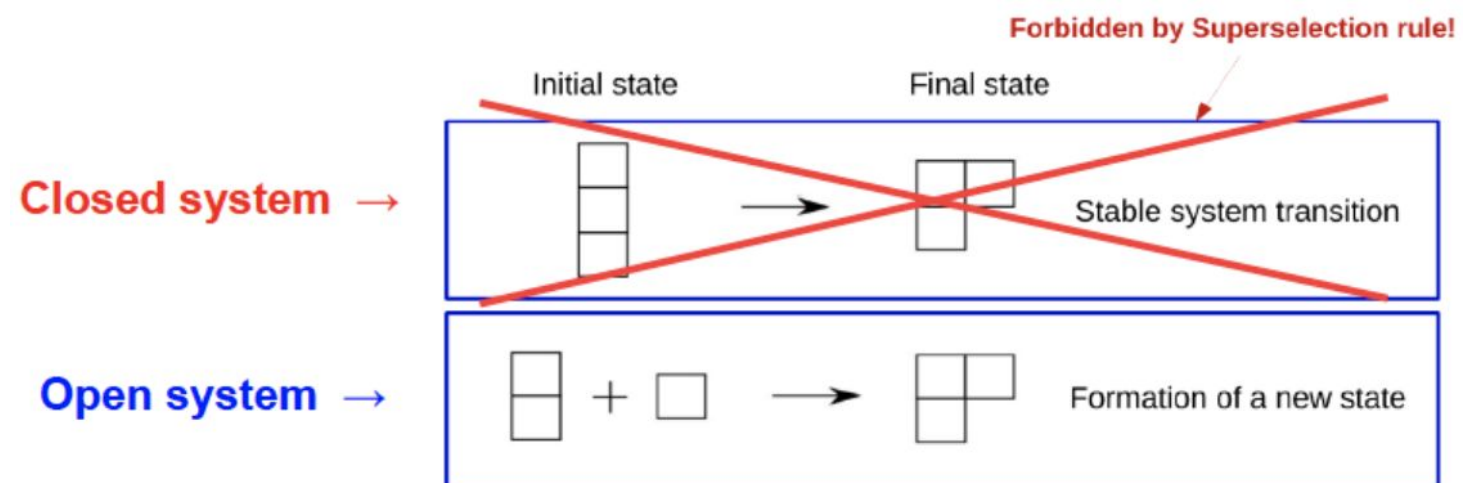
If the w.f. has a small mixed symmetry component the symmetric world Hamiltonian would only connect mixed symmetry states to mixed symmetry states.

Local QFT - Greenberg & Mohapatra (Quon Model), Ignatiev, Kuzmin, Rahal, Campa ... are subjected to M-G superselection rule: transition probability between two symmetry states is zero



introduce new fermions (current) in a pre-existing identical fermion system and check for PEP-violating atomic

transitions **VIP Open Systems & GATOR**



# From theory to Open Systems experiments

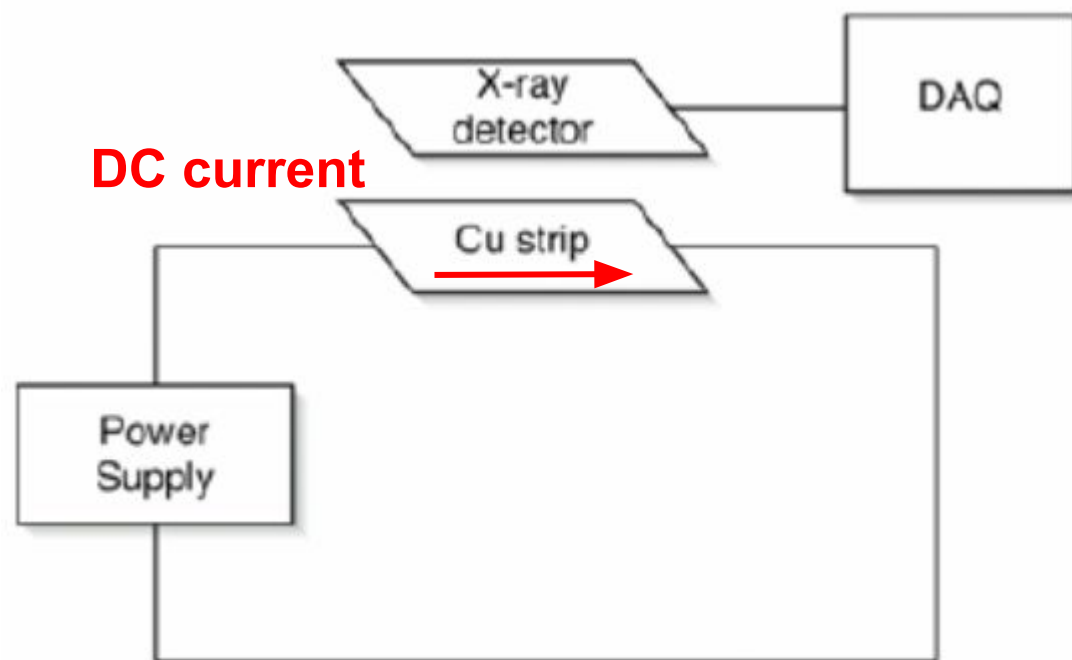
The PEP violation probability  $\beta^2$  is related to the  $q$  parameter by

$$\beta^2 = 1 + q$$

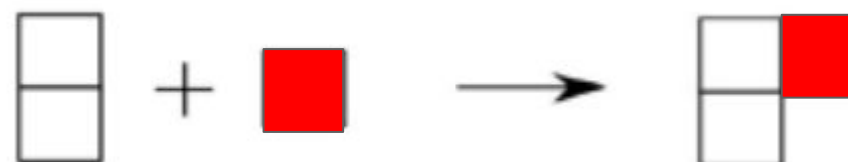
such probability is the anomalous component of the two-identical fermions density matrix

$$\rho_2 = (1 - \beta^2)\rho_a + \beta^2\rho_s$$

a high sensitivity test of  $\beta^2$  consists in (Ramberg E. and Snow G. A. 1990 Phys. Lett. B 238 438)



If the symmetry state formed by a *new current* electron with the electrons of the target is such that the K shell of an atom accommodates two equal spin electrons:

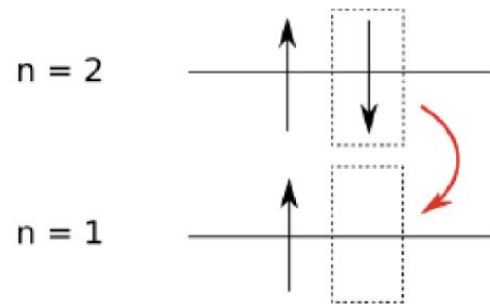


Then the X-ray detector will measure (with a certain efficiency) .....

# From theory to Open Systems experiments

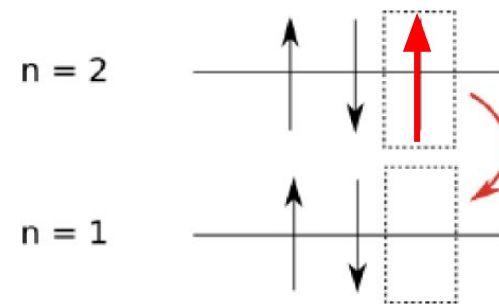
Then the X-ray detector will measure (with a certain efficiency) **a photon emitted by the new electron** when performing the PEP-violating atomic transition

Allowed transition  
 $2p \rightarrow 1s$  ( $K\alpha$ )



$\sim 8.05$  keV in Cu

Pauli-forbidden transition  
 $2p \rightarrow 1s$  ( $K\alpha$ )



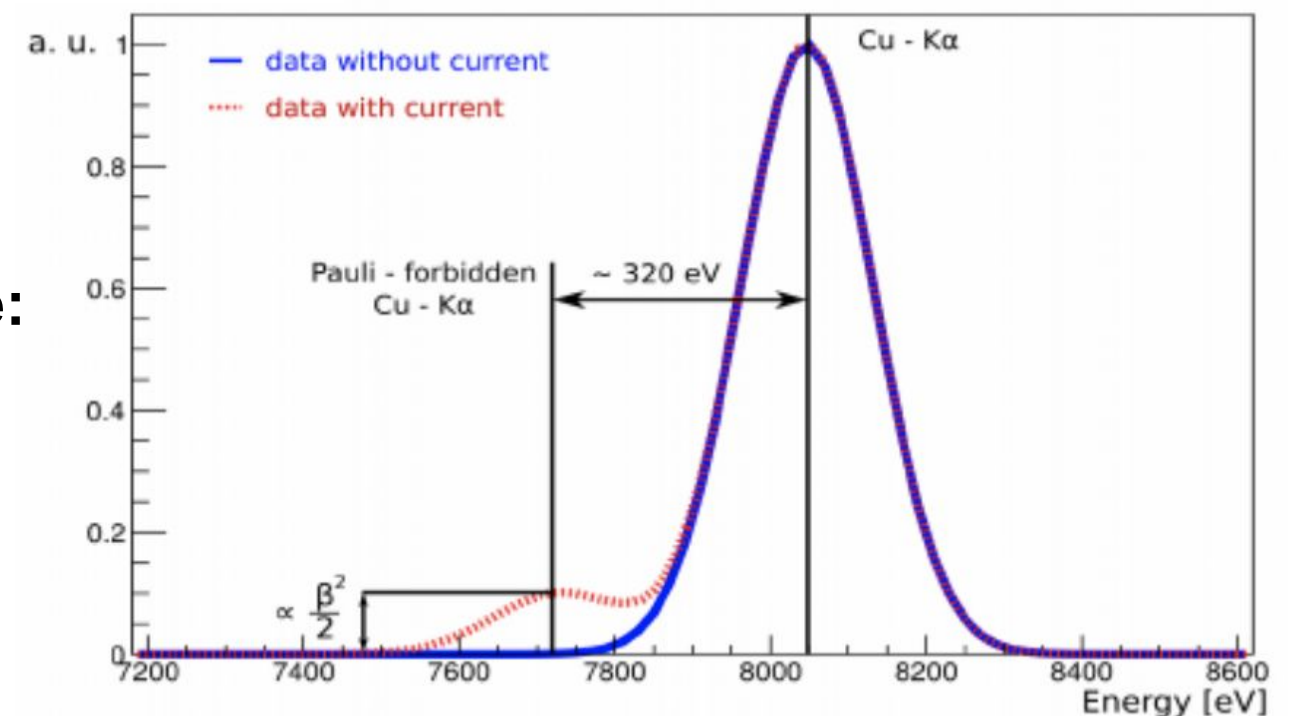
$\sim 7.7$  keV in Cu

Paul Indelicato (Ecole Normale Supérieure et Université Pierre et Marie Curie)

Multiconfiguration Dirac-Fock approach

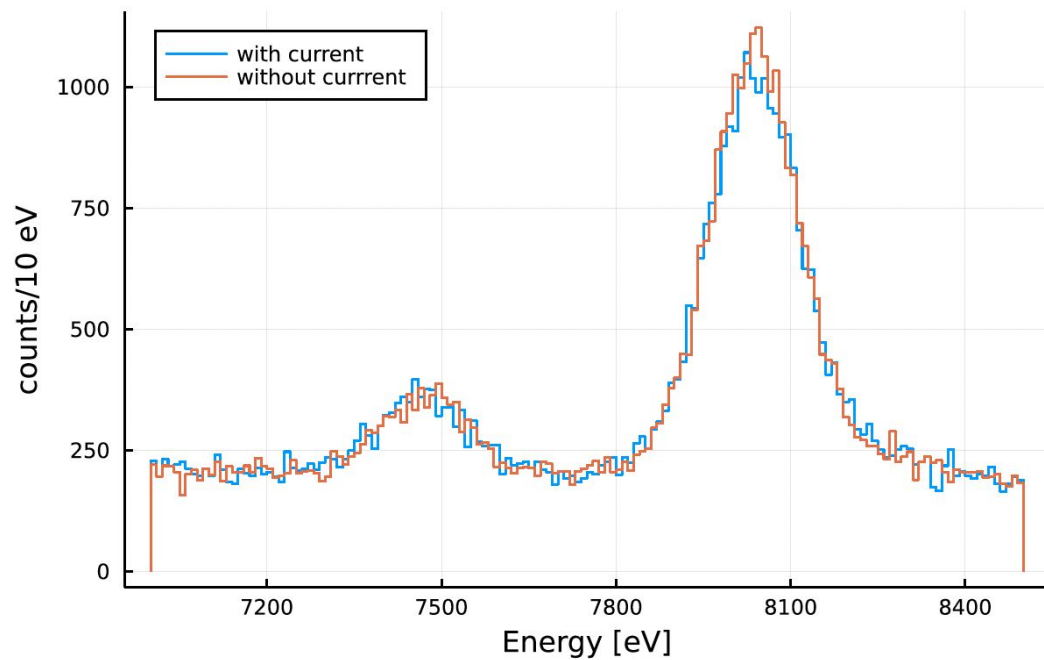
Accounts for the shielding of the two inner electrons

In presence of **signal** you expect to measure:

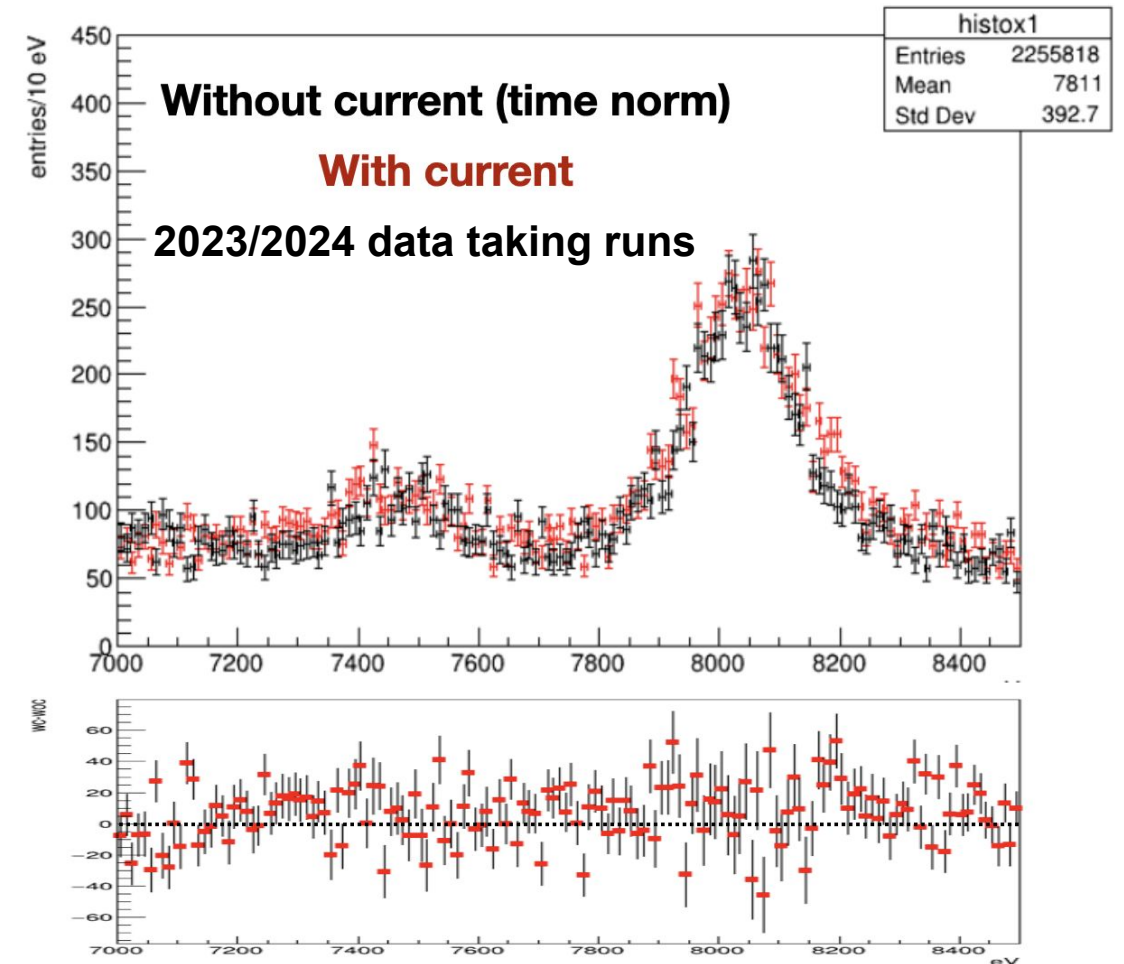


# VIP-2 Open Systems (see F. Sgaramella's talk)

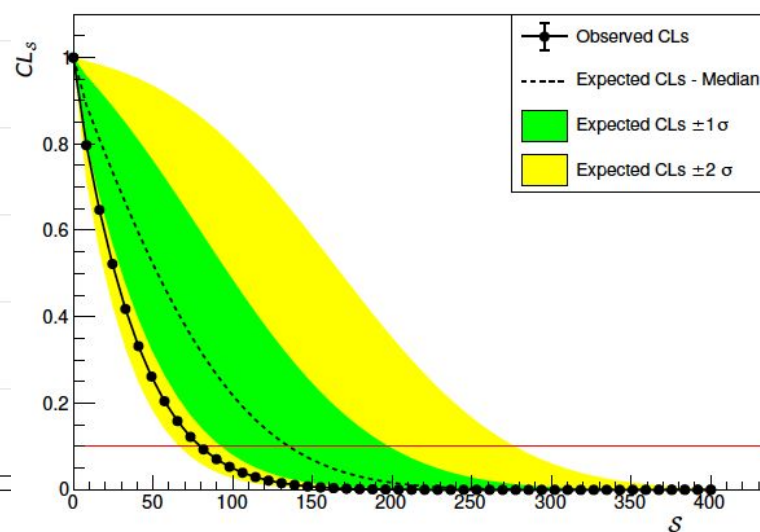
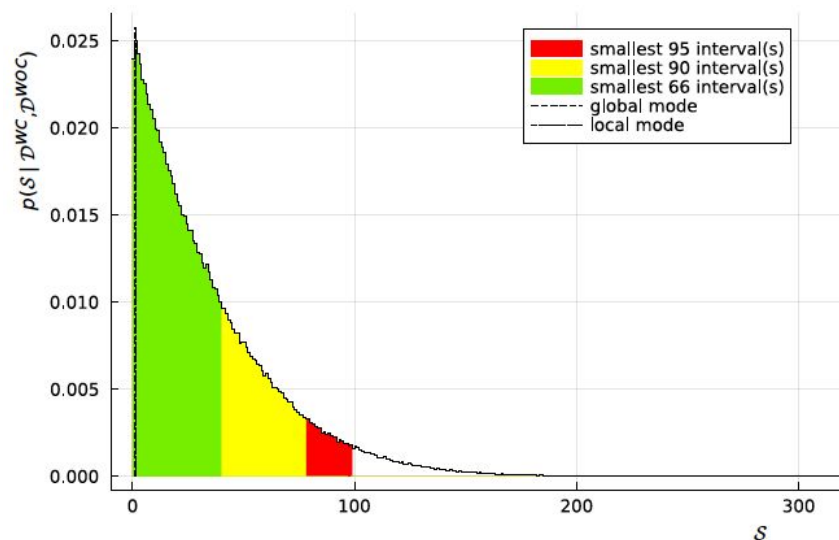
Total acquired statistics data analysis under publication (see also *Symmetry* 2023, 15(2), 480)



VIP-2 calibrated data in the region-of-interest 7000-8500 eV, of about two years of data taking (May 2019 to May 2021). The spectrum of the data acquired with a current circulating in the target is shown in blue. Data taken without current in the target, used as reference and control, shown in red. The copper and nickel  $K_{\alpha}$  lines are visible in the spectra.



**Bayesian analysis validated by means of frequentist CLs exclusion method, exploiting Neyman construction for a robust evaluation of the CLs. Further improvement of the limits on PEPV probability:**



$$\beta^2/2 < 3.1 \cdot 10^{-31} \quad \text{SCATTERING}$$

$$\beta^2/2 < 2.4 \cdot 10^{-43} \quad \text{RANDOM WALK}$$

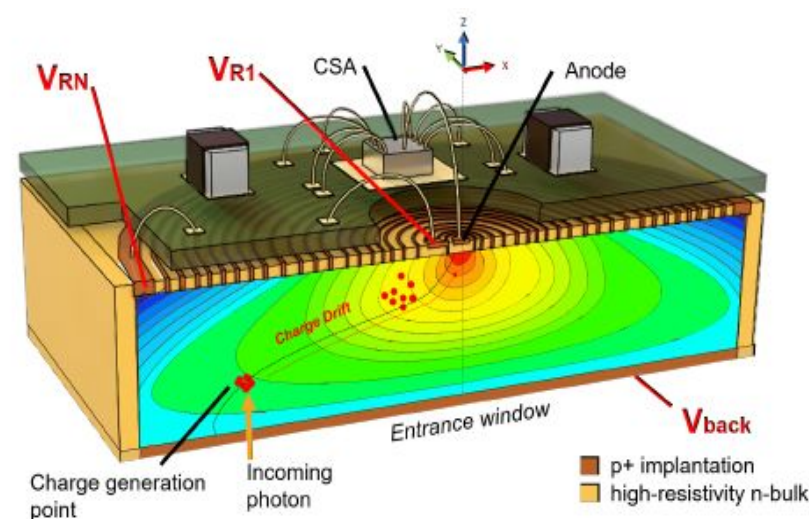
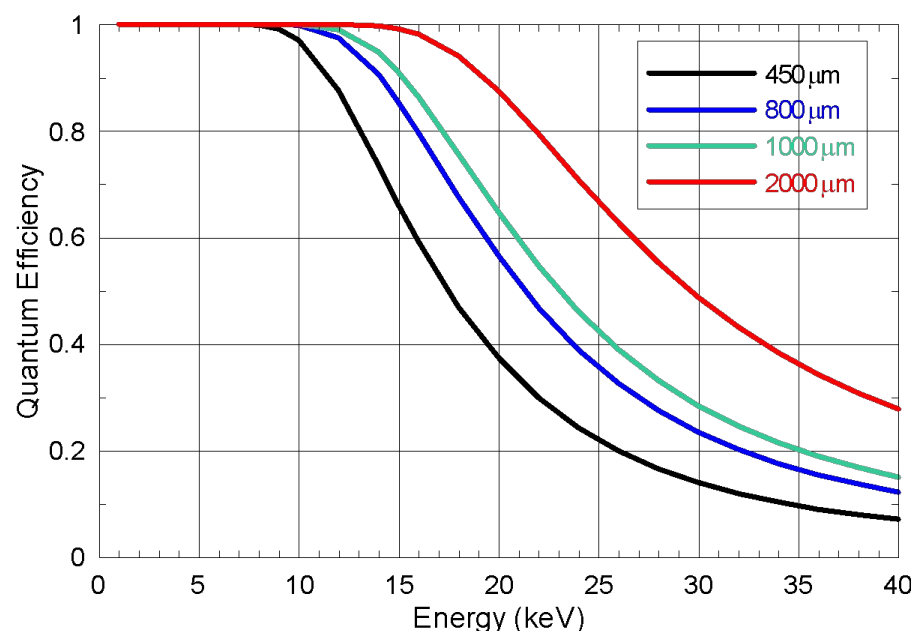
# VIP-3 : scanning $\beta^2$ over the periodic table

Okun, L.:

“it is specifically the fundamental nature of the Pauli principle which would make such tests, over the entire periodic table, of special interest”

L. Possible violation of the Pauli principle in atoms. JETP Lett. 1987, 46, 529532

see also *Universe* 2023, 9(7), 321



Improved quantum efficiency + double active area  $\sim 41 \text{ cm}^2$   $\rightarrow$  increased geometrical efficiency =

scan of  $\beta^2$  with comparable sensitivity to VIP-2 for zirconium, silver, tin ( $Z \in 40-50$ )

installation early 2025

# R&D of a possible VIP-3.5

**VIP-3.5** - further improvement in the quantum efficiency -> layered structures of 1mm thick SDDs to perform a scan of  $\beta^2/2$  with comparable sensitivity to VIP-2/3 till  $Z \sim 60$ :

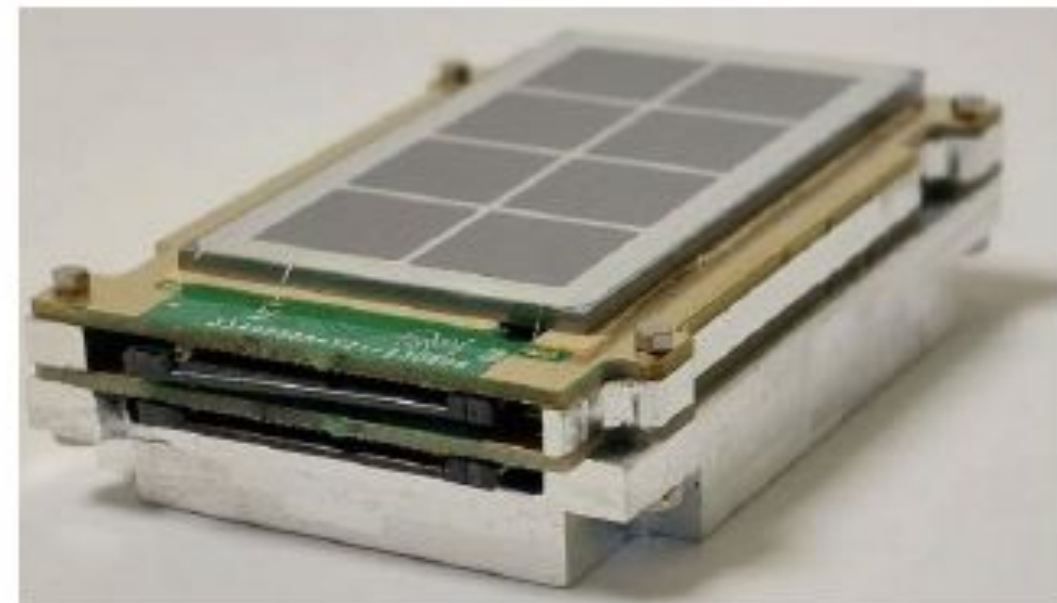
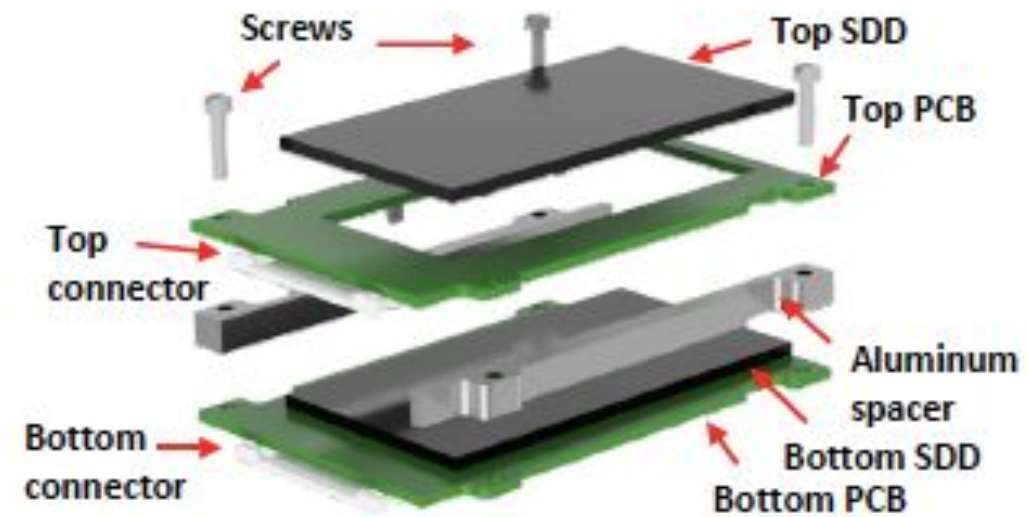
R&D ongoing

Stacked-detector assembly:

- two identical PCB carriers, at a distance of 2mm;
- Aluminum spacers on the sides for mechanical support and thermal conduction;
- Four screws to hold the system together and provide additional thermal conductivity.

A first stacked detection module has been assembled and tested:

- readout performed with the SFERA ASIC, a 16-channel analog pulse processor designed for both X and  $\gamma$ -ray detectors;



# search for PEP violation with GATOR

(see A. Bismarck's talk)

## THE GOAL:

measurement of  $\beta^2/2$  in Pb ( $Z = 82$ ) respecting MG superselection ([Found.Phys. 42 \(2012\)](#)), at energies not accessible with SDD detectors

Transitions in Pb	allow. (keV)	forb. (keV)
1s - 2p <sub>3/2</sub> K <sub><math>\alpha</math>1</sub>	74.961	73.713
1s - 2p <sub>1/2</sub> K <sub><math>\alpha</math>2</sub>	72.798	71.652
1s - 3p <sub>3/2</sub> K <sub><math>\beta</math>1</sub>	84.939	83.856
1s - 4p <sub>1/2(3/2)</sub> K <sub><math>\beta</math>2</sub>	87.320	86.418
1s - 3p <sub>1/2</sub> K <sub><math>\beta</math>3</sub>	84.450	83.385

using the GATOR facility: high-performance low-background germanium spectrometer.

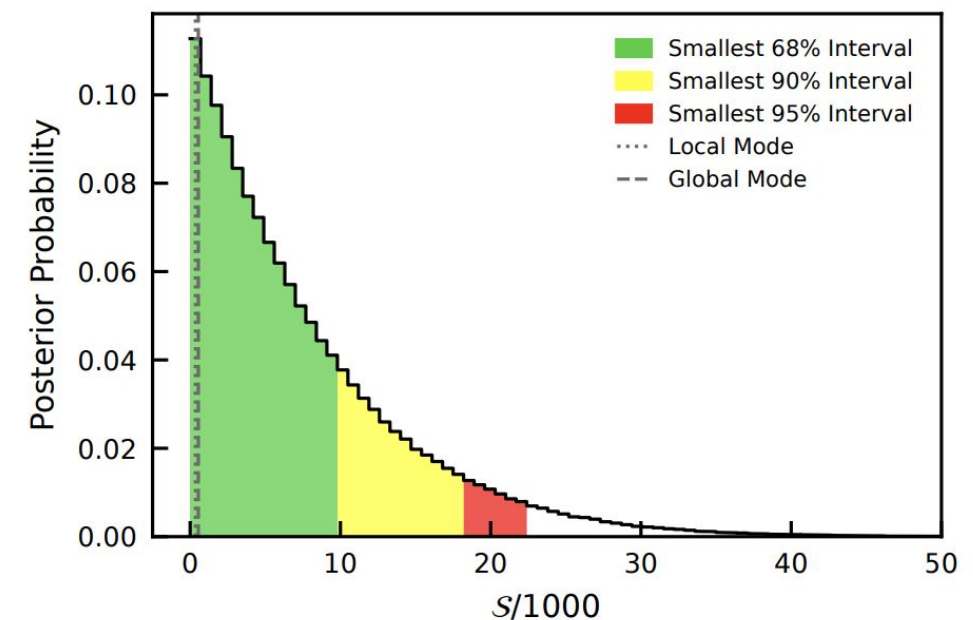
Analysis of the data collected during 2023 (41 days with a circulating current of 40 A and 56 days without current) finalized:

*paper under finalization:*

$$\beta^2/2 < 4.8 \cdot 10^{-29} \quad \text{Bayesian}$$

$$\beta^2/2 < 5.7 \cdot 10^{-29} \quad \text{Frequentist}$$

with probability 0.9

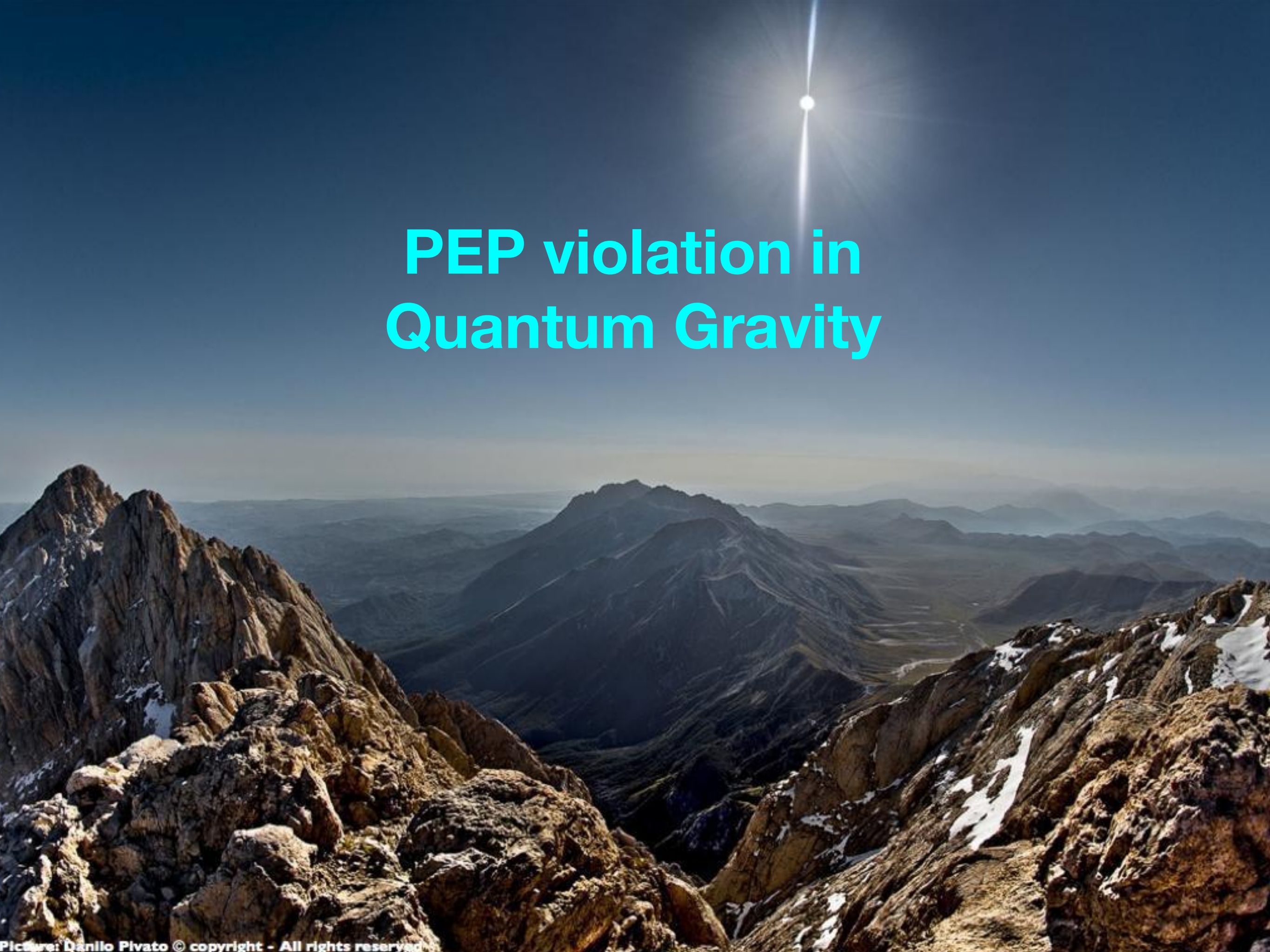


**Fig. 5** Marginalized posterior distribution of the parameter of interest  $\mathcal{S}/1000$ , obtained from the Bayesian analysis. The 90 % upper limit is indicated by the yellow band.

# ***possible future plans for the GATOR - VIP collaboration***

**Possible future plans are under discussion:**

- **implement the setup with a chiller-based target cooling system to increment the circulating current to 400 A,**
- **possibility to (additionally) implement the setup with a new readout electronics to perform a test of the anisotropy effect in PEP violating atomic transitions, in the context of Quantum Gravity theories (see the next slides).**

A high-altitude mountain landscape with a bright sun in the sky and the text "PEP violation in Quantum Gravity" overlaid. The scene shows rugged, rocky mountain peaks with patches of snow, set against a clear blue sky. The sun is positioned in the upper right, creating a lens flare effect. The text is centered in the upper half of the image.

# PEP violation in Quantum Gravity

# *PEP violation in quantum gravity*

## Non-commutativity of S-T:

- in quantum mechanics (relatively large-scales/low-energies) phase space is a smooth manifold.
- On distances of the order of  $\ell_p$  this breaks down, Heisenberg uncertainty + GR  $\rightarrow$  black hole formation  $\rightarrow$  the smooth manifold structure is lost.
- The notion of a point becomes meaningless and the simple commutation relation between space-time points is no longer expected to hold (first suggested by Snyder (1947) and Heisenberg (1954)).

Non-commutative Quantum Gravity, GUP, CPT deformation ... - Marcianò, Addazzi, Balachandran, Mavromatos, Illuminati ...

- Messiah-Greenberg superselection rule is violated
- PEP violation probability: a) depends on the transition energy b) depends on the energy scale of new-physics emergence c) is subject to not isotropic corrections



**VIP-2 Closed Systems** - High Purity Ge detectors, set of ultra-radiopure targets to check  $\delta^2(E)$  with a systematic scan over Z, tests of directionality.

# *PEP violation in quantum gravity*

Quantum gravity models can embed PEP violating transitions

PEP is a consequence of the spin statistics theorem based on: Lorentz/Poincaré and CPT symmetries; locality; unitarity and causality. Deeply related to the very same nature of space and time



non-commutativity of space-time operators is common to several quantum gravity frameworks (e.g.  $k$ -Poincaré,  $\theta$ -Poincaré)



non-commutativity induces a deformation of the Lorentz symmetry and of the locality → naturally encodes the violation of PEP not constrained by MG

PEP violation is suppressed with  $\delta^2 (E, \Lambda)$

$E$  is the characteristic transition energy,  $\Lambda$  is the scale of the space-time non-commutativity emergence.

A. P. Balachandran, G. Mangano, A. Pinzul and S. Vaidya, Int. J. Mod. Phys. A 21 (2006) 3111

A.P. Balachandran, T.R. Govindarajan, G. Mangano, A. Pinzul, B.A. Qureshi and S. Vaidya, Phys. Rev. D 75 (2007)

Collaboration with A. Addazi, A. Marcianò (Int.J.Mod.Phys.A 35 (2020) 32, 2042003)

# *PEP violation in quantum gravity*

Theoretical prediction *Int.J.Mod.Phys.A* 35 (2020) 32, 2042003

specific calculation of **atomic levels transitions probabilities** for  $\theta$ -Poincaré

$$W \simeq W_0 \phi_{PEPV}, \quad \phi_{PEPV} = \delta^2 \simeq \frac{D E_N \Delta E}{2 \Lambda \Lambda} \quad \phi_{PEPV} = \delta^2 \simeq \frac{C \bar{E}_1 \bar{E}_2}{2 \Lambda \Lambda}$$

for **non-vanishing (vanishing) electric like components** of the  $\theta_{\mu\nu}$  tensor.

Connection with quon algebra (in the case of quon fields however the  $q$  factor does not show any energy dependence):

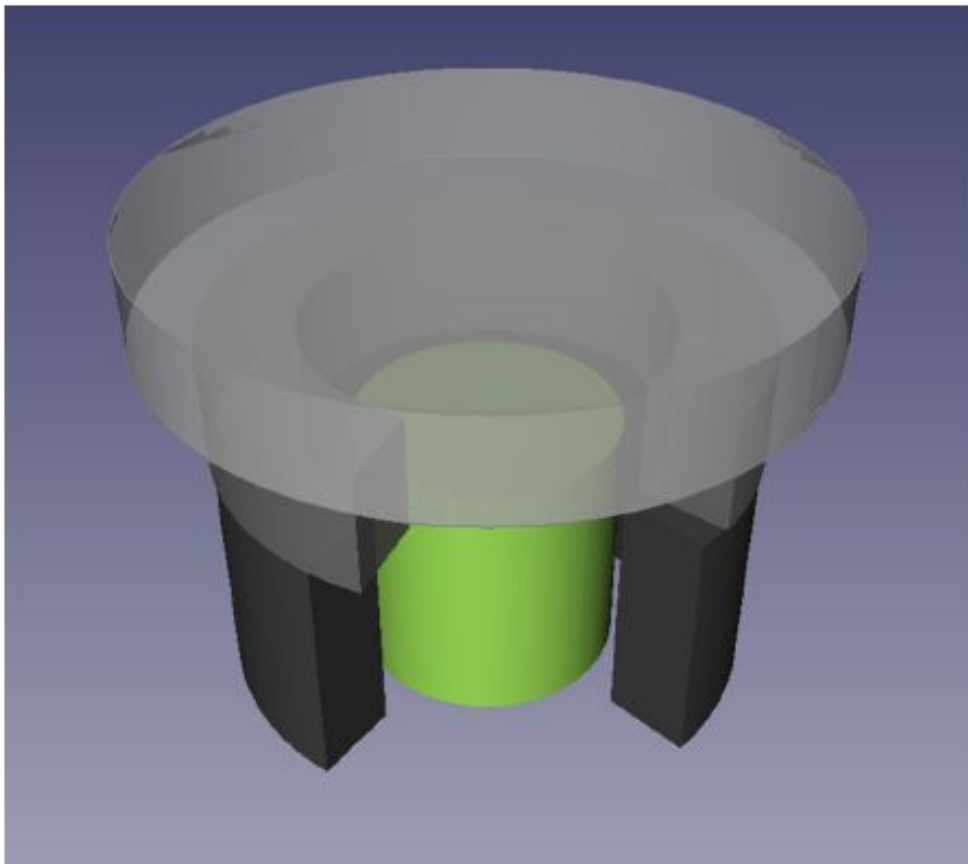
$$q(E) = -1 + 2\delta^2(E)$$

An **experimental bound on the probability that PEP may be violated** in atomic transition processes, **straightforwardly translates into a bound on the new physics scale  $\Lambda$** , consistently with the choice of the  $\theta_{0i}$  components.

# ***Closed Systems experimental apparatus***

## **High Purity Ge detector based setup:**

- high purity co-axial p-type germanium detector (HPGe), diameter of 8.0 cm, length of 8.0 cm, surrounded by an inactive layer of lithium-doped germanium of 0.075 mm.
- The target material is composed of three cylindrical sections of radio-pure Roman lead, completely surrounding the detector.



- Passive shielding: inner - electrolytic copper, outer - lead

- 10B-polyethylene plates reduce the neutron flux towards the detector

- shield + cryostat enclosed in air tight steel housing flushed with nitrogen to avoid contact with external air (and thus radon).

- Acquisition time  $\Delta t \approx 70d \approx 6.1 \cdot 10^6s$

**K. P. et al., Eur. Phys. J. C (2020) 80: 508**

**<https://doi.org/10.1140/epjc/s10052-020-8040-5>**

Fig. 1 Schematic representation of the Ge crystal (in green) and the surrounding lead target cylindrical sections (in grey)

# Statistical model

- The *pdf* of the expected number of total signal counts  $S$  given the measured distribution is:

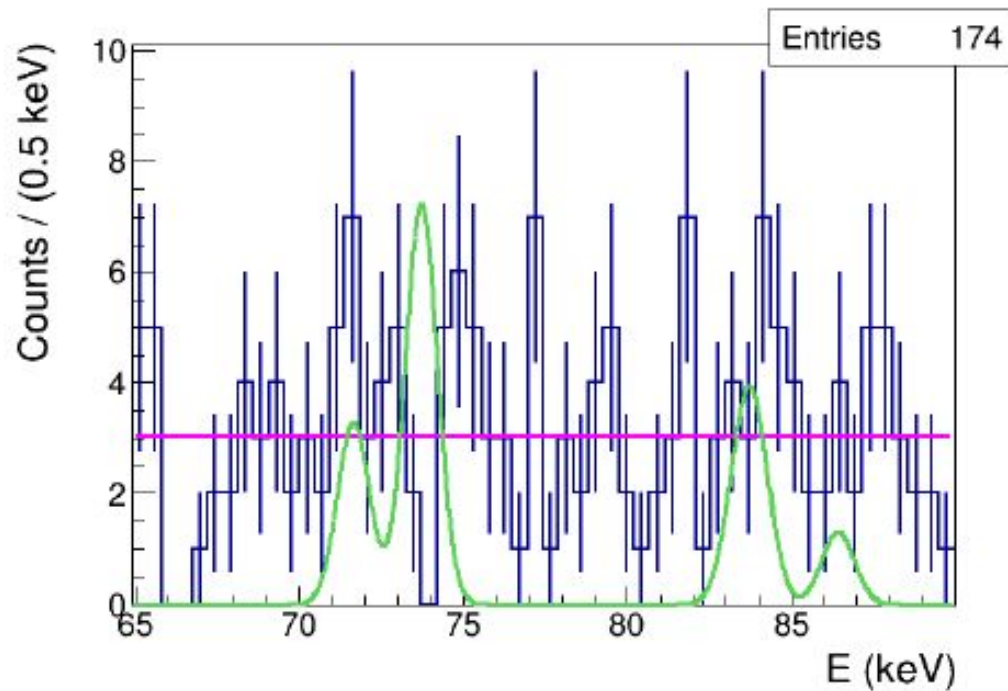


FIG. 1. The measured X-ray spectrum, in the region of the  $K_\alpha$  and  $K_\beta$  standard and violating transitions in Pb, is shown in blue; the magenta line represents the fit of the background distribution. The green line corresponds to the shape of the expected signal distribution (with arbitrary normalization) for  $\theta_{0i} \neq 0$ .

The prior for  $S$  consistent with existing limits [Found. Phys. 42, 1015-1030 (2012)].



$$P(S|data) = \int_0^\infty \int_{\mathcal{D}_p} P(S, B|data, \mathbf{p}) d^m \mathbf{p} dB$$

$$P(S, B|data, \mathbf{p}) =$$

$$= \frac{P(data|S, B, \mathbf{p}) \cdot f(\mathbf{p}) \cdot P_0(S) \cdot P_0(B)}{\int P(data|S, B, \mathbf{p}) \cdot f(\mathbf{p}) \cdot P_0(S) \cdot P_0(B) d^m \mathbf{p} dS dB}$$

- the likelihood is weighted on the joint *pdf* of the experimental parameters

$$P(data|S, B, \mathbf{p}) = \prod_{i=1}^N \frac{\lambda_i(S, B, \mathbf{p})^{n_i} e^{-\lambda_i(S, B, \mathbf{p})}}{n_i!}$$

$$\lambda_i(S, B) = B \cdot \int_{\Delta E_i} f_B(E, \alpha) dE + S \cdot \int_{\Delta E_i} f_S(E, \sigma) dE$$

# Statistical model

- First analysis which accounts for the predicted energy dependence of the PEP violation probability. Expected rate of  $K_{\alpha 1}$  transitions:

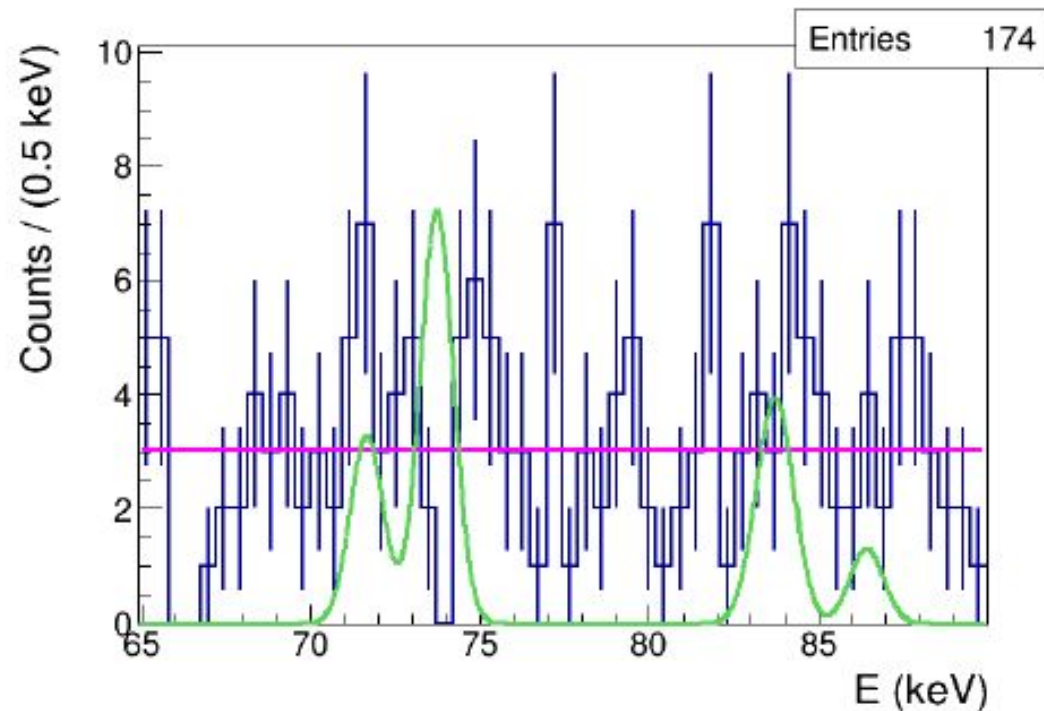


FIG. 1. The measured X-ray spectrum, in the region of the  $K_{\alpha}$  and  $K_{\beta}$  standard and violating transitions in Pb, is shown in blue; the magenta line represents the fit of the background distribution. The green line corresponds to the shape of the expected signal distribution (with arbitrary normalization) for  $\theta_{0i} \neq 0$ .

$$\Gamma_{K_{\alpha 1}} = \frac{\delta^2(E_{K_{\alpha 1}})}{\tau_{K_{\alpha 1}}} \cdot \frac{BR_{K_{\alpha 1}}}{BR_{K_{\alpha 1}} + BR_{K_{\alpha 2}}} \cdot 6 \cdot N_{atom} \cdot \epsilon(E_{K_{\alpha 1}}).$$

- probability to observe  $n$  transitions in the time  $t$ :

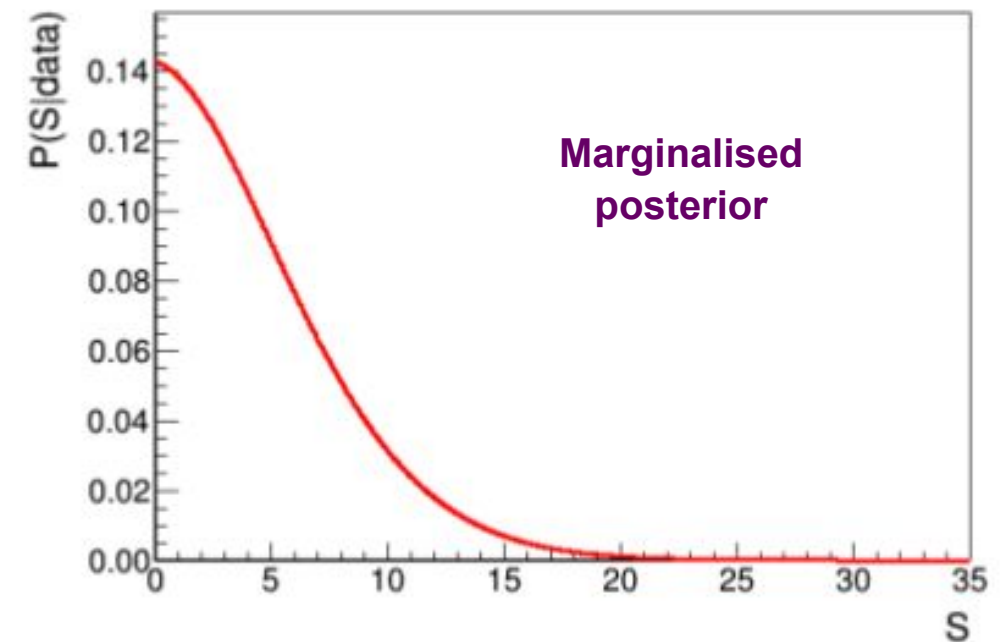
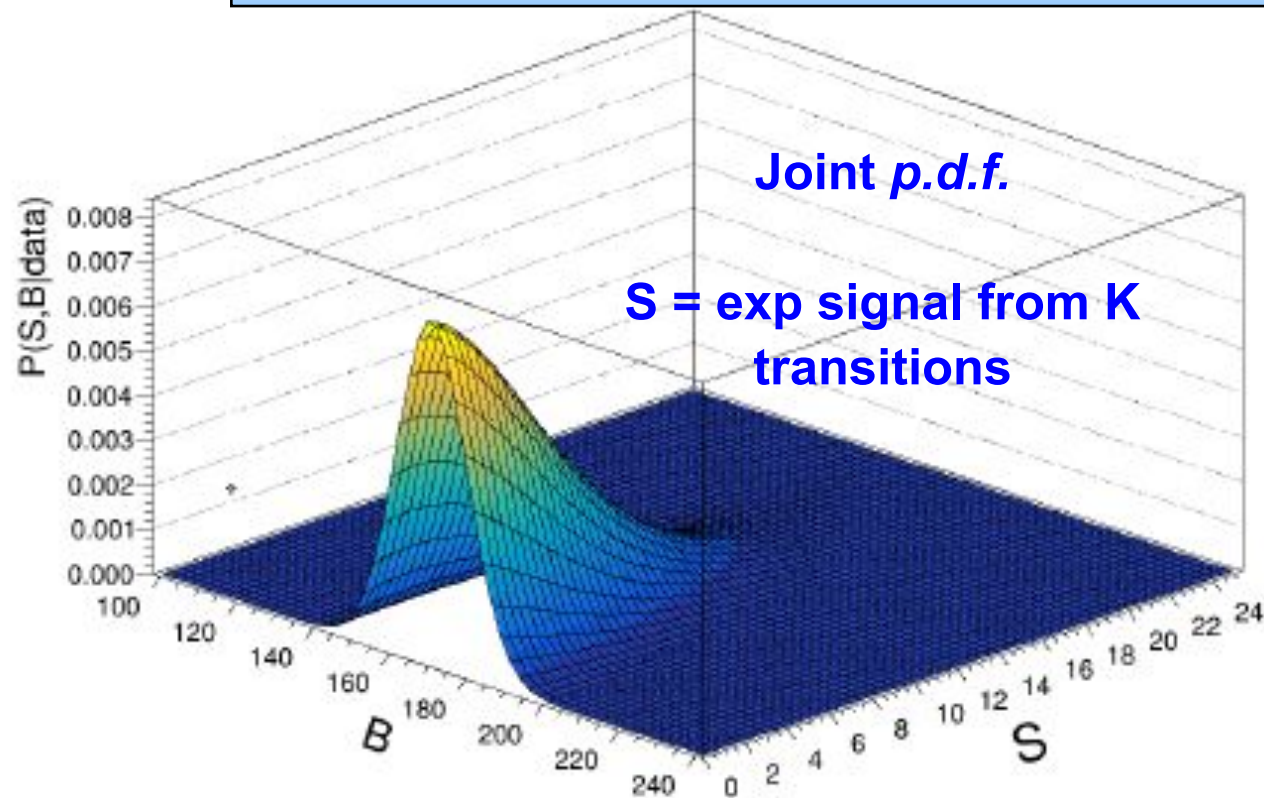
$$P(n; t) = \frac{(\Gamma_{K_{\alpha 1}} t)^n e^{-\Gamma_{K_{\alpha 1}} t}}{n!},$$

$$f_S(E, k) = \frac{1}{N} \cdot \sum_{K=1}^{N_K} \Gamma_K \frac{1}{\sqrt{2\pi\sigma_K^2}} \cdot e^{-\frac{(E-E_K)^2}{2\sigma_K^2}}$$

- upper limit on the non-commutativity scale:

$$\mu = \sum_{K=1}^{N_K} \mu_K = \frac{\aleph}{\Lambda^k} < \bar{S}$$

# Results



From which an upper limit on the non-commutativity scale is obtained (90% Probability):

$\theta_{0i}$	$\bar{S}$	lower limit on $\Lambda$ (Planck scales)
$\theta_{0i} = 0$	13.2990	$6.9 \cdot 10^{-2}$
$\theta_{0i} \neq 0$	18.1515	$2.6 \cdot 10^2$

K. P. et al., PRL 129, 131301 (2022)

K. P. et al., PRD 107, 026002 (2023)

see also A. Addazi, P. Belli, R. Bernabei and A. Marciano, Chin. Phys. C 42 (2018) no.9, 094001

# Generalized analysis

- Generalized analysis based on an analytic expansion of the PEP violation prob.

$$M_k : \delta^2(E) = \frac{E^k}{\Lambda^k} + O(E^{k+1})$$

-  $k = 1$  corresponds to  $k$ -Poincaré. Different quantization procedures lead to different predictions:

- Arzano-Marcianò procedure - PEP violation is suppressed with a probability proportional to  $\delta^2 = E / \Lambda$
- Freidel-Kowalski-Glikman-Nowak procedure - PEP violation is missing.

So experimental investigation of statistics violations provides important down-top indications on the “right” quantization procedure: **the AM  $k$ -Poincaré field’s quantization model is ruled out.**

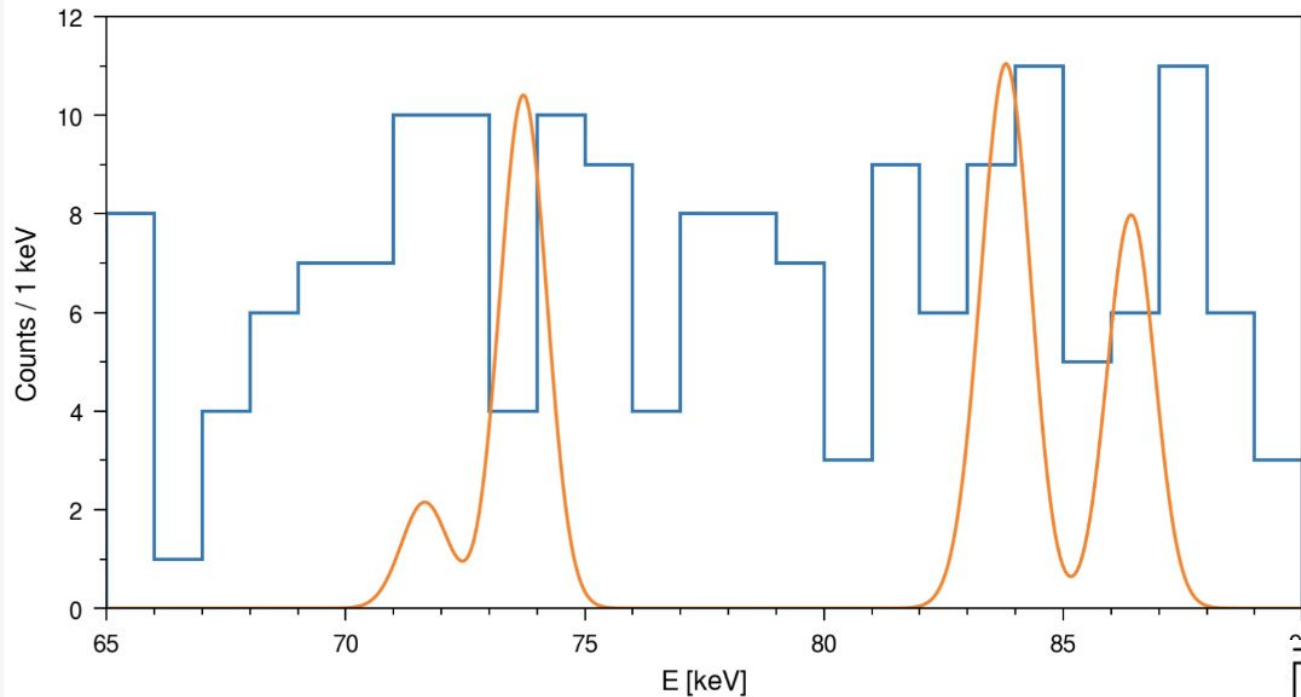
-  $k = 2$  corresponds to  $\theta$ -Poincaré: excluded up to  $\Lambda > 1.6 \cdot 10^{-1}$  Planck scales

-  $k = 3$  corresponds to “triply special relativity” model by Kowalski-Glikman–Smolin (KS). First measurement ever, excluded up to  $\Lambda > 5.6 \cdot 10^{-9}$  Planck scales -> experimental guidance towards future developments of the model with two invariant energy scales accounting for the deformation of the (non-commutative) space-time symmetries.

# Generalized analysis

## - The normalised signal shape for the $M_3$ parametrization:

**Figure 1.** The figure shows the measured X-ray spectrum corresponding to an acquisition time of  $\Delta t \approx 6.1 \cdot 10^6$  s in the region of interest. For a comparison, the expected signal distribution (with arbitrary normalization) is also shown in orange for the  $A_3$  analysis and the  $M_3$  parametrization.



- The sensitivity on  $\Lambda$  increases with  $E$   
 -> the analysis is repeated by searching for PEP violation signal in  $K\alpha$ ,  $K\beta$  and  $K\alpha + K\beta$  transitions.

Universe 2023, 9(7), 321

$A_i, M_k$	$\bar{S}$	lower limit on $\Lambda$ in unit of Planck scale
$A_1, k = 1$	11.4913	$3.1 \cdot 10^{21}$
$A_1, k = 2$	11.3776	$1.4 \cdot 10^{-1}$
$A_1, k = 3$	11.2610	$4.9 \cdot 10^{-9}$
$A_2, k = 1$	15.1408	$2.8 \cdot 10^{21}$
$A_2, k = 2$	15.1640	$1.4 \cdot 10^{-1}$
$A_2, k = 3$	15.1859	$5.1 \cdot 10^{-9}$
$A_3, k = 1$	18.7270	$4.2 \cdot 10^{21}$
$A_3, k = 2$	19.1847	$1.6 \cdot 10^{-1}$
$A_3, k = 3$	19.5993	$5.6 \cdot 10^{-9}$

# Preliminary analysis on PEPV Generalized Uncertainty Principle

Generally related to the existence of a **minimal length** - as predicted by several QG models -  
E.g. GUP structure emerges from **string theory** in the high energy limit.

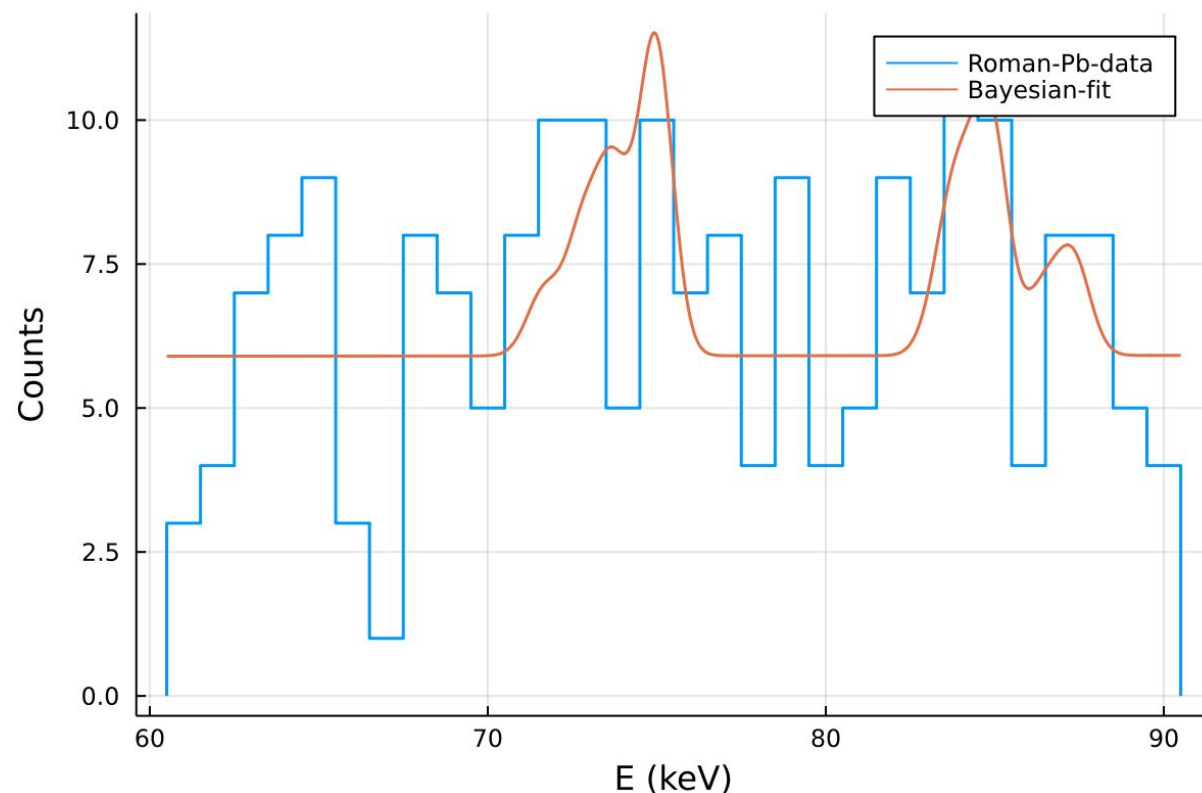
The construction of field theories in this context implies **deformations of the statistics:**

Theory already developed in collaboration with Illuminati, Bosso and Luciano

➔ PEP atomic tests suitable to investigate GUP models. **FIRST STUDY EVER!**

Violation of the PEP depends on the energy and on  $\Lambda_{GUP}$  as

$$\delta^2(E, \beta) = \frac{m \Delta E}{\Lambda_{GUP}^2}$$



Preliminary result!

$\Lambda_{GUP} > 0.52$  Planck scales

A scenic view of a mountain range with a bright sun in the sky. The sun is positioned in the upper right quadrant, creating a lens flare effect. The mountains are rugged and rocky, with some snow patches visible on the slopes. The sky is a clear, pale blue.

**R&D activity for the development of an experiment dedicated to test anisotropy effects in PEP violating atomic transitions**

# *HPGe implementation for directionality measurements*

## **THE IDEA:**

- **to implement an HPGe based setup, Machine Learning augmented, to be able to measure the direction of the incoming photon.**
- **This will be achieved by a precise study and characterization of the detector's pulse shapes.**

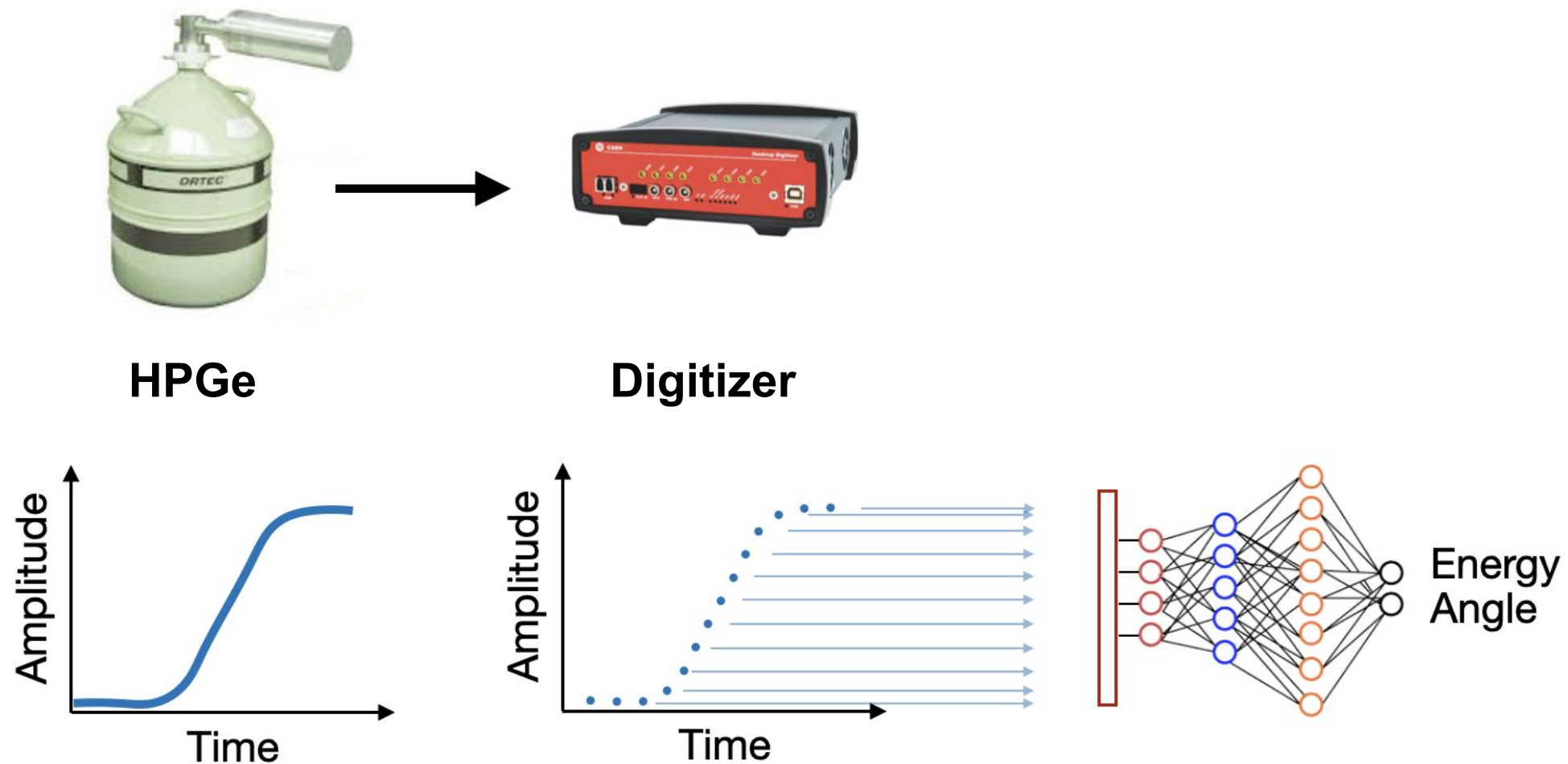
## **IN DETAIL:**

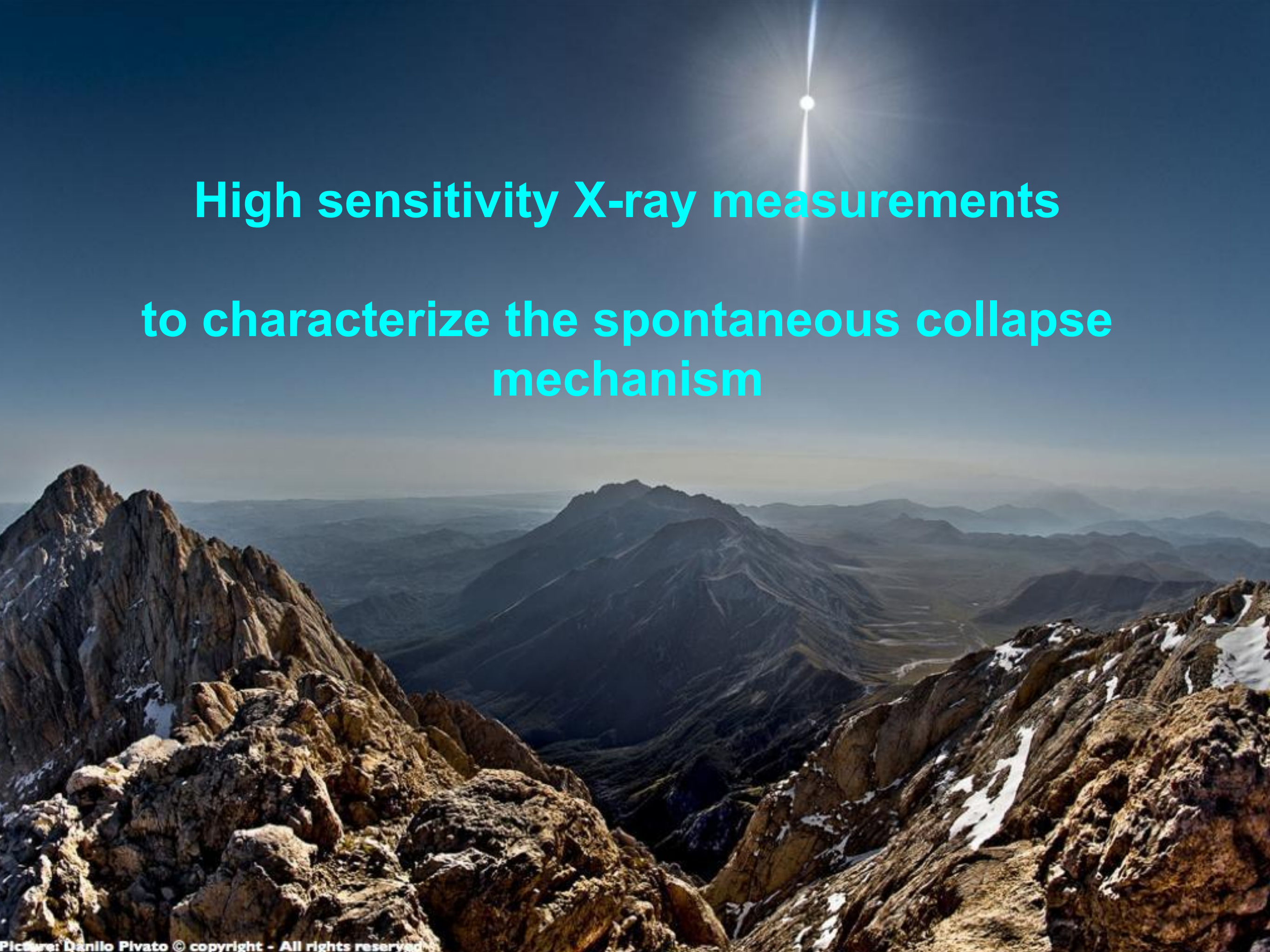
- **recent pioneering study**  
(<https://www.sciencedirect.com/science/article/pii/S0168900222004879>)  
**extracted the complex relationship between the shape of the signal and the direction from which the gamma-ray enters the detector active volume using a two-steps ML technique.**
- **A Ba-133 radioactive source, placed at 0, 45, 90 and 180 degrees with respect to the axis of the detector is used for calibration sample acquisition.**

# *HPGe implementation for directionality measurements*

Schematic view below of the data acquisition and ML architecture analysis.

First, the preamplified signal is acquired by the HPGe coaxial p-type detector. The analogue signal is then digitized with high sampling rate 250 MS/s with 14 bits resolution (provided by the Caen DT5725). A convolutional neural network model will provide the angle and the energy.



A high-altitude mountain landscape with a bright sun flare in the sky. The foreground shows rugged, rocky terrain with patches of snow. The background features a vast, hazy mountain range under a clear blue sky.

**High sensitivity X-ray measurements  
to characterize the spontaneous collapse  
mechanism**

# Quantum and Gravity

## DYNAMICAL COLLAPSE MODELS:

- Why the quantum properties (superposition) do not carry over to the macro-world?
- Stochastic and non-linear modifications of the Schrodinger dynamics -> **spontaneous collapse**, progressive reduction of the superposition, proportional to the increase of the mass of the system

“spontaneous universal collapse in massive degrees of freedom, assuming a fundamental gravity-related irreversibility, may have perspectives for quantum cosmology as well”

L. Diósi (2023) J. Phys.: Conf. Ser. 2533 012005)

**Spontaneous decoherence** induced by space-time indeterminacy

&

**Irreversibility in Quantum Gravity/Cosmology** at the Planck scale

lead to the same structure of master equations

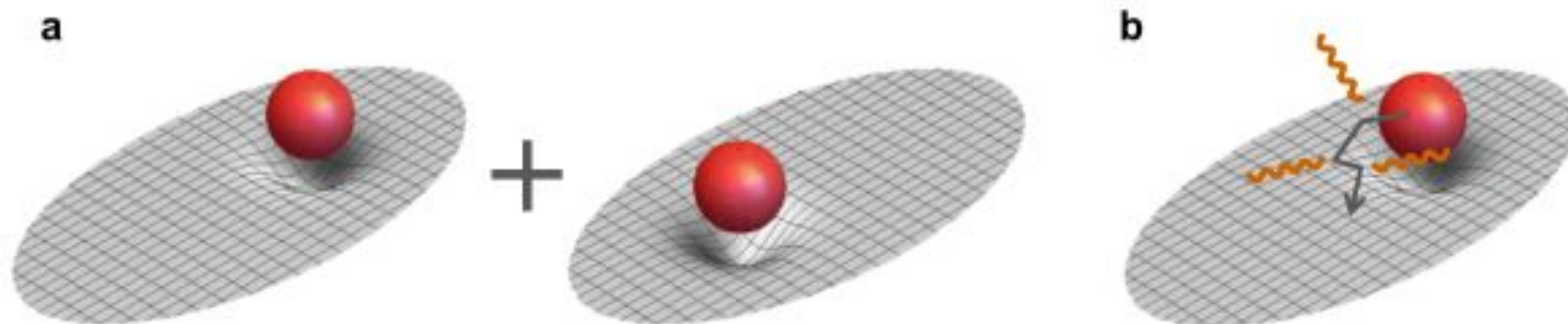
this spectacular connection can be experimentally tested !

# Gravity induced collapse: the Diosi-Penrose model

*Diósi: QT requires an absolute indeterminacy of the gravitational field, -> the local gravitational potential should be regarded as a stochastic variable, whose mean value coincides with the Newton potential, and the correlation function is:*

$$\langle \phi(\mathbf{r}, t) \phi(\mathbf{r}', t') \rangle - \langle \phi(\mathbf{r}, t) \rangle \langle \phi(\mathbf{r}', t') \rangle \sim \frac{\hbar G}{|\mathbf{r} - \mathbf{r}'|} \delta(t - t')$$

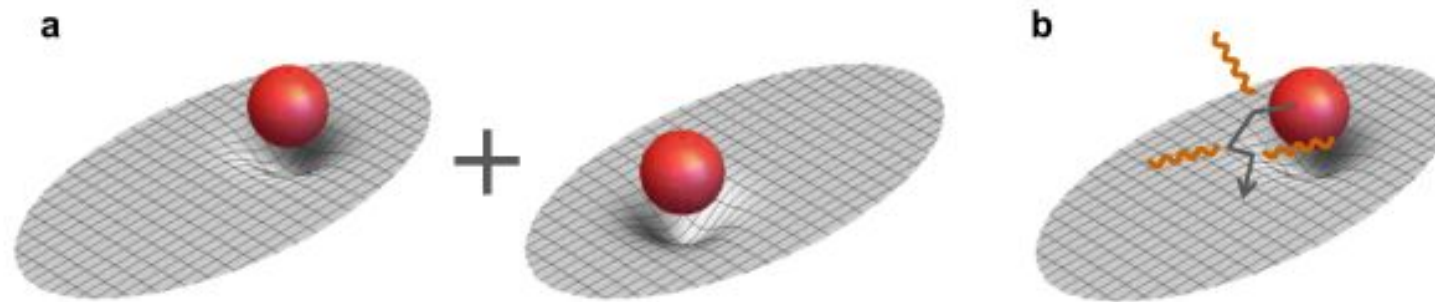
*Penrose: When a system is in a spatial quantum superposition, a corresponding superposition of two different space-times is generated. The superposition is unstable and decays in time. The more massive the system in the superposition, the larger the difference in the two space-times and the faster the wave-function collapse.*



# Radiation measurements to test the collapse

- Unavoidable side effect of the [stochastic collapse dynamics](#):  
a [Brownian-like diffusion of the system in space](#) Phys. Rev. Lett. 130, 230202 (2023).

Collapse probability is Poissonian in  $t$  -> Lindblad dynamics for the statistical operator -> free particle average square momentum increases in time.



- Then [charged particles emit spontaneous radiation](#). We search for spontaneous radiation emission from a germanium crystal and the surrounding materials in the experimental apparatus.

**Strategy:** simulate the background from all the known emission processes -> perform a Bayesian comparison of the residual spectrum with the theoretical prediction -> extract the pdf of the model parameters -> bound the parameters.

# Spontaneous emission in the $\gamma$ -rays regime

- *CSL - s. e. photons rate:*

$$\left. \frac{d\Gamma}{dE} \right|_t^{CSL} = \frac{\hbar \lambda}{4 \pi^2 \epsilon_0 c^3 r_C^2 m_0^2 E} (N_p^2 + N_e)$$

- *DP - s. e. photons rate:*

$$\left. \frac{d\Gamma}{dE} \right|_t^{DP} = \frac{G}{12 \pi^{3/2} \epsilon_0 c^3 R_0^3 E} \{N_p^2 + N_e\}$$

the photon w.l.  $\lambda_\gamma$  is intermediate between the nuclear dimension and the lower atomic orbit radius  $\rightarrow$  protons emit coherently, electrons emit independently

$\lambda$  - collapse strength

$r_c$  - correlation length

see e. g. S. L. Adler, JPA 40, (2007) 2935, Adler, S.L.; Bassi, A.; Donadi, S., JPA 46, (2013) 245304.

$R_0$  - size of the particle mass density. See e.g. Diósi, L. J. Phys. Conf. Ser. 442, 012001 (2013)., Penrose, R. Found. Phys. 44, 557-575 (2014).

# Spontaneous emission in the *X-rays* regime

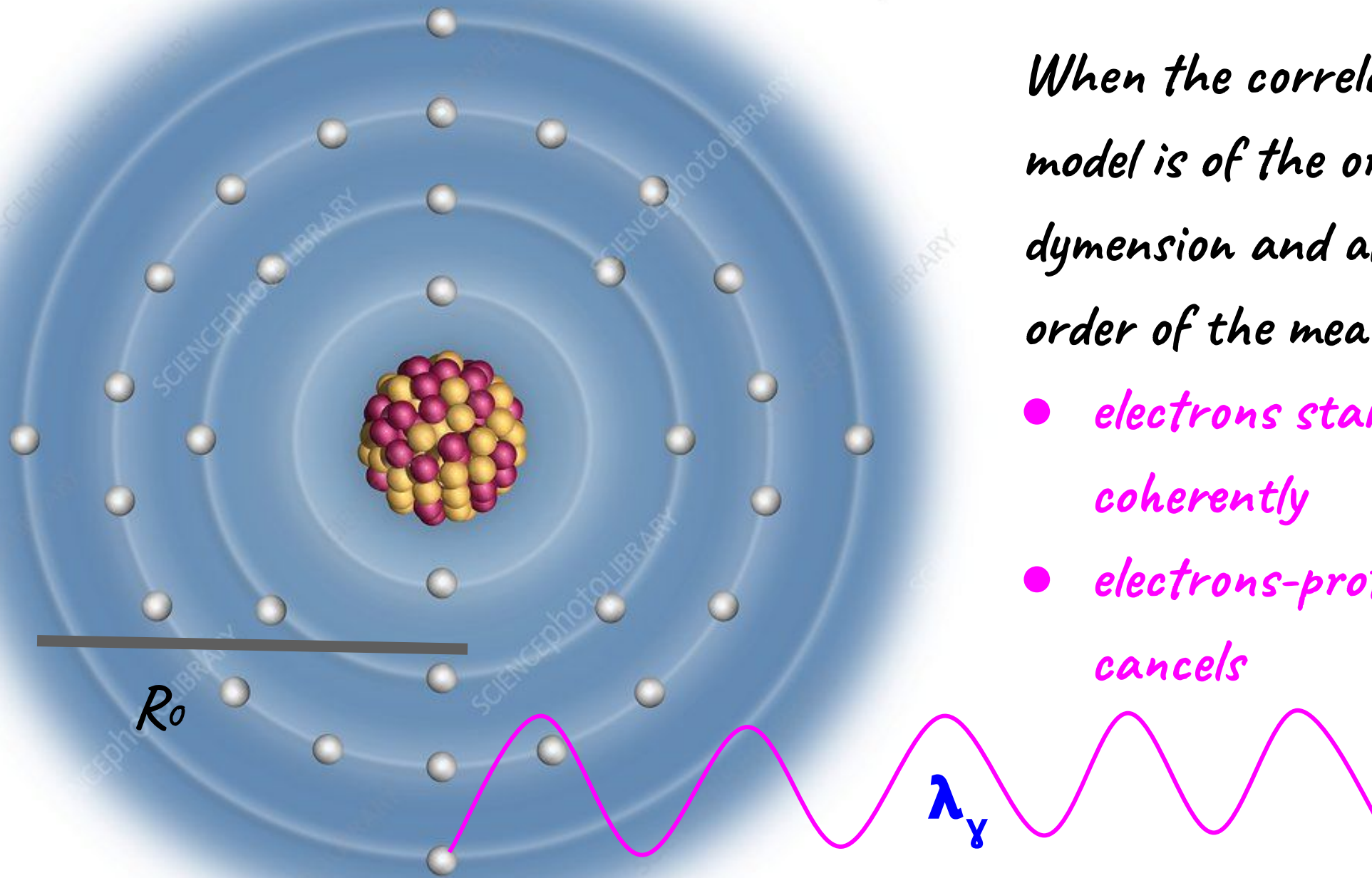
In the low-energy regime, the photon w.l. is comparable to the atomic orbits dimensions

e.g.  $\lambda_{dB}(E=15 \text{ keV}) = 0.8 \text{ \AA}$

$r_{1s} = 0.025 \text{ \AA}; r_{4p} = 1.5 \text{ \AA}$

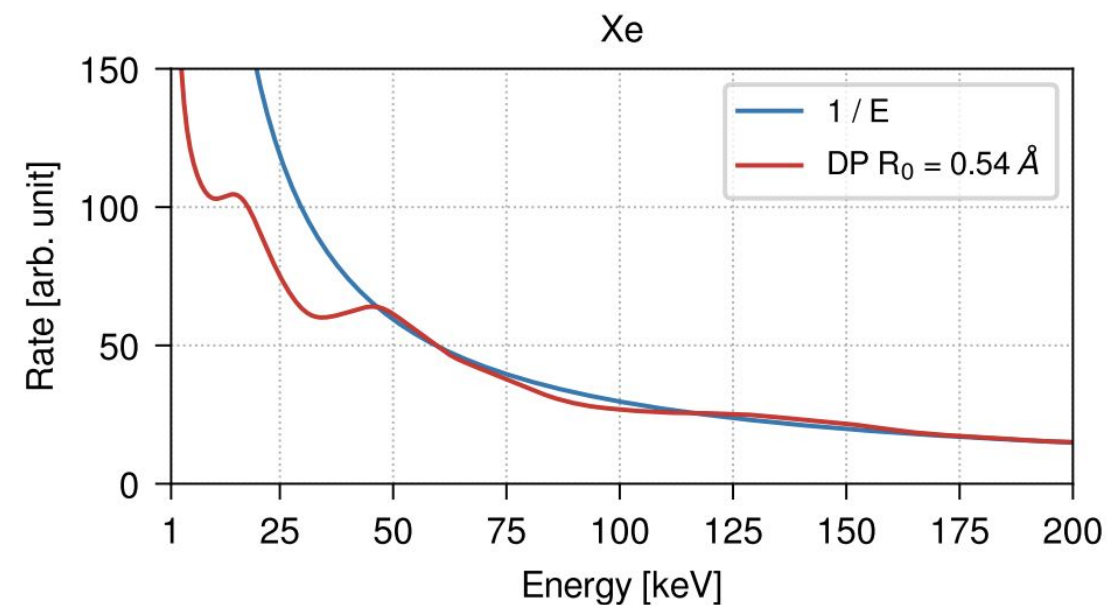
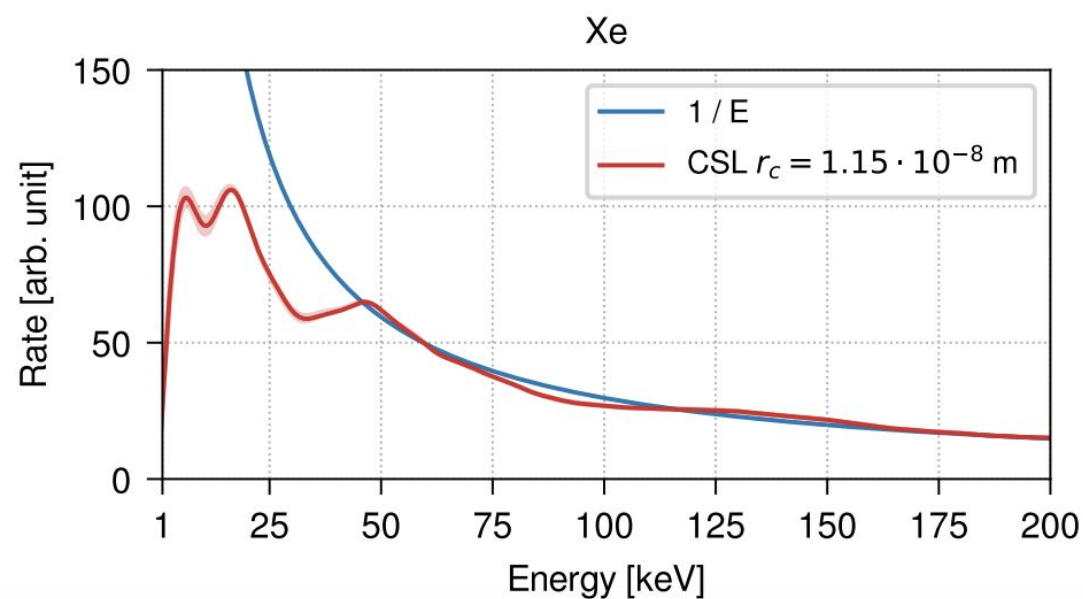
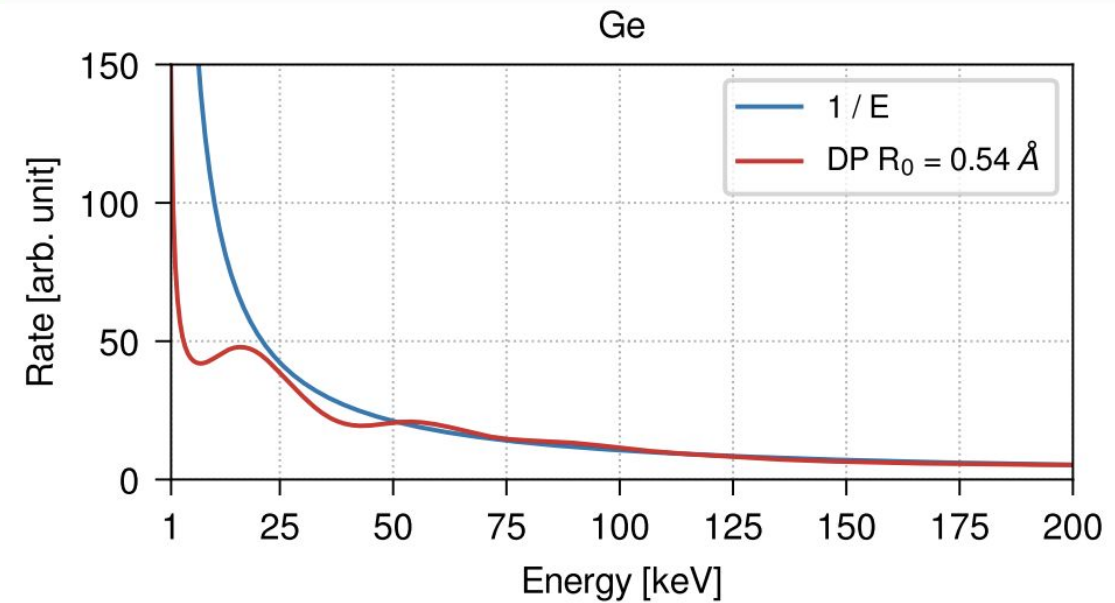
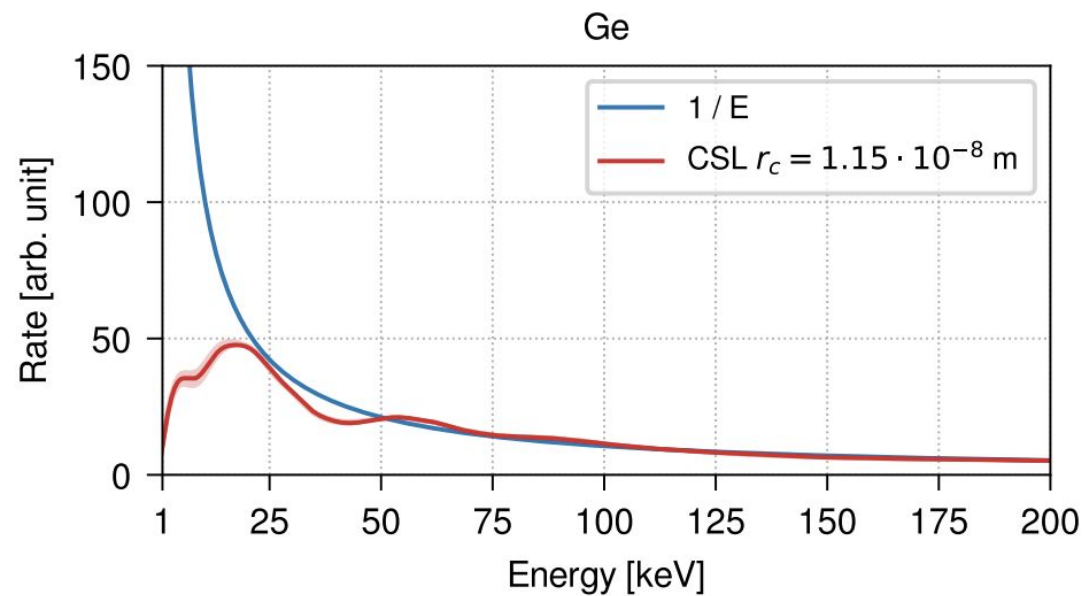
When the correlation length of the model is of the order of the atomic dimension and also  $\lambda_\gamma$  is of the order of the mean atomic radii:

- *electrons start to emit coherently*
- *electrons-protons contribution cancels*



# Spontaneous emission in the *X-rays* regime

see *S. Manti's* talk



- *at each energy the atomic structure influences the expected S.E. spectrum shape*
- *the S.E. spectrum shape is different for different collapse models.*

arXiv:2301.09920v1 [quant-ph] <https://doi.org/10.48550/arXiv.2301.09920>

# Spontaneous emission in the *X-rays* regime

*accepted in PRL*

$$\frac{d\Gamma}{dE} \Big|_t^{DP} = \frac{Ge^2}{12\pi^{5/2}\epsilon_0 c^3 R_0^3 E} \left\{ N_p^2 + N_e + 2 \sum_{o o' \text{ pairs}} N_o N_{o'} \frac{\sin \left[ \frac{\beta |\rho_o - \rho_{o'}| E}{\hbar c} \right]}{\left[ \frac{\beta |\rho_o - \rho_{o'}| E}{\hbar c} \right]} e^{-\frac{\beta^2 (\rho_o - \rho_{o'})^2}{4R_0^2}} + \right. \\ \left. + \sum_o N_o (N_o - 1) e^{-\frac{(\alpha \rho_o)^2}{4R_0^2}} \cdot \frac{\sin \left( \frac{\alpha \rho_o E}{\hbar c} \right)}{\left( \frac{\alpha \rho_o E}{\hbar c} \right)} - 2N_p \sum_o N_o \frac{\sin \left( \frac{\rho_o E}{\hbar c} \right)}{\left( \frac{\rho_o E}{\hbar c} \right)} \cdot e^{-\frac{\rho_o^2}{4R_0^2}} \right\}$$

*first prediction of a distinctive experimental signature for different collapse mechanisms! Opens up a world of new experimental challenges, to test established and new models linking gravitation to quantum mechanics.*

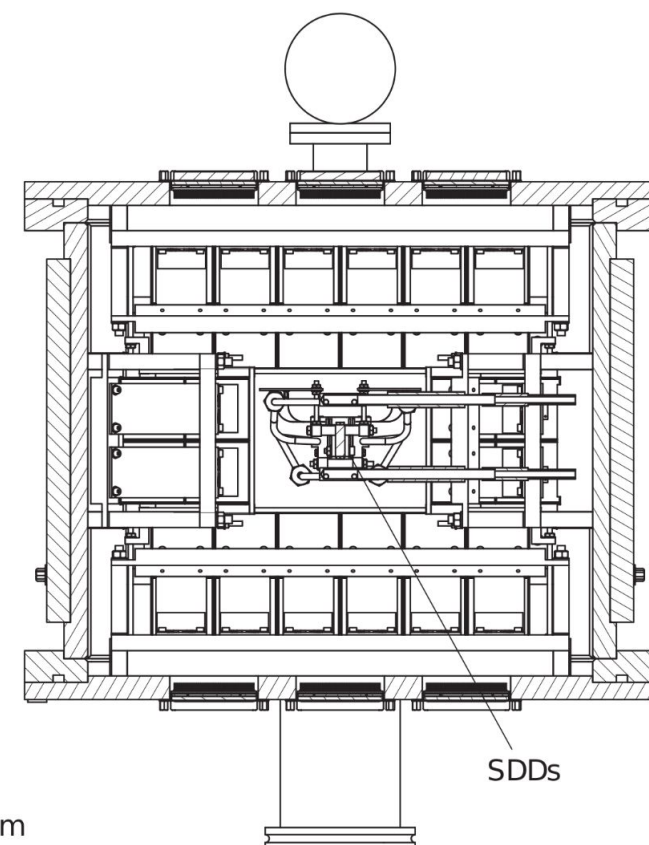
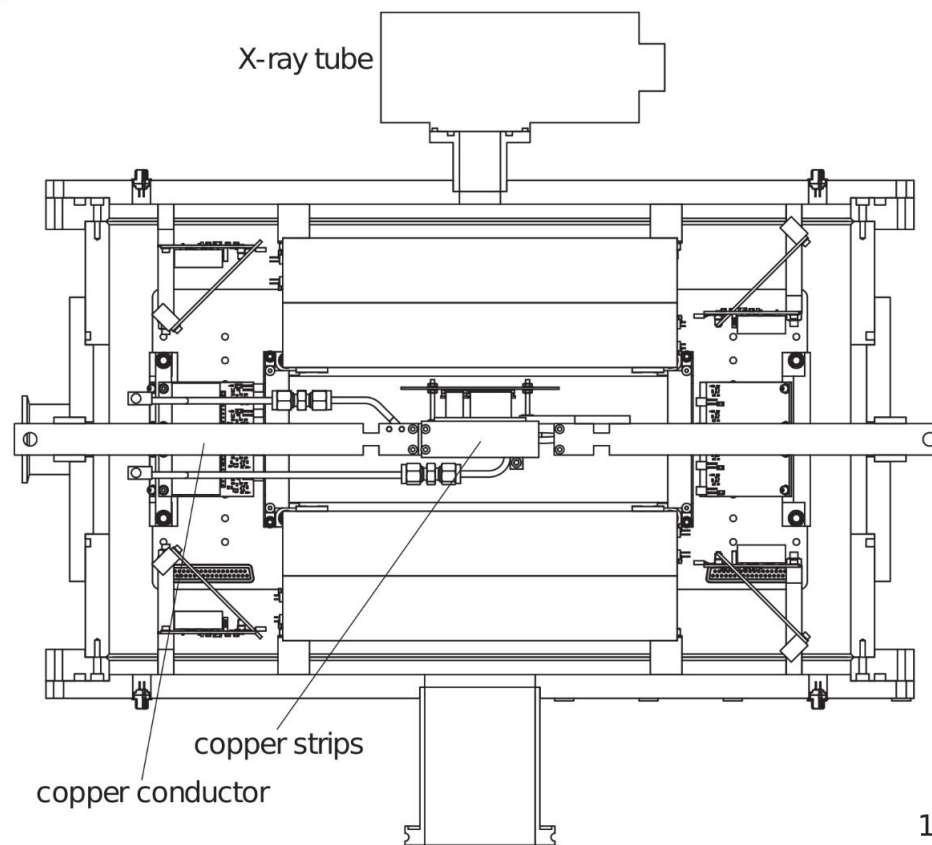
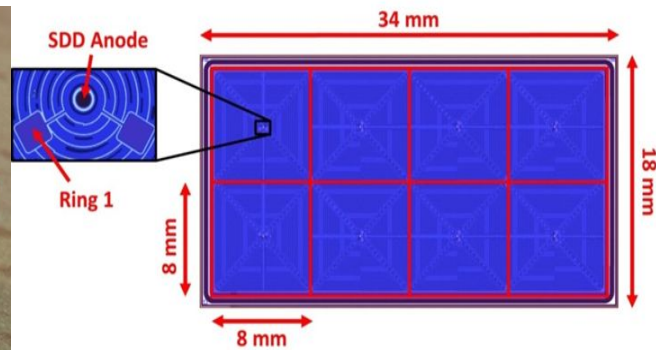
*R&D of a dedicated experiment ongoing.*

***Spare slides***

# VIP-2 Open Systems - present status and results

## VIP-2 Open Systems -

- SDD detectors 450 $\mu$ m thick (high resolution 190 eV FWHM at 8 keV) -> [ML/DP analysis improvement of 10 eV \(Meas. Sci. Technol. 35 \(2024\) 025501\)](#)
- 4 arrays of 2x4 SDDs, liquid Argon closed circuit cooling
- 2 strip shaped Cu targets (cooled by closed chiller circuit -> with [INCREASED](#) 200A (peak) circulating current  $\sim$ 1  $^{\circ}$ K heating in the SDDs)





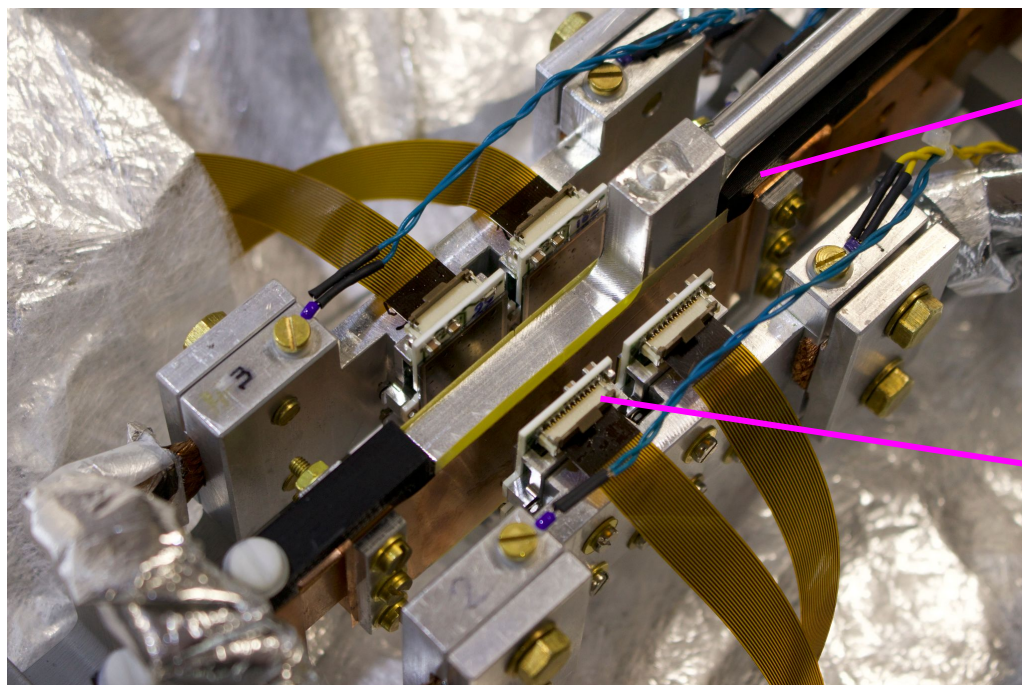
# VIP-2 Open systems apparatus activity

# VIP-2 Open systems maintenance/renovation

- After maintenance of the setup: chamber regeneration, maintenance of inner shielding cooling system, revision and cleaning of the pumps, under-vacuum washing of the inner components, maintenance of the SDDs electronics and system, rebuilding of the copper target which was ruined,
- in view of the longer duration of the VIP-2 run, due to delays in the new 1mm SDD production (by FBK, see below) we performed the following renovation activity:
  - we built and substituted the target cooling system (which was damaged),
  - a safer current feedthrough - with super-flexible Cu cables of 50 mm<sup>2</sup> section - was installed.

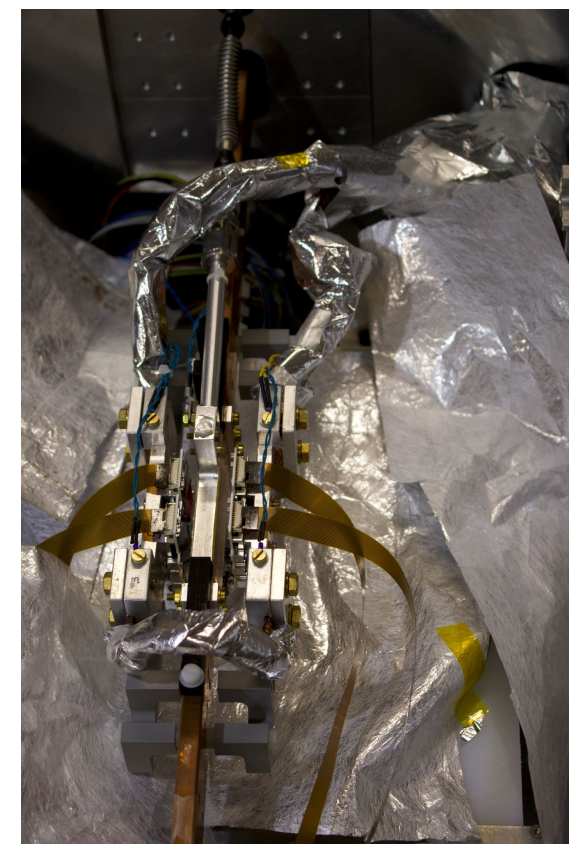
These interventions allowed to increase the circulating current to 200 A.

- Vacuum instability problems of the chamber were solved, and 2 o.m. were gained in pressure (from  $7 \times 10^{-5}$  mb to  $6 \times 10^{-7}$  mb).
- substitution of damaged SDDs -> factor 2 gain in acceptance



New target cooling system  
&  
New current feedthrough  
higher circulating current

New 450  $\mu$ m SDD arrays  
higher acceptance



# VIP-2 Open systems activity 2023-now

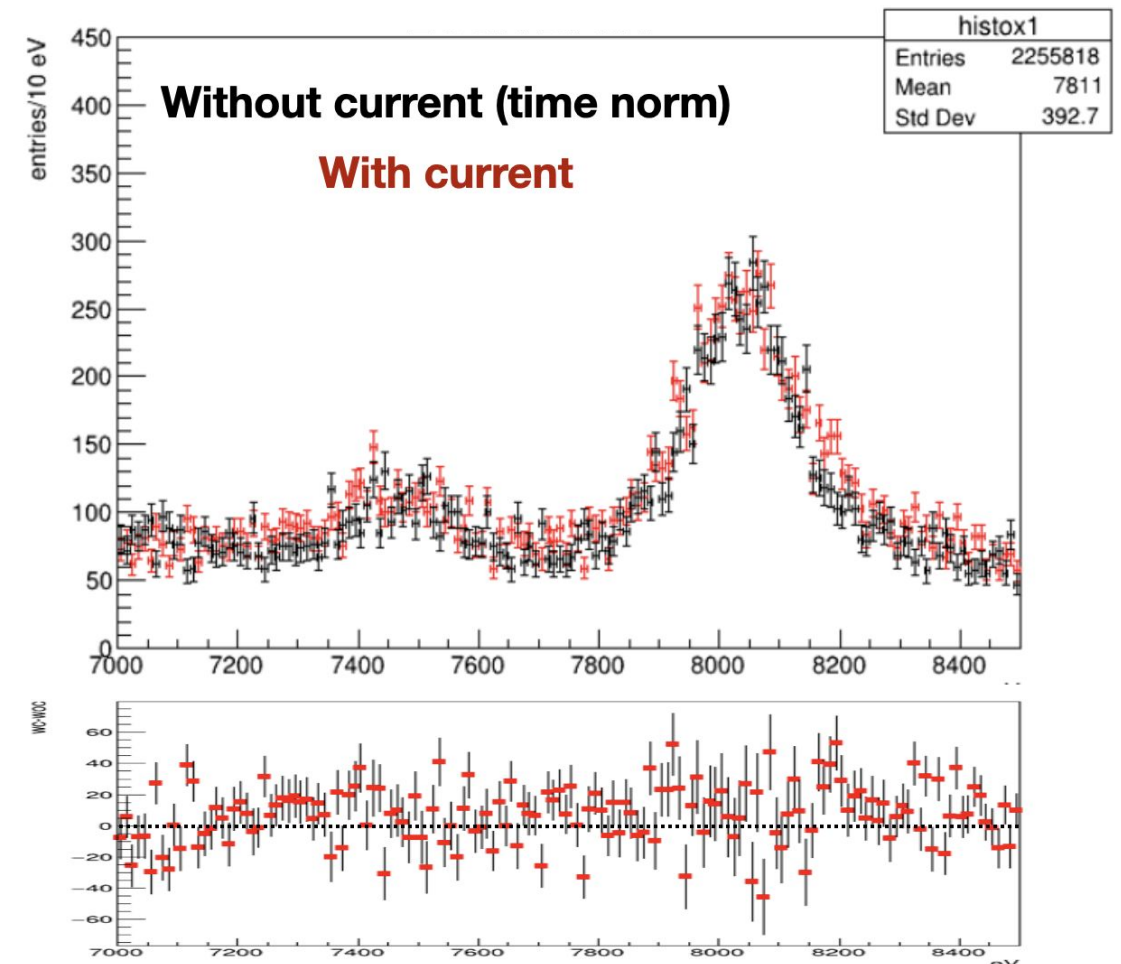
## Chronology of the activity:

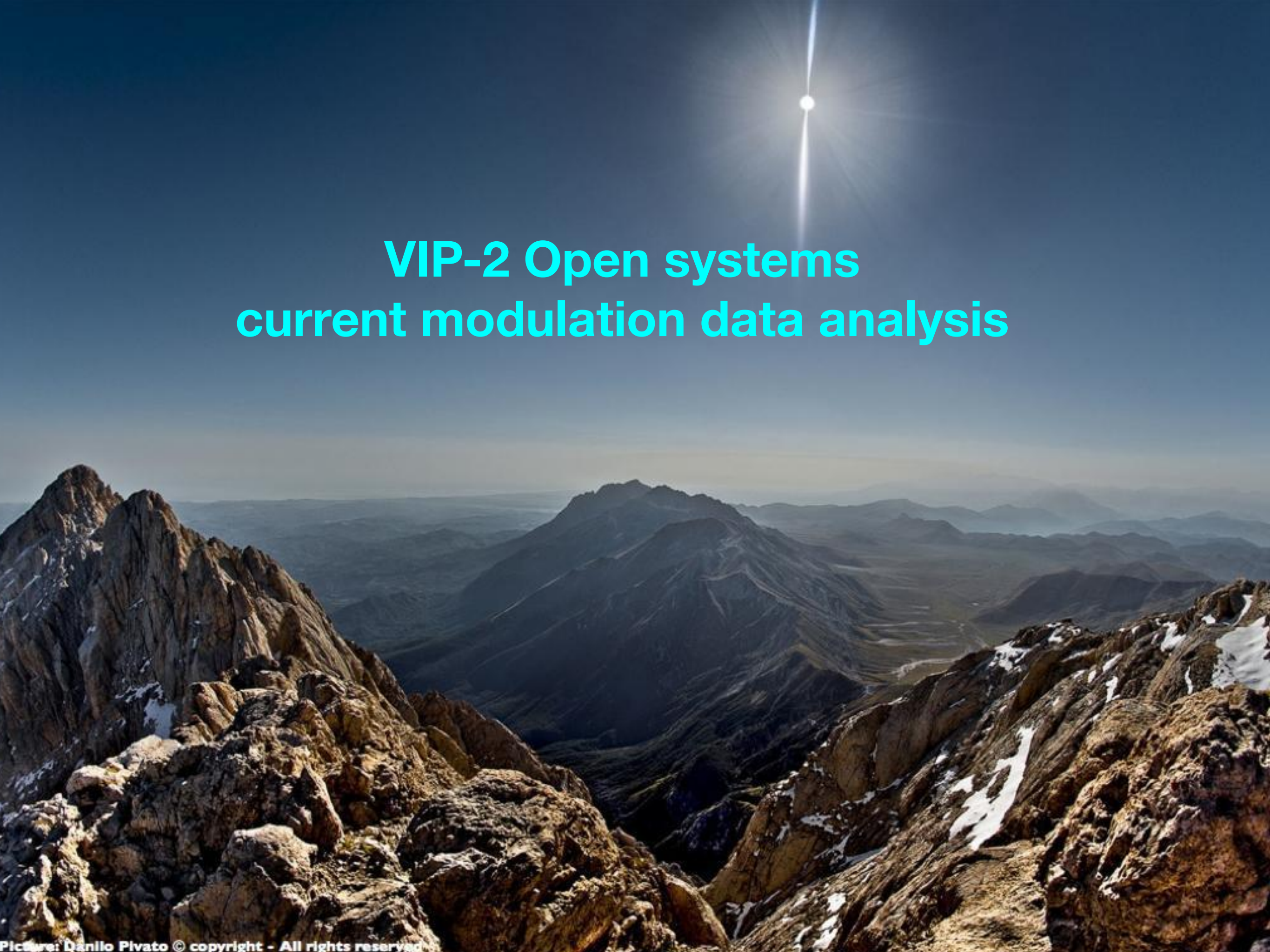
- (March - May) 2023 - substitution target cooling system, installation new current feedthrough, maintenance vacuum chamber, substitution damaged SDDs
- (May - July) 2023 - data taking with current (without shielding to monitor the system parameters)
- July 2023 - Shielding installation
- August 2023 - data taking with current (electric noise due to power supply connection solved)
- (September - December) 2023 - data taking with current  $I = 200$  A
- December 2023 - now - data taking without current

## Plan for 2024:

- to balance the acquisition periods with & without current
- to start a modulated current acquisition till the installation of VIP-3

[2023-2024 calibrated data under analysis:](#)



A scenic mountain landscape with a bright sun in the sky and snow-dusted peaks. The sun is positioned in the upper right quadrant, creating a lens flare effect. The mountains are rugged and rocky, with patches of snow. The sky is a clear, deep blue.

# VIP-2 Open systems current modulation data analysis

# Refined current modulation run analysis

Modulated current test run (68 days) the wc-woc alternation is automatized with a fixed period of 100 s: 50 s of wc phase, 50 s of woc.

A simultaneous spectral and Discrete Fourier Transform Bayesian analysis is performed:

leads to a 32% reduction of the 0.9 probability constraint on the PEPV signal:

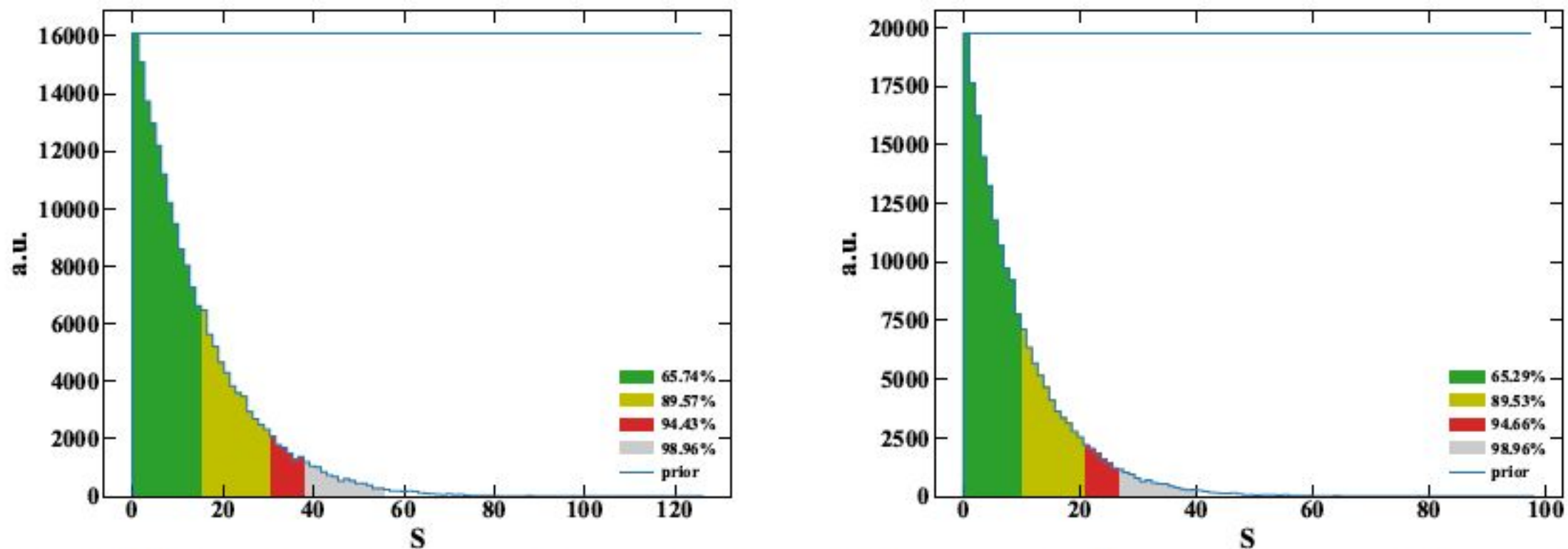


Fig. 6 Marginalized posterior distribution of  $S$  using only the spectral analysis as per Section 3 (left) and spectral+modulated combined as per Section 5 (right). Colored regions represent the distribution areas; the blue lines represent the prior representation.

$$\left. \frac{\beta^2}{2} \right|_{\text{comb}} < 8.50 \cdot 10^{-31} \quad (\text{scattering})$$

$$\left. \frac{\beta^2}{2} \right|_{\text{comb}} < 6.74 \cdot 10^{-43} \quad (\text{close encounters})$$

**UNDER REVIEW**  
**(milestone fulfilled)**

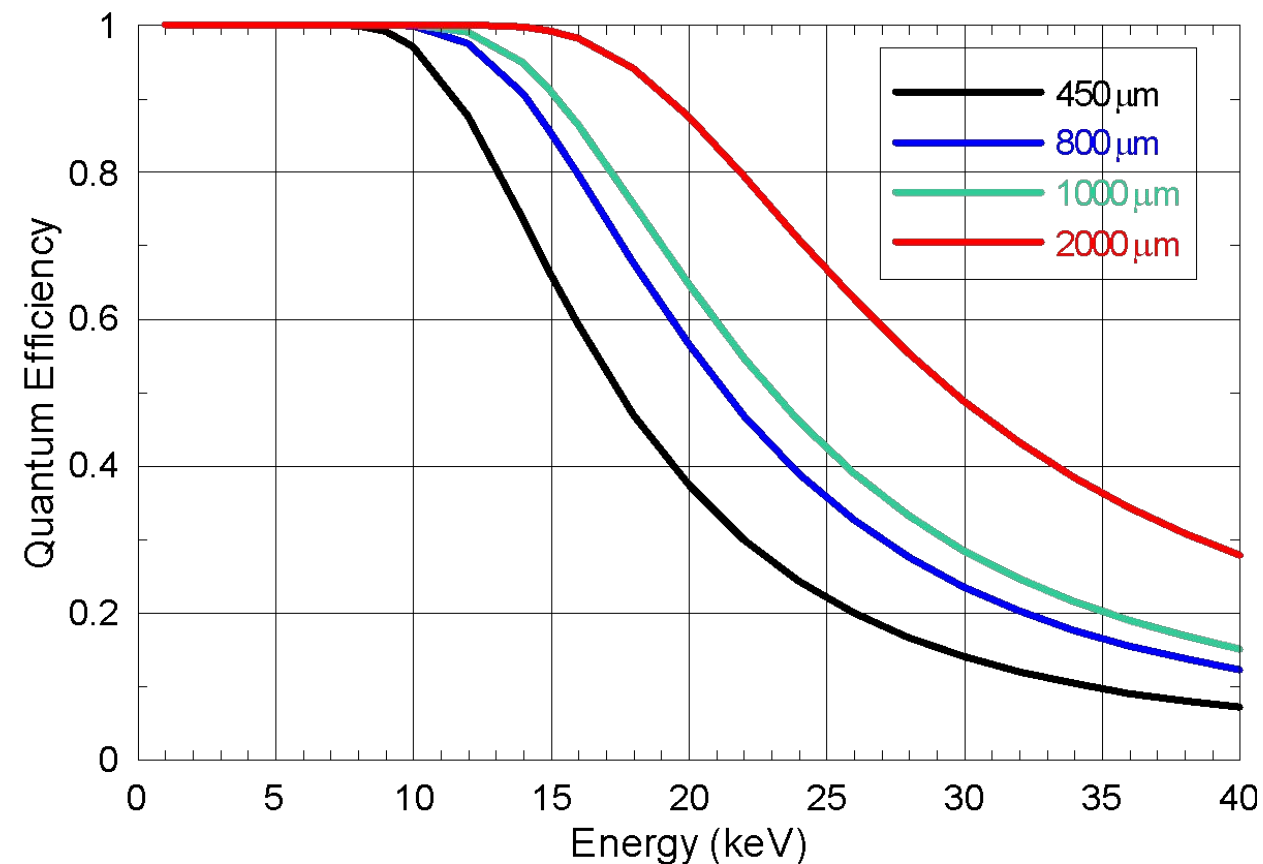




# Update on the activity for the future VIP-3 experiment

# VIP-3 activity 2023-now

Scan the PEP violation probability as a function of Z (i.e. of Energy)



Okun, L.:

“The special place enjoyed by the Pauli principle in modern theoretical physics does not mean that this principle does not require further and exhaustive experimental tests. On the contrary, it is specifically the fundamental nature of the Pauli principle which would make such tests, over the entire periodic table, of special interest”

L. Possible violation of the Pauli principle in atoms. JETP Lett.  
1987, 46, 529532

dependence on Z vastly discussed in our recent papers e.g. *Universe* 2023, 9(7), 321

# VIP-3 activity 2023-now

- Production of the new SDDs 1mm by FBK (Trento) finalized,
- regular meetings with Politecnico di Milano for the electronics development,
- proved increment of a factor 2 in efficiency at  $\sim 20$  keV keeping fixed E resolution (with respect present technological limits for 450 $\mu$ m) -> investigation PEP for electrons at higher Z (Ag, Sn, Zr and Pd),
- in Ag  $K\alpha_1$  tran. shift 482.70 eV with respect to the standard line (478.80 eV for the  $K\alpha_2$ )

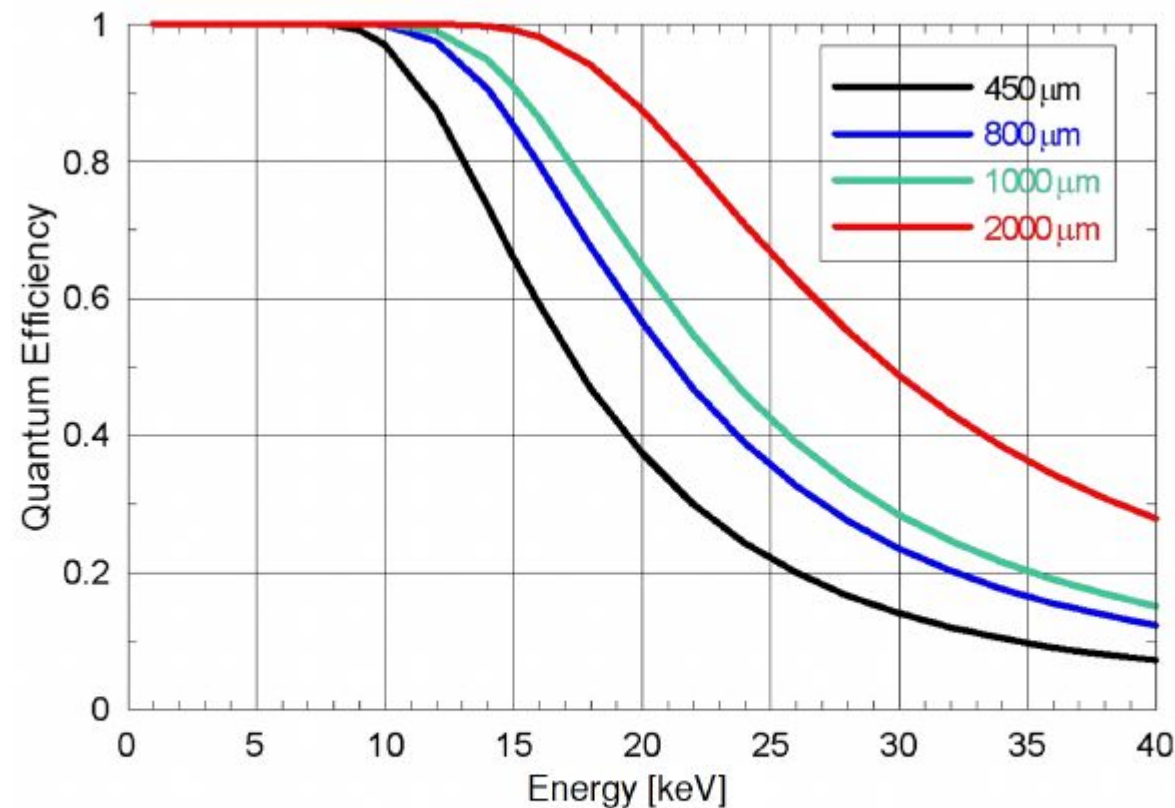


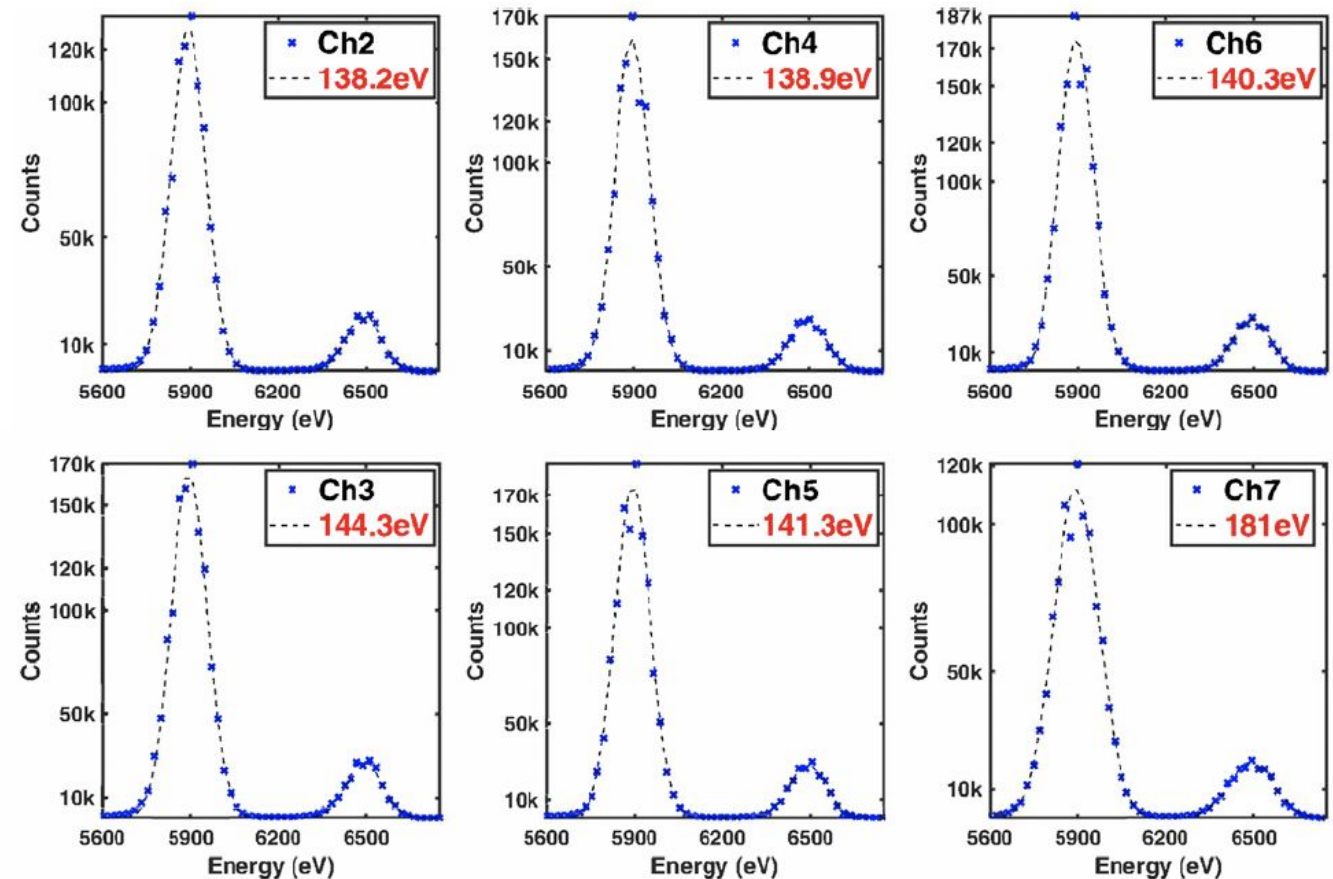
**Fig. 4** The figure shows the quantum efficiency as a function of the energy, for SDD devices of various thicknesses. The black curve corresponds to the detectors currently used in VIP-2, the green curve shows the efficiency achievable with the new 1 mm thick SDDs which we are presently developing for the VIP-3 experiment.

# VIP-3 activity 2023-now

- prototypes bonded and successfully characterized :
  - Optimization of the operational parameters of the new SDD, including the voltage of the focusing electrode;
  - Good spectroscopic performance of the new 1-mm-thick SDDs.

Spectroscopic measurements with a first prototype with partially working channels:

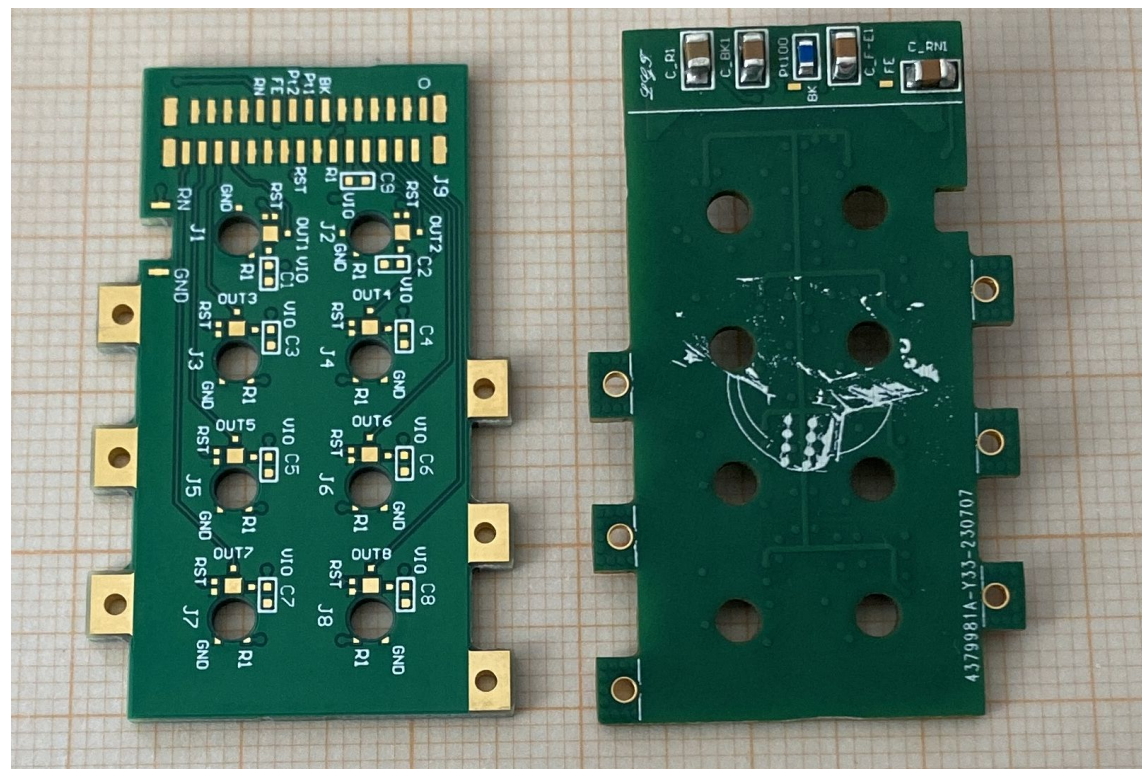
- irradiation with an  $^{55}\text{Fe}$  X-ray source;
- detector temperature:  $-30^\circ\text{C}$ ;
- spectra acquired with SFERA APP, shaping time  $6\ \mu\text{s}$ ;
- best energy resolution @5.9keV (Mn- $K\alpha$  peak ):  $138.2\ \text{eV}$ , (channel 2).



# VIP-3 activity 2023-now

## Design of the PCB support prototype finalized, prototype realized for testing:

- PCB dimensions modified to host a wider SDD chip (enlarged ~1 mm on each side wrt previous arrays);
- new bias line for the new focusing electrode on the window;
- new connector: from 20 to 30 pins to reduce noise and cross-talk problems;
- optimization of the material (FR4 under study) to minimize the presence of impurities -> contamination measurements ongoing.



## NEXT STEPS:

- thermal cycles in the cryostat with the new modules to verify their mechanical robustness
- PCB production (setting final geometry)
- PCB bonding

# VIP-3 activity 2023-now

## Design of the PCB support prototype finalized:

- PCB dimensions modified to host a wider SDD chip (enlarged ~1 mm on each side wrt previous arrays);
- new bias line for the new focusing electrode on the window;
- new connector: from 20 to 30 pins to reduce noise and cross-talk problems
- optimization of the material (FR4 under study) to minimize the presence of impurities -> contamination measurements ongoing.

## NEXT STEPS:

- thermal cycles in the cryostat with the new modules to verify their mechanical robustness
- PCB production (setting final geometry)
- PCB bonding
  
- **HENCE - the design of all the mechanical components, for which the final geometry of the SDD apparatus is necessary, is started** (new thermal contact between the cold-finger and SDDs detectors, new target cooling system)

Production phase of these components (o.m. 1 month) is conditioned to the green light of Politecnico di Milano

**ALL THE REST OF THE VIP-3 SETUP IS READY OR UNDER FINALIZATION:**

# VIP-3 activity 2023-now

- Finalization of the new SDDs readout electronics:

a new system, continuous reset based, dedicated to VIP is under finalization

- SDD readout board - design completed, prototype under realization

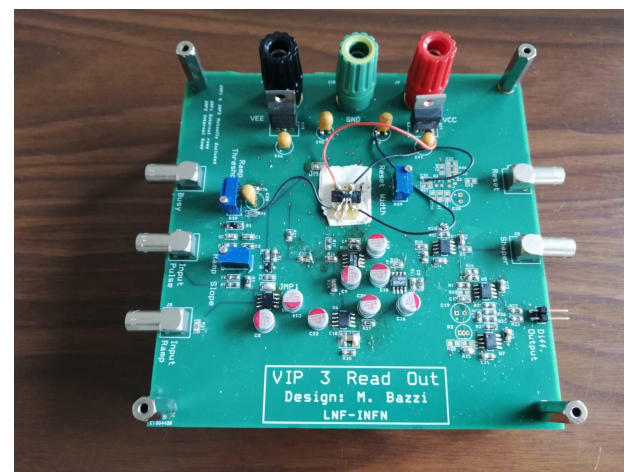
- flat cable: readout board - peak sensing

ADC - READY

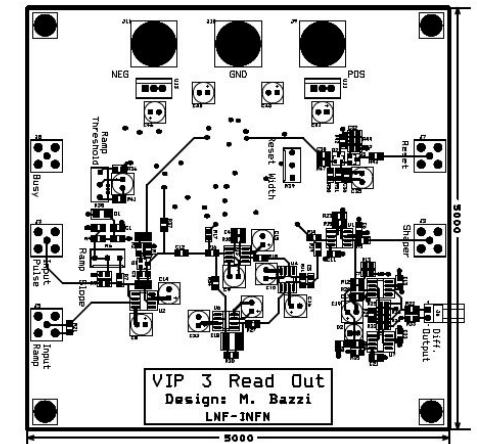
- peak sensing ADC – DAQ - READY

- flat cable: SDD - new front end electronics - design completed,

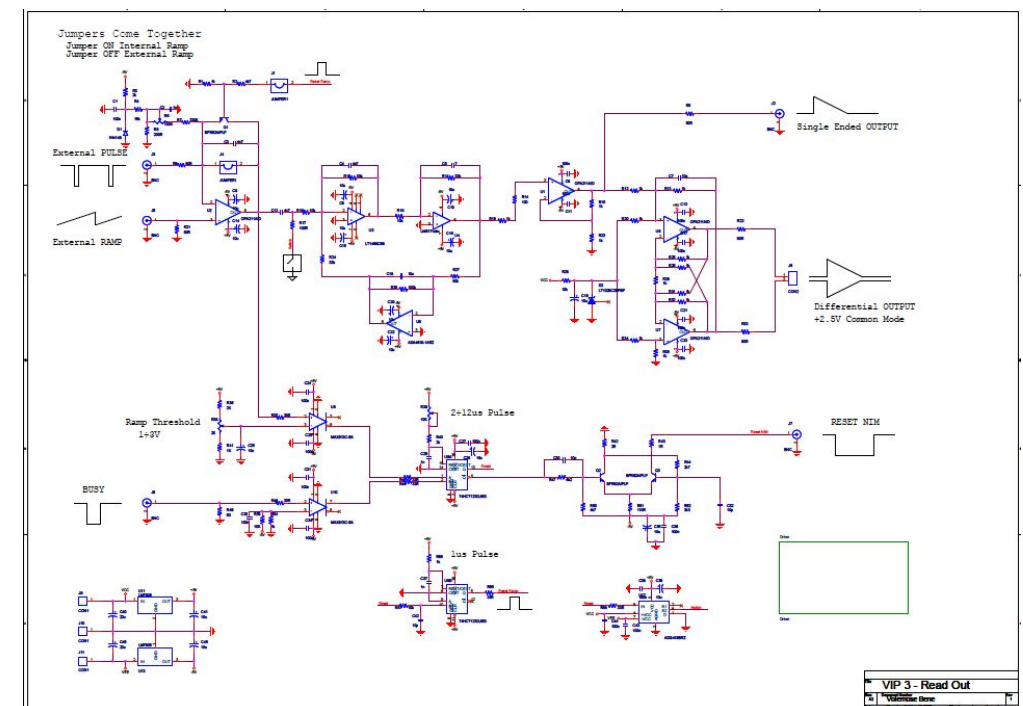
prototype realized and under test:



- internal buffer-board - READY

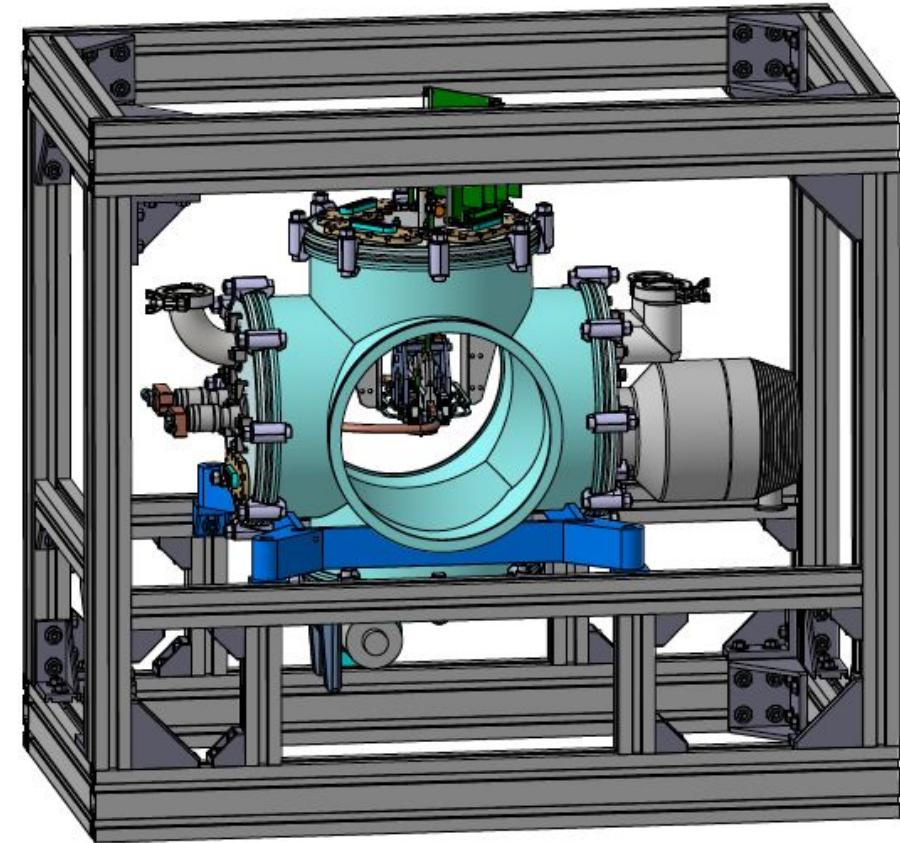
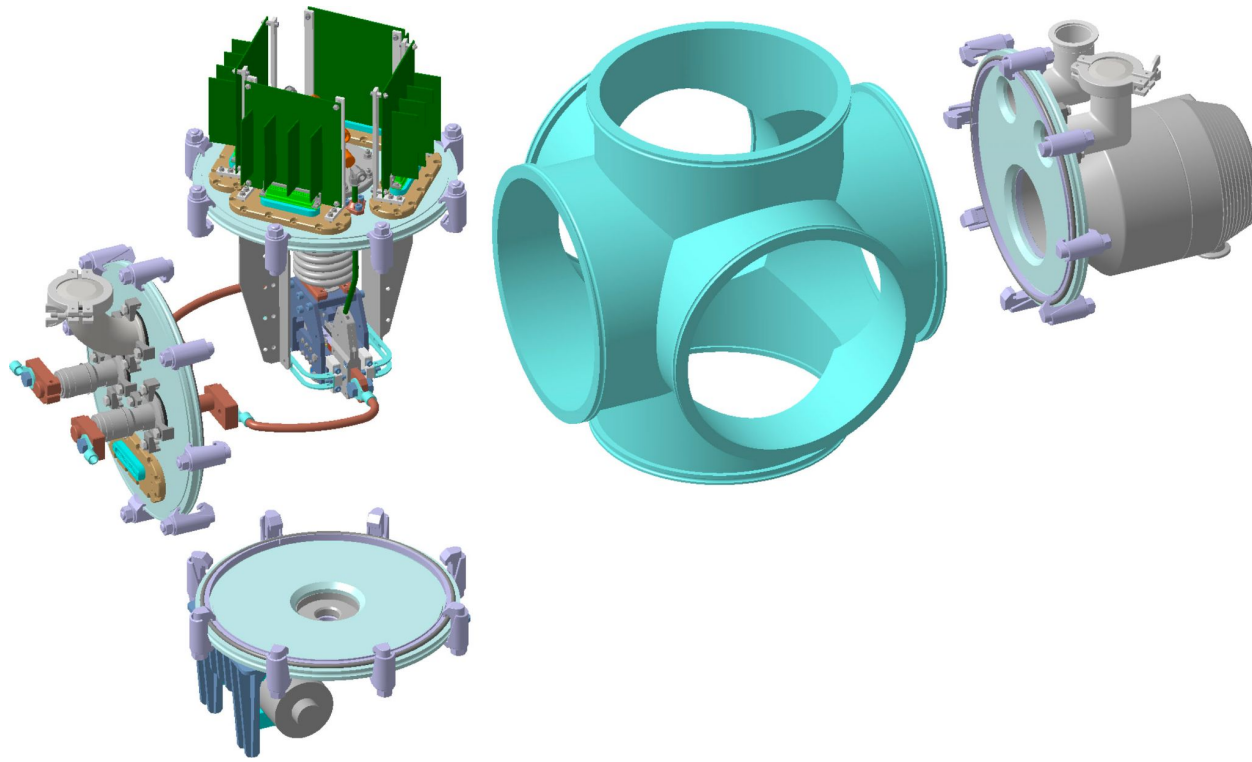


DRILL CHART				
SYM	DIAM	TOL	QTY	NOTE
*	0.020		35	
x	0.028		3	
+	0.031		39	
o	0.037		2	
o	0.050		5	
#	0.054		6	
%	0.067		20	
^	0.135		4	
o	0.170		3	
TOTAL			137	



# VIP-3 activity 2023-now

- - realization of the new vacuum chamber - **READY**



**(milestone fulfilled)**



# ***The VIP experiments - collapse theories***

**J. Oppenheim:**

**"Quantum theory and Einstein's theory of general relativity are mathematically incompatible with each other, so it's important to understand how this contradiction is resolved. Should spacetime be quantized, or should we modify quantum theory, or is it something else entirely?"**

**A Postquantum Theory of Classical Gravity?**

**Phys. Rev. X 13, 041040 – Published 4 December 2023**

# ***Postquantum theory of classical gravity***

- **Consistent theory of classical gravity coupled to quantum field theory.**
- **The dynamics is linear in the density matrix, completely positive, and trace preserving, and reduces to Einstein's theory of general relativity in the classical limit.**
- **The assumption that general relativity is classical modifies the dynamical laws of quantum mechanics; the theory must be fundamentally stochastic in both the metric degrees of freedom and in the quantum matter fields.**
- **The measurement postulate of quantum mechanics is not needed; the interaction of the quantum degrees of freedom with classical space-time necessarily causes decoherence in the quantum system.**



# ***Paper published in Measurement Science and Technology***

*Meas. Sci. Technol. 35 (2024) 025501*

## **Novel Machine Learning and Differentiable Programming Techniques applied to the VIP-2 Underground Experiment**

**Abstract.** In this work, we present novel Machine Learning and Differentiable Programming enhanced calibration techniques used to improve the energy resolution of the Silicon Drift Detectors (SDDs) of the VIP-2 underground experiment at the Gran Sasso National Laboratory (LNGS). We achieve for the first time a Full Width at Half Maximum (FWHM) in VIP-2 below 180 eV at 8 keV, improving around 10 eV on the previous state-of-the-art. SDDs energy resolution is a key parameter in the VIP-2 experiment, which is dedicated to searches for physics beyond the standard quantum theory, targeting Pauli Exclusion Principle (PEP) violating atomic transitions. Additionally, we show that this method can correct for potential miscalibrations, requiring less fine-tuning with respect to standard methods.



# Refined current modulation run analysis

Modulated current test run (68 days) the wc-woc alternation is automatized with a fixed period of 100 s: 50 s of wc phase, 50 s of woc.

## Spectral analysis:

$$p(\theta | \mathcal{D}^{woc}, \mathcal{D}^{wc}) = \frac{\mathcal{L}(\mathcal{D}^{woc}, \mathcal{D}^{wc} | \theta) \cdot p(\theta)}{\int d\theta \mathcal{L}(\mathcal{D}^{woc}, \mathcal{D}^{wc} | \theta) \cdot p(\theta)}$$

$$\mathcal{L}(\mathcal{D}^{woc}, \mathcal{D}^{wc} | \theta) = \mathcal{L}^{woc}(\mathcal{D}^{woc}, \mathcal{F}^{woc}(\theta | E)) \cdot \mathcal{L}^{wc}(\mathcal{D}^{wc}, \mathcal{F}^{wc}(\theta | E))$$

$$\begin{aligned} \mathcal{L}^{woc}(\mathcal{D}^{woc}, \mathcal{F}^{woc}) &= \\ &= \prod_i \mathcal{P}(\mathcal{D}_i^{woc} | \mathcal{F}^{woc}(E_i | \theta)) \end{aligned}$$

$$\begin{aligned} \mathcal{F}^{woc}(E_i | \theta) &= \\ &= a \cdot (E_i - E_{PEPV}^{Cu}) + b + \\ &+ \{A^{Ni} \cdot \mathcal{N}(E_i - E_{K\alpha}^{Ni}, \sigma^{Ni}) + \\ &+ A^{Cu} \cdot [\mathcal{N}(E_i - E_{K\alpha 1}^{Cu}, \sigma^{Cu}) + \\ &+ 0.51 \cdot \mathcal{N}(E_i - E_{K\alpha 1}^{Cu} + 19.95, \sigma^{Cu})]\} w_{bin} \end{aligned}$$

$$\begin{aligned} \mathcal{L}^{wc}(\mathcal{D}^{wc}, \mathcal{F}^{wc}) &= \\ &= \prod_i \mathcal{P}(\mathcal{D}_i^{wc} | \mathcal{F}^{wc}(E_i | \theta)) \end{aligned}$$

$$\begin{aligned} \mathcal{F}^{wc}(E_i | \theta) &= \\ &= a \cdot (E_i - E_{PEPV}^{Cu}) + b + \\ &+ \{A^{Ni} \cdot \mathcal{N}(E_i - E_{K\alpha}^{Ni}, \sigma^{Ni}) + \\ &+ A^{Cu} \cdot [\mathcal{N}(E_i - E_{K\alpha 1}^{Cu}, \sigma^{Cu}) + \\ &+ 0.51 \cdot \mathcal{N}(E_i - E_{K\alpha 1}^{Cu} + 19.95, \sigma^{Cu})] + S \cdot \mathcal{N}(E_i - E_{PEPV}^{Cu}, \sigma^{Cu})\} w_{bin} \end{aligned}$$

The priors  $p(\theta)$  are defined in order to consider the parameters of the two models independent. Systematic uncertainties in the calibration are considered as prior normal distributions of the lines centroids ( $\sigma = 2\text{eV}$ ). Systematic uncertainties in the detector resolution are considered in the priors. The systematic uncertainty on the data timestamp is considered as a scaling factor (normally distributed prior with  $\sigma = 1\text{s}$ ).

# Refined current modulation run analysis

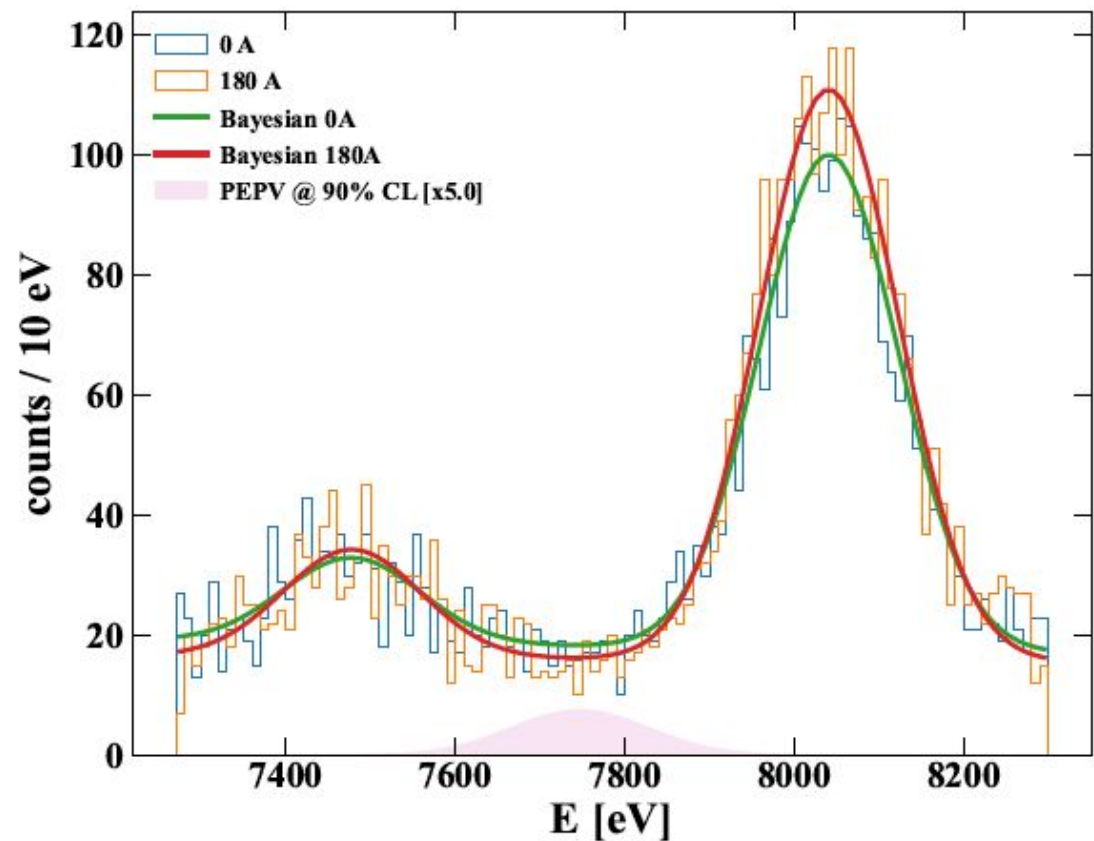


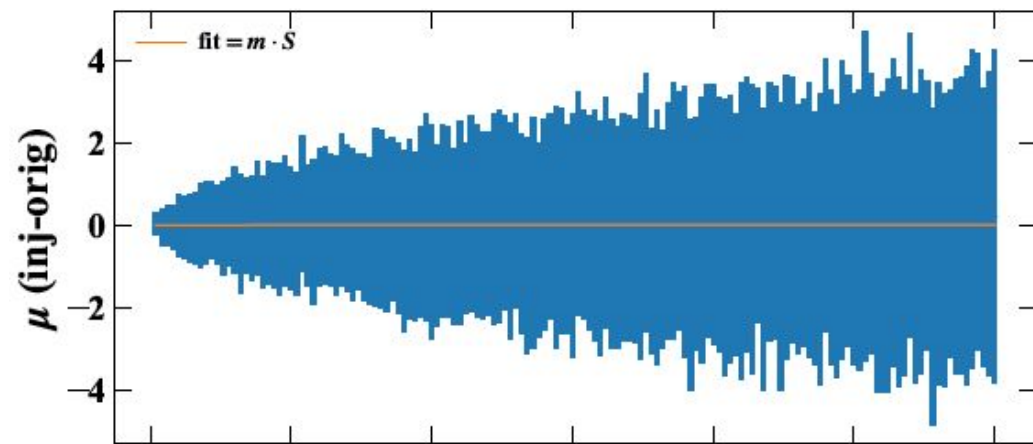
Fig. 3 Energy spectra of the VIP-2 calibrated data without (blue) and with (orange) the current. Their Bayesian optimizations are shown (green and red, respectively); the signal component distribution inside the upper limit at 90% of C.L. is shown in pink, magnified by a factor of 100.

$$\left. \frac{\beta^2}{2} \right|_{\text{spec}} < 1.25 \cdot 10^{-30} \quad (\text{scattering})$$
$$\left. \frac{\beta^2}{2} \right|_{\text{spec}} < 9.94 \cdot 10^{-43} \quad (\text{close encounters})$$

## Simultaneous DFT analysis with FFT algorithm:

- same energy range of the spectral analysis: from 7270 to 8300 eV,
- we identify a Region of Interest (ROI) as a 150 eV neighborhood (left and right) of the PEPV energy. Exceeding events might belong to about 95% of the PEPV distribution (signal-enriched region).
- The remaining signal-depleted part is the Background.
- $D = B + S$ , where B has an unknown behavior. We characterize D empirically as a function of hypothetical S, to understand the DFT central harmonic dependencies from the signal presence. We assume a Normal distribution with a mean  $\mu$  and a variance Var to describe fluctuations.
- 100 synthetic data sets are generated for each signal hypothesis and compared with the original data set (synthetic – original).

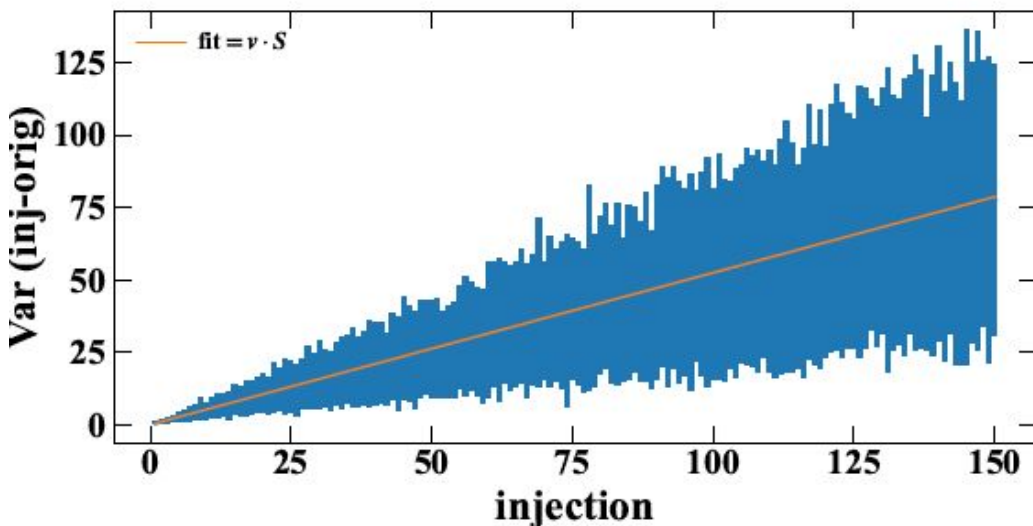
# Update on the current modulation run analysis



- A linear fit is performed (orange lines), with the slope as a free parameter (the intercept fixed to 0, no variation of the original case from itself).
- $\mu$  turns to be independent from the signal, Var highlights a linear dependence from possible signals.
- a data-driven model for Var is built as function of  $S$ :

$$\text{Var} = V_0 + v \cdot S$$

- $V_0$  unknown baseline variance.



- Based on this pre-analysis new likelihood factors are built for the amplitudes of the data DFT harmonics:

$$\begin{aligned} \mathcal{L}(\mathcal{A}, \mu, \text{Var}) &= \\ &= \prod_{i=1}^N \mathcal{N}(\mathcal{A}_i | \mu_i, \text{Var} = V_0 + v \cdot f(\sigma^{\text{Cu}})S) \end{aligned}$$

and a new Bayesian analysis is performed based on a global likelihood:

$$\begin{aligned} \mathcal{L}(\mathcal{D}^{\text{woc}}, \mathcal{D}^{\text{wc}}, \mathcal{A}^{\text{ROI}}, \mathcal{A}^{\text{BKG}} | \theta) &= \\ &= \mathcal{L}^{\text{woc}}(\mathcal{D}^{\text{woc}} | \theta) \cdot \mathcal{L}^{\text{wc}}(\mathcal{D}^{\text{wc}} | \theta) \cdot \\ &\quad \cdot \mathcal{L}^{\text{ROI}}(\mathcal{A}^{\text{ROI}} | \theta) \cdot \mathcal{L}^{\text{BKG}}(\mathcal{A}^{\text{BKG}} | \theta) \end{aligned}$$

# ***Refined current modulation run analysis***

**We build a synthetic data set from the data  $D$  by subtracting random events from the wc bins as a signal  $S$  hypothesis. The resulting central harmonics are the DFT of a possible  $B$ . The mean and variance of the differences from the original data set will show their behavior as a function of  $S$  without any assumption on  $D$  and  $B$ .**

**quindi qui ottengo per ogni ipotesi di segnale i conteggi in funzione della frequenza del corrispondente bkg. Poi studio la media e la varianza delle armoniche centrali in funzione dell'ipotesi di  $S$**



# VIP-3 activity 2023-now

- Production of the new SDDs 1mm by FBK (Trento) finalized, sent to PoliMi in July 2023 for testing:

## Recap of the Production Timeline

FC  
BF

Aug 2021 –  
Jan 2023

### SDD production process

The production of the batch has been suspended twice because of two periods during which FBK laboratories were not operational:

- Nov 2021 – Mar 2022: installation of a new clean room in FBK
- Jul 2022 – September 2022: major maintenance of FBK clean room

Feb 2023 –  
May 2023

### Test of SDD batch using automatic probers

- All SDD arrays and most of test structures tested @RT using dedicated probecards
- SDD arrays also tested at low temperature (-30° C)
- Report of the results presented

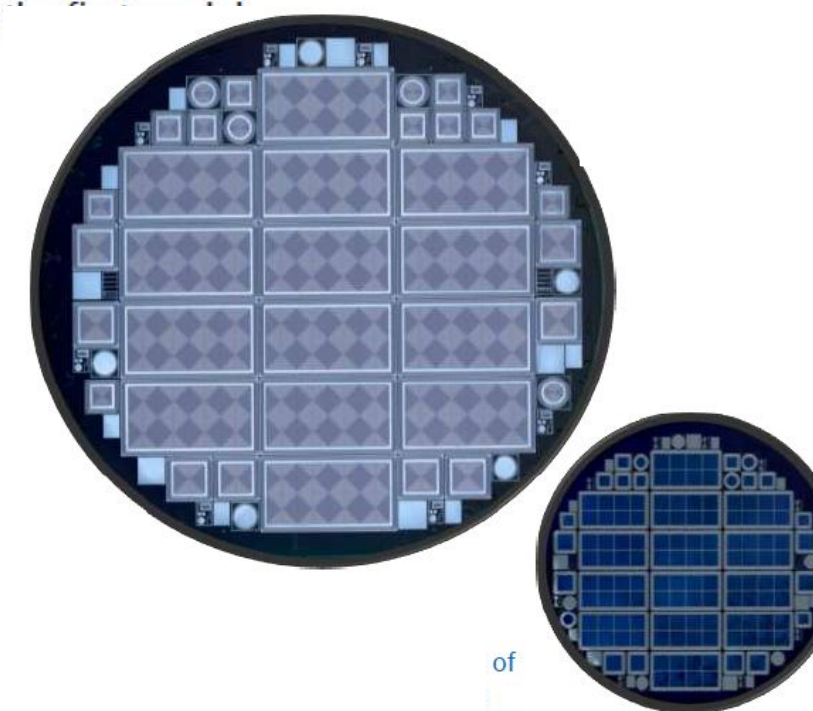
May 2023 –  
Jun 2023

### Test of SDD batch using automatic probers

- Two 1-mm-thick wafers and one 450-um-thick wafer selected and diced to prepare prototypes

Jul 2023

### Delivery of first SDD samples to PoliMi



of  
1...

## VIP-3 activity 2023-now

New SDDs 1mm thick, further improvements:

- pixel dimensions of 7.9 mm x 7.9 mm, geometry of the SDD arrays 2x4 matrix, total chip dimensions are 35.6 mm x 19.8 mm i.e. ~ 2 mm wider than the previous chips,
- width of the last ring extended in order to improve collection at the border of the active area.
- introduction of a layout solution on the window-side, to reduce the charge sharing effect,
- the robustness of the bonding pads was enhanced,
- planned configuration: 8 SDD arrays, facing two target strips (w.r to the 4 SDD arrays in VIP-2) total - 64 SDD cells = double active area ~ 41 cm<sup>2</sup> -> increased geometrical efficiency.

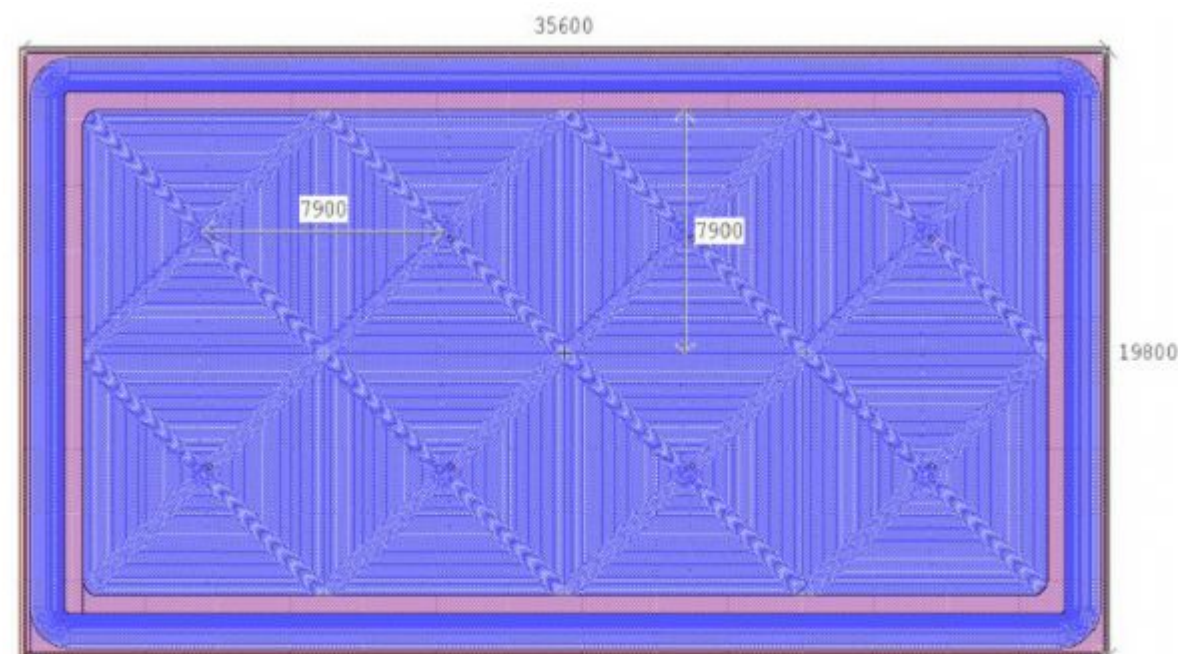
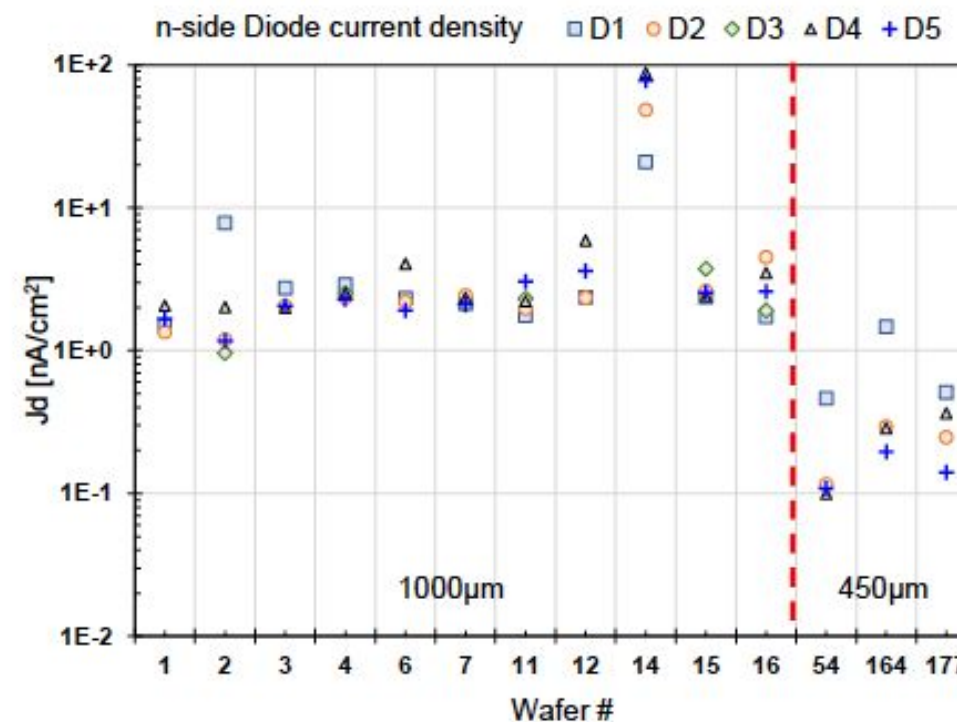
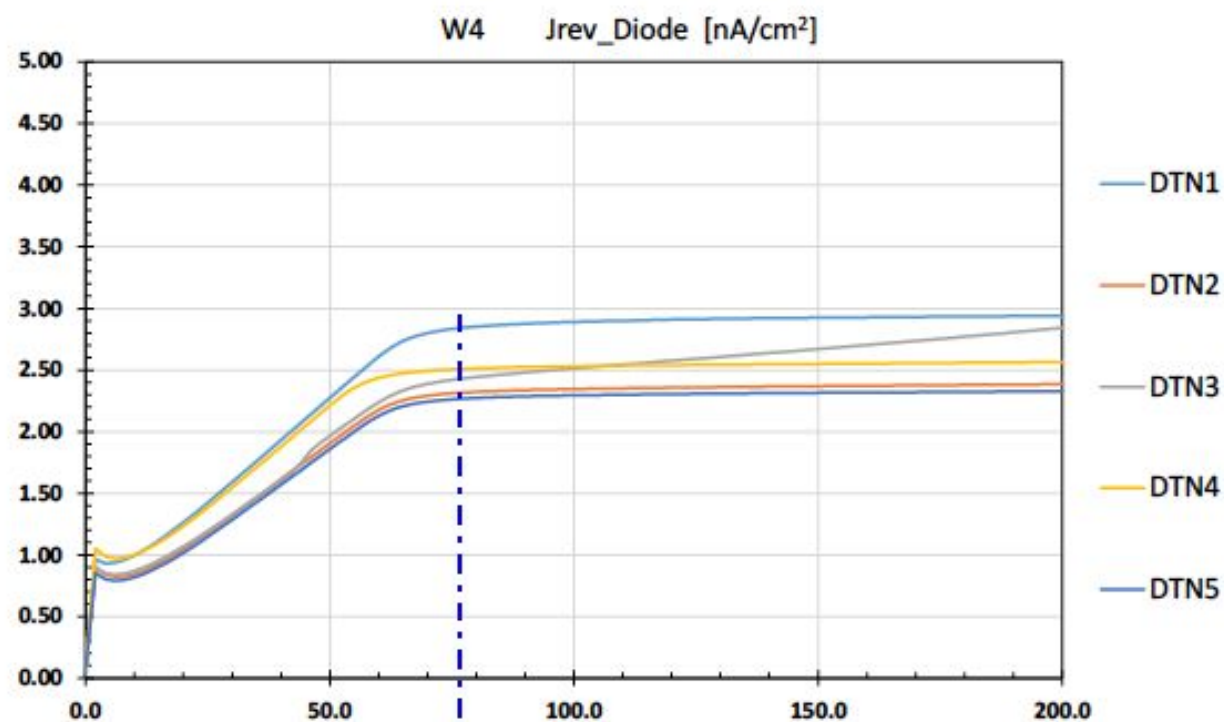


**Fig. 5** The figure shows the layout of the main SDD array, which is being produced for the VIP-3 experiment from the anode side.

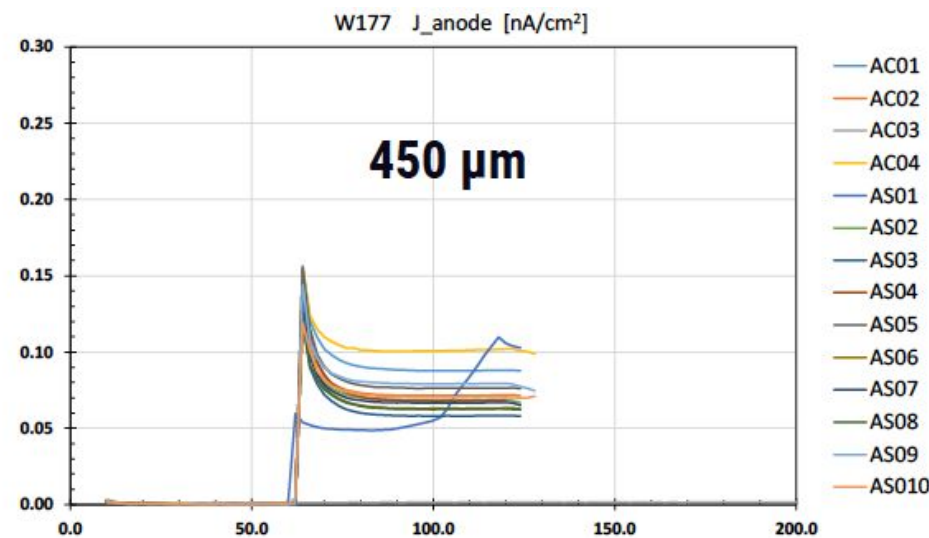
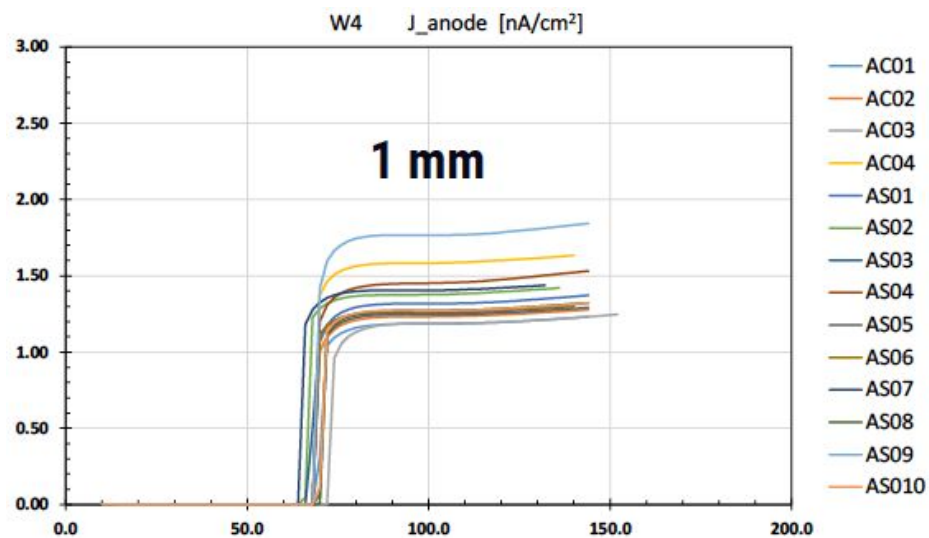
# VIP-3 activity 2023-now

## successful tests:



Estimated depletion voltage for all wafers ~70V

Very good results in terms of Leakage Current Density @ 24°C, 100V (except for W14)



- Bias conditions:  $V_{\text{anode}}=0V // V_{\text{Ring1}}=-10V // V_{\text{Bulk}}=0V // V_{\text{LastRing}}=-10V \rightarrow 2 \times V_{\text{depl}} (\sim -140V)$
- Current measurement at all terminals
- Estimated depletion voltage for all wafers ~65÷75V

## *VIP-3 activity 2023-now*

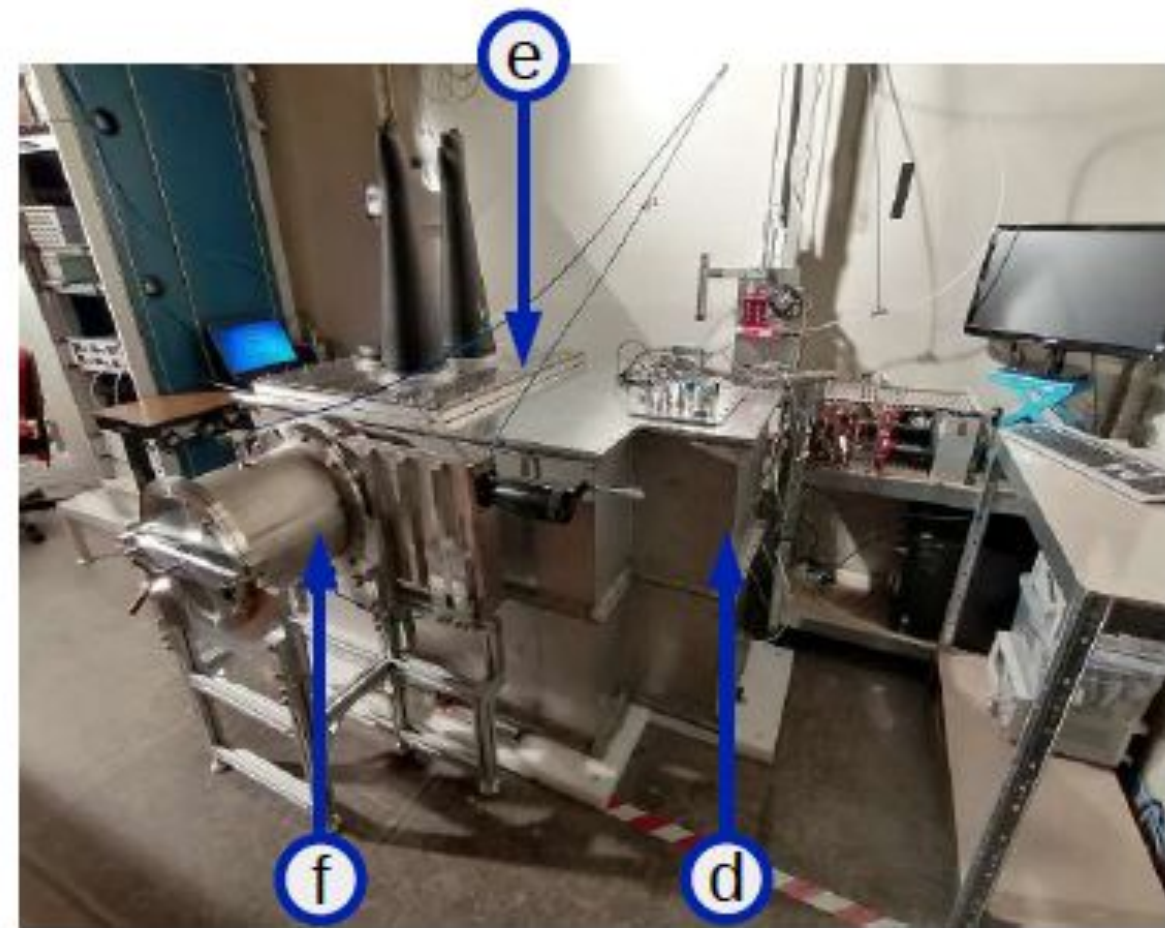
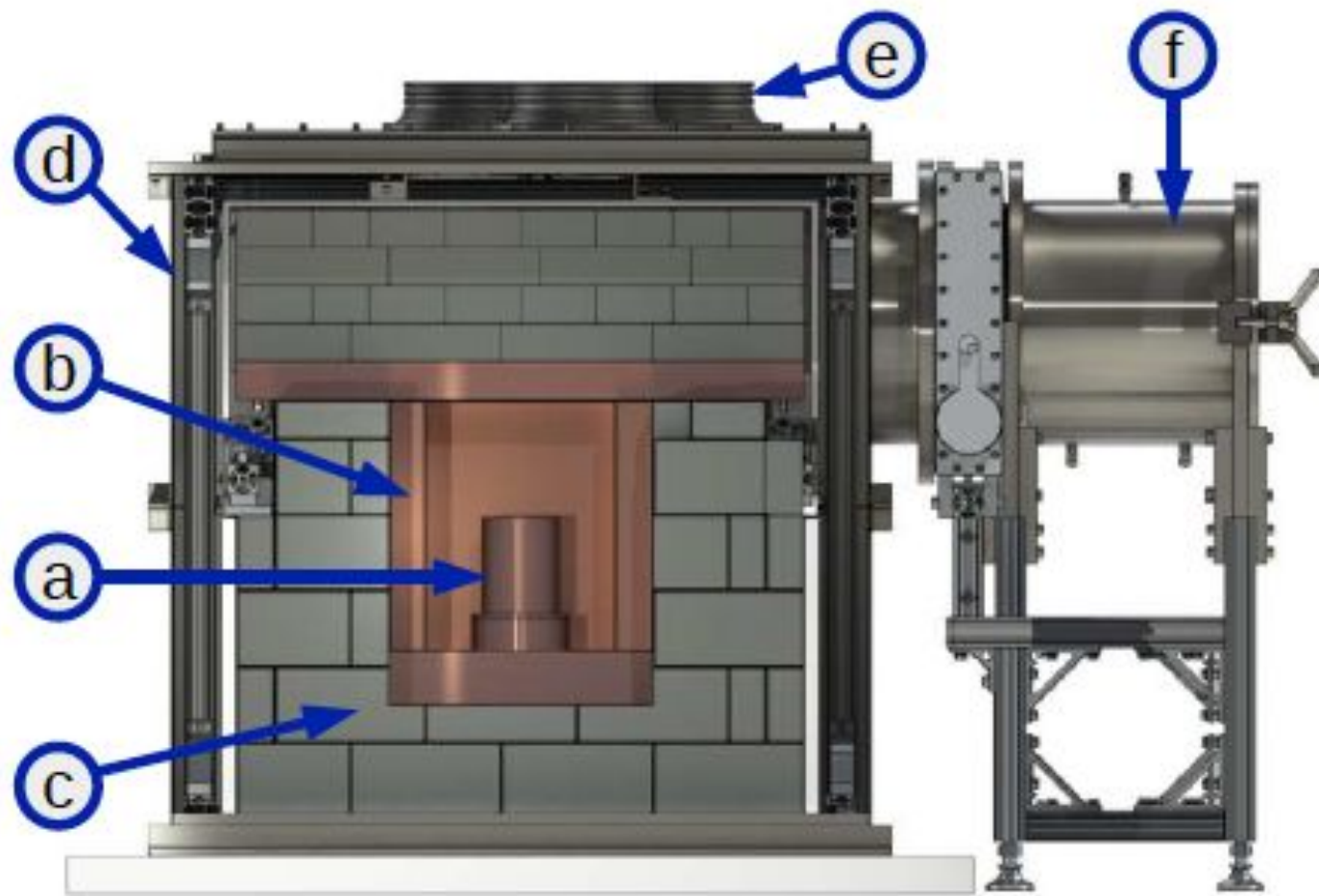
**NEW SDDS VALIDATION AND FINAL GEOMETRY** undergoing at POLITECNICO DI MILANO:

- **realization of the new thermal contact between the cold-finger and SDDs detectors**  
- under design
- **realization of the new target cooling system made in pure copper** - under design



# ***GATOR detector cooling & shielding***

## The Gator Detector

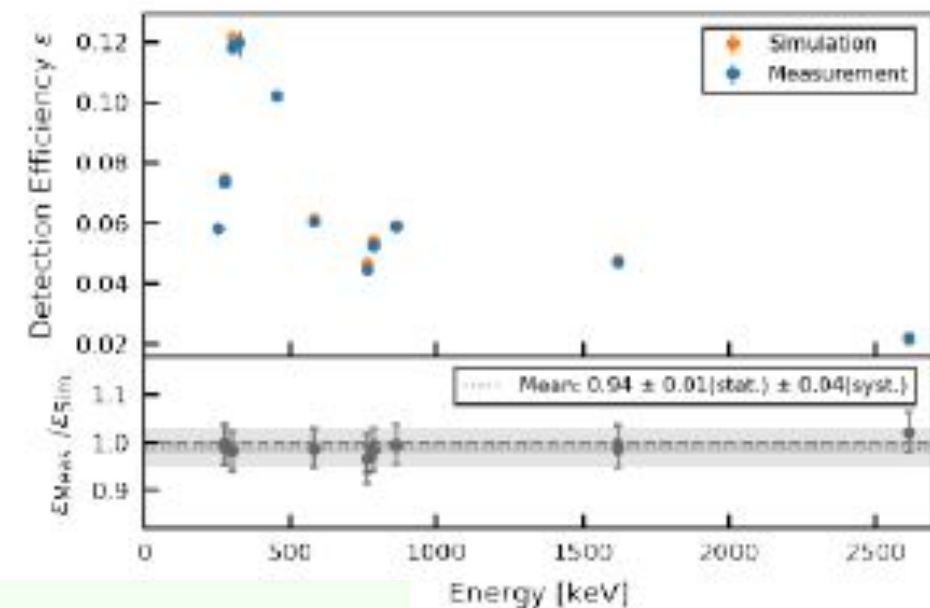
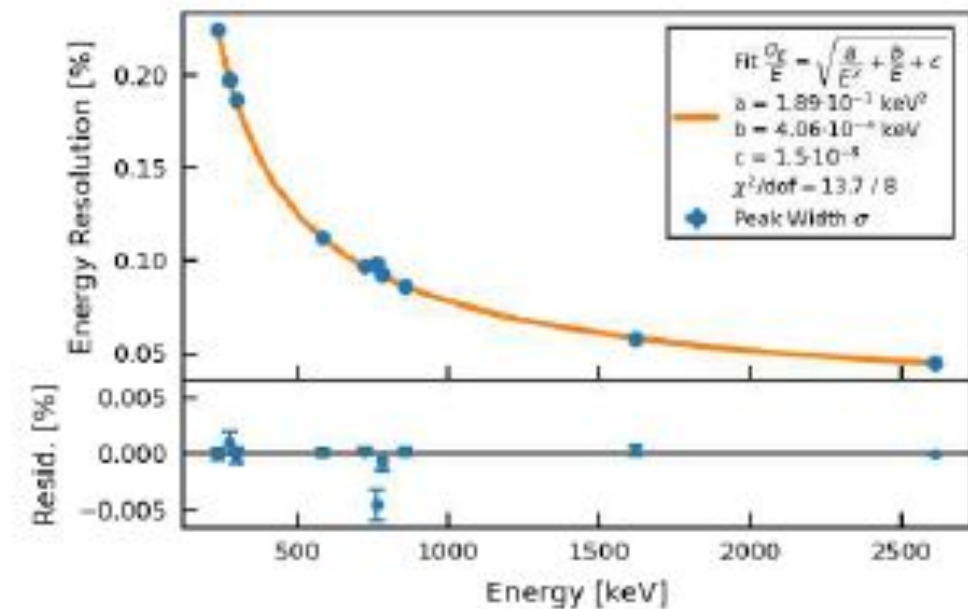


**(a)** HPGe detector inside Cu-OFE cryostat (cooled with LN<sub>2</sub> via copper coldfinger), **(b)** OFHC Cu cavity, **(c)** lead shield, polyethylene sheet, **(d)** airtight stainless steel enclosure (purged with GN<sub>2</sub>), **(e)** glove ports, **(f)** sample load lock

# GATOR detector - resolution

## Energy Range and Resolution

- Covered MCA energy range: approx. 10 – 2700 keV
- Analysis range: approx. 35 – 2700 keV (noise-dominated for  $E \lesssim 35$  keV)
- Regular calibrations of the detector with radioactive sources (e.g.  $^{228}\text{Th}$ ) or high-activity samples
  - FWHM at 74.96 keV (1s–2p<sub>3/2</sub> K $\alpha$ 1 transition in Pb): ~ 1.1 keV
  - Verification of simulated efficiencies and consistent activities related lines



energy shift among standard and PEPV K $\alpha$ 1 transitions is 1.25 keV

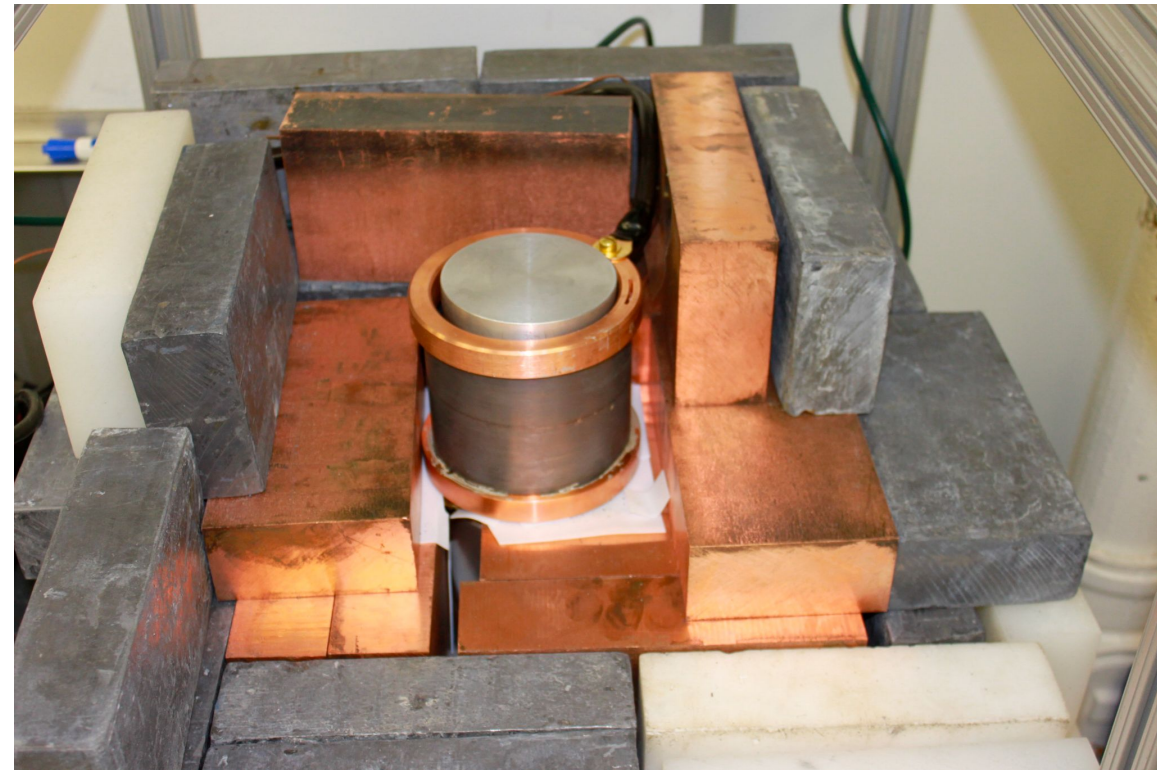
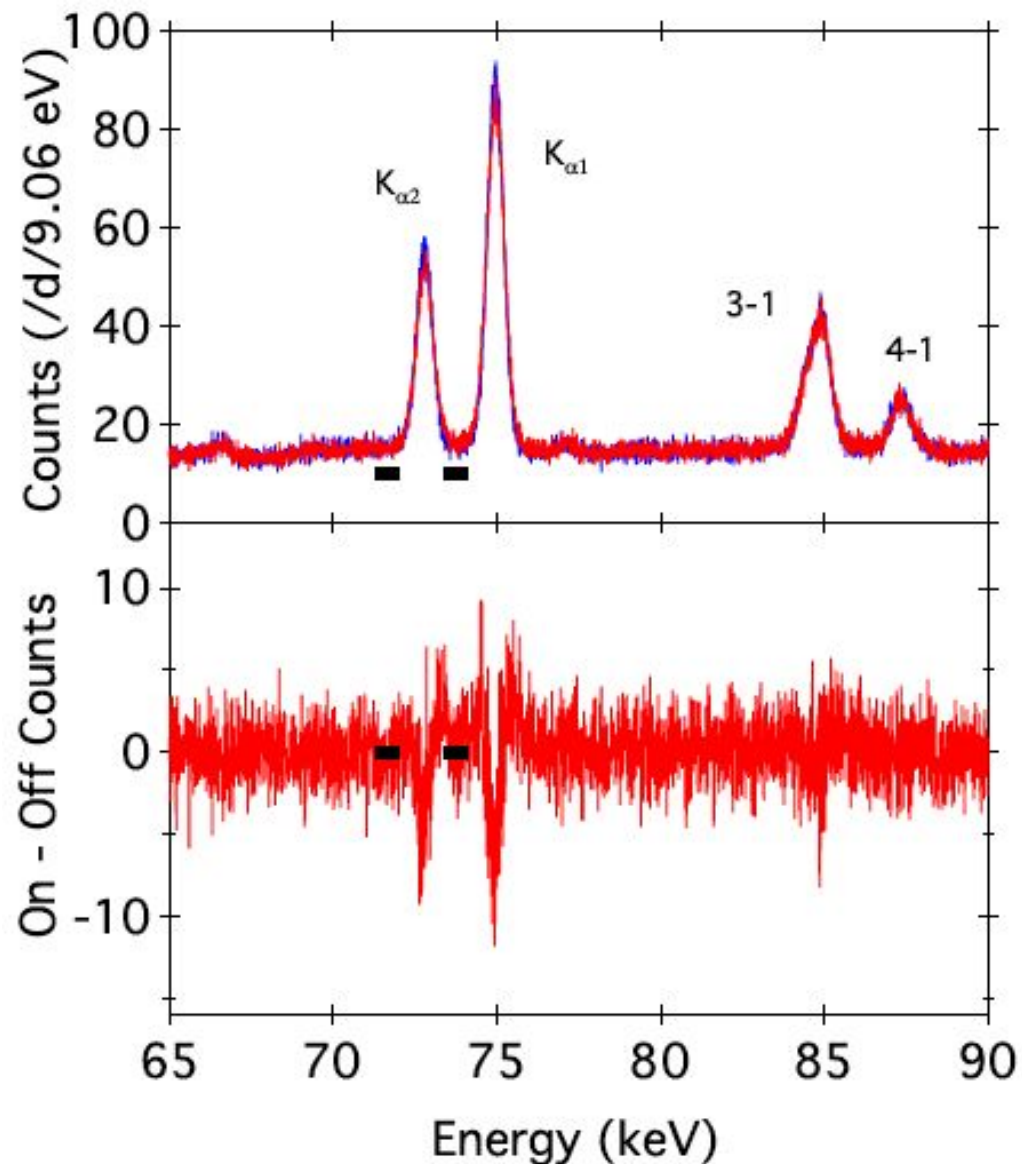


# Previous exploratory measurement

## Found.Phys. 42 (2012) 1015-1030

Exploratory measurement performed above ground:

- point-contact Ge detector
- Pb target
- 110 A circulating current



obtained limit:

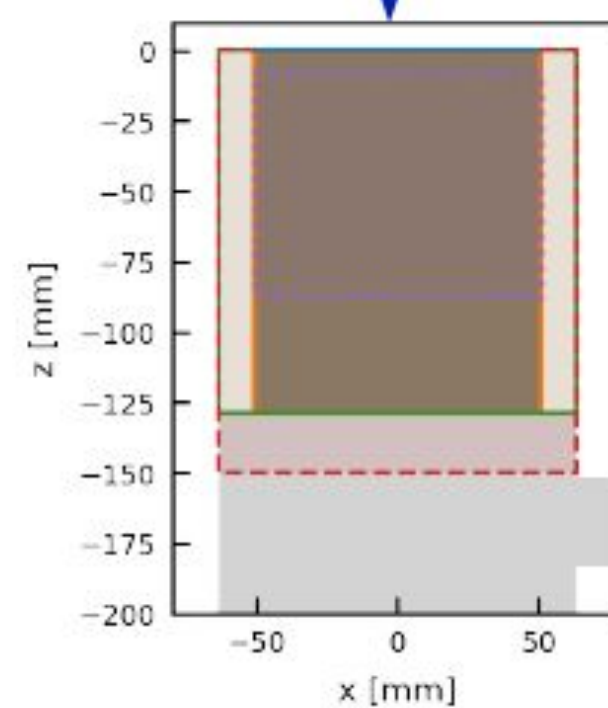
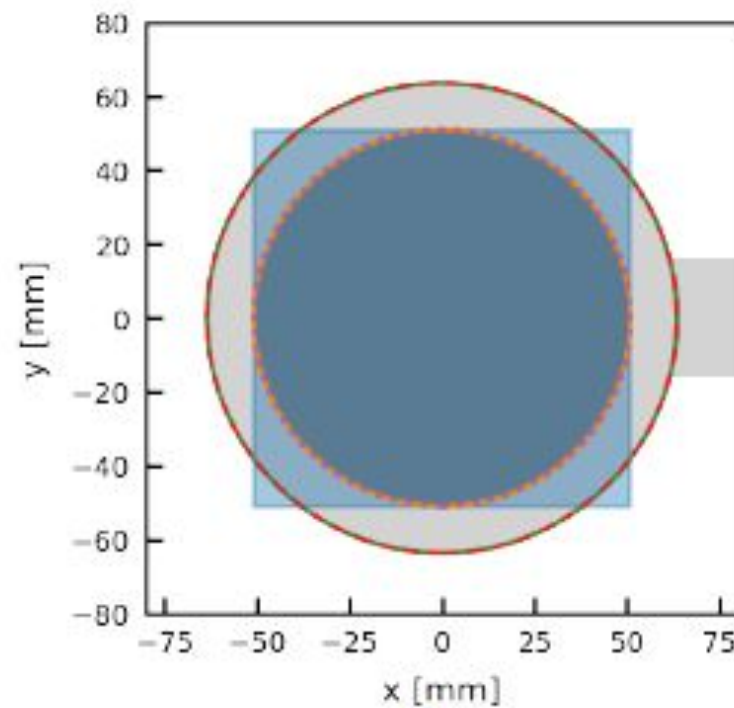
$$\beta^2/2 < 1.5 \cdot 10^{-27}$$

Goal of the

VIP - GATOR dedicated measurement  
about 2 o.m. improvement

# MC simulations for the optimization of the target geometry

## Investigated Geometries Pb Conductor



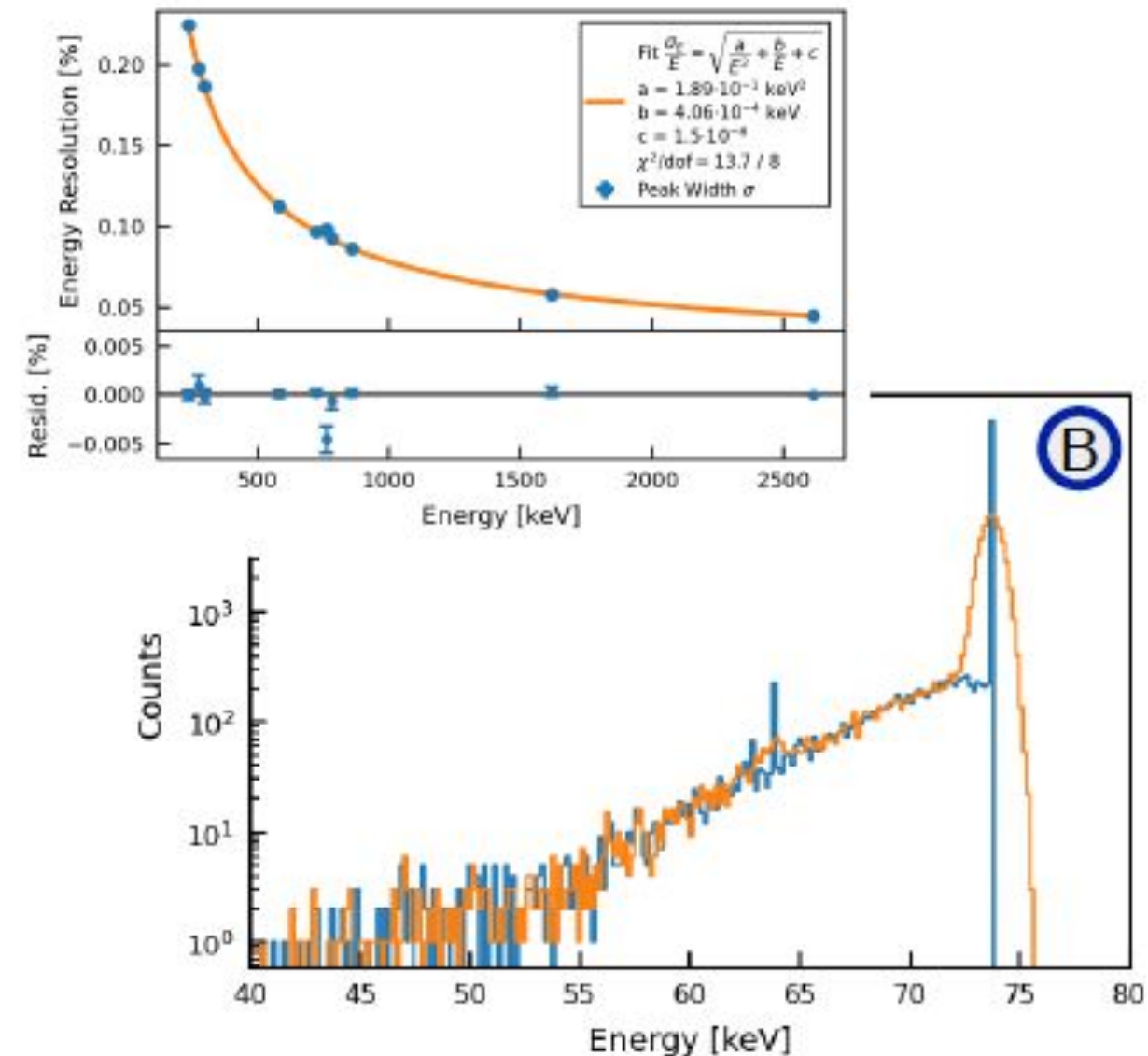
- Cu Cryostat Endcap:  
 $D_{\text{outer}} = 101.6 \text{ mm}$   
 $\Delta z = 129.05 \text{ mm}$
- Cu Cryostat Base  
 (+ Coldfinger):  
 $D_{\text{outer}} = 127.0 \text{ mm}$
- Hollow Cylinder:  
 $D_{\text{inner}} = 101.8 \text{ mm}$   
 $\Delta z = 129.05 \text{ mm}$
- Hollow Cylinder:  
 $D_{\text{inner}} = 127.2 \text{ mm}$   
 $\Delta z = 129.05 \text{ mm}$
- Hollow Cylinder:  
 $D_{\text{inner}} = 127.2 \text{ mm}$   
 $\Delta z = 150.0 \text{ mm}$
- Hollow Cylinder:  
 $D_{\text{inner}} = 127.2 \text{ mm}$   
 $\Delta z = 79.8 \text{ mm}$   
 (Sensitive Vol. Sim.)
- Plate:  
 $\Delta x = \Delta y = 101.6 \text{ mm}$



# Detection efficiency simulations for various geometries

## Geant4 Simulations

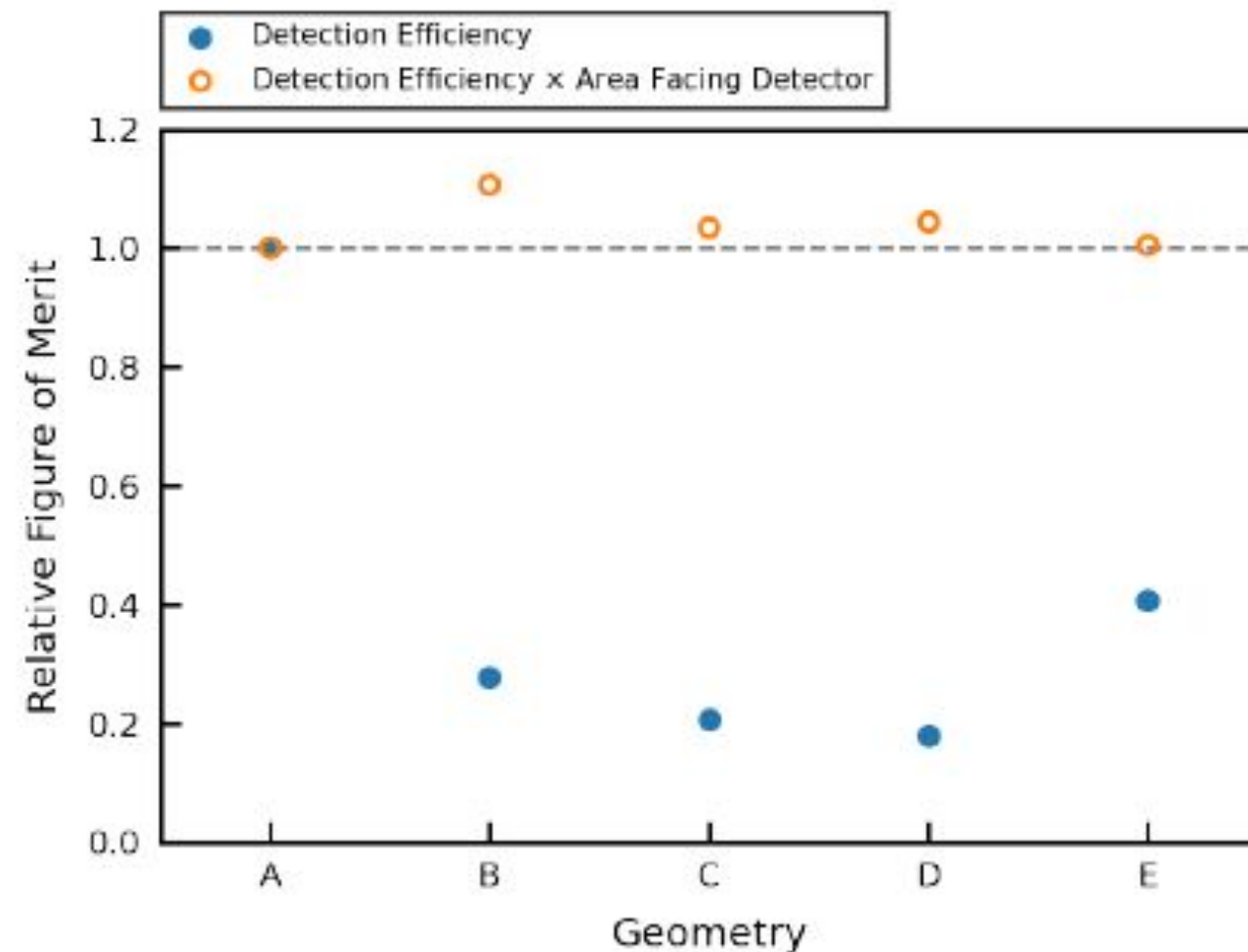
- Geant4 simulations with framework for sample efficiency simulations\*
- Number of simulated gammas:  $10^7 - 10^8$  (depending on thickness)
- Gamma energy: 73.713 keV (energy of PEP violating Pb  $K_{\alpha 1}$ )
- Reduced length (0.1  $\mu\text{m}$ ) and energy (250 eV) cuts in *PhysicsList*
- Energy-resolution smearing, binning according to Gator MCA



# Detection efficiency simulations for various geometries

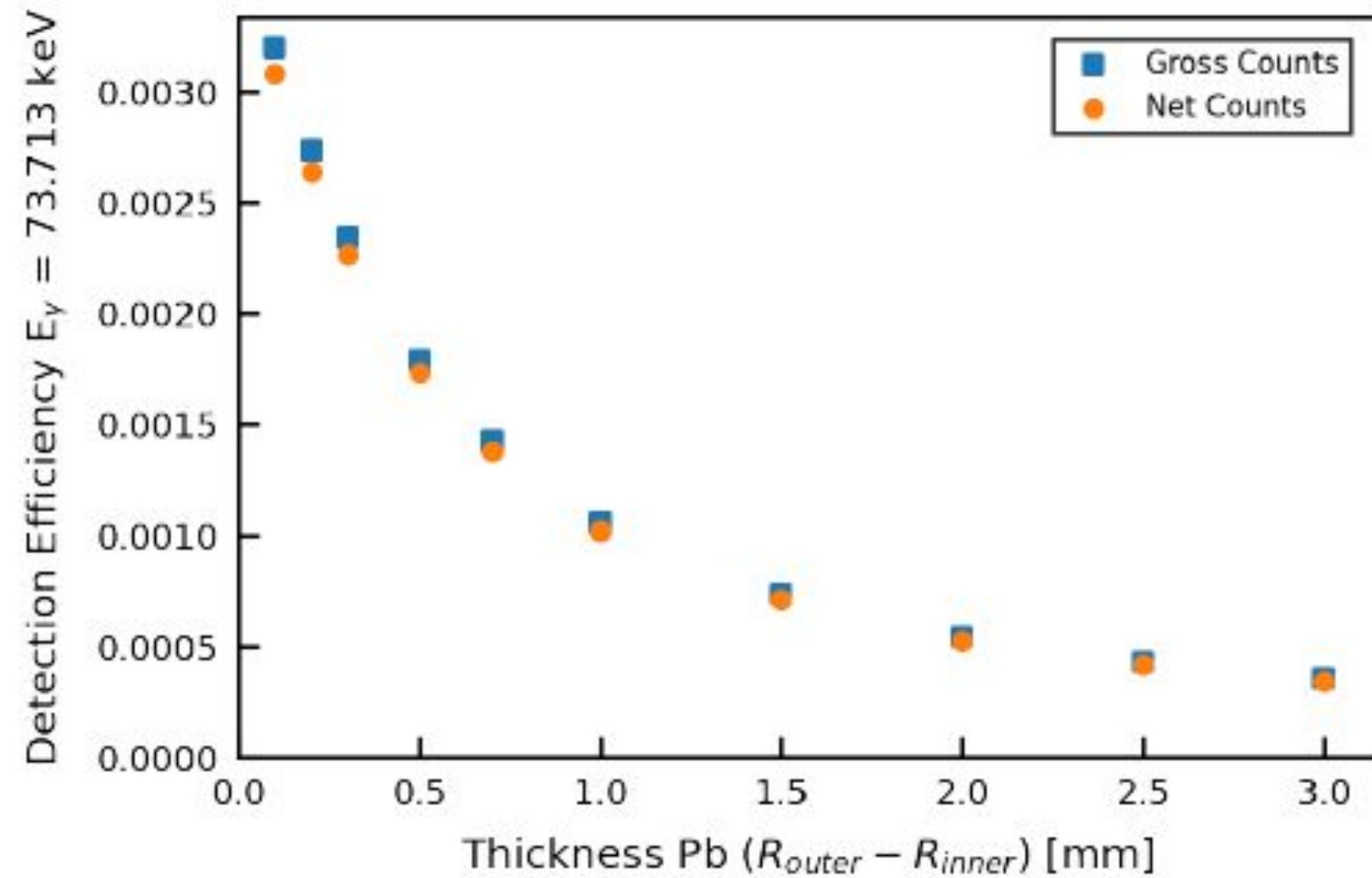
## Figure of Merit for Geometry

- For same current density  $j$ , the integral charge  $q$  and hence the number of eventual X-rays scales with the volume
  - Scale efficiencies for given thickness (here 25  $\mu\text{m}$ ) with conductor area facing the detector for figure or merit
- Maximum deviation FOM  $\sim 10\%$ 
  - Select most convenient geometry\*
- Other impacts from geometry, e.g. induced B-field, resistance ( $R \sim L/A$ ), and power dissipation resulting in heat-up, weight / required holder,... need to be considered as well



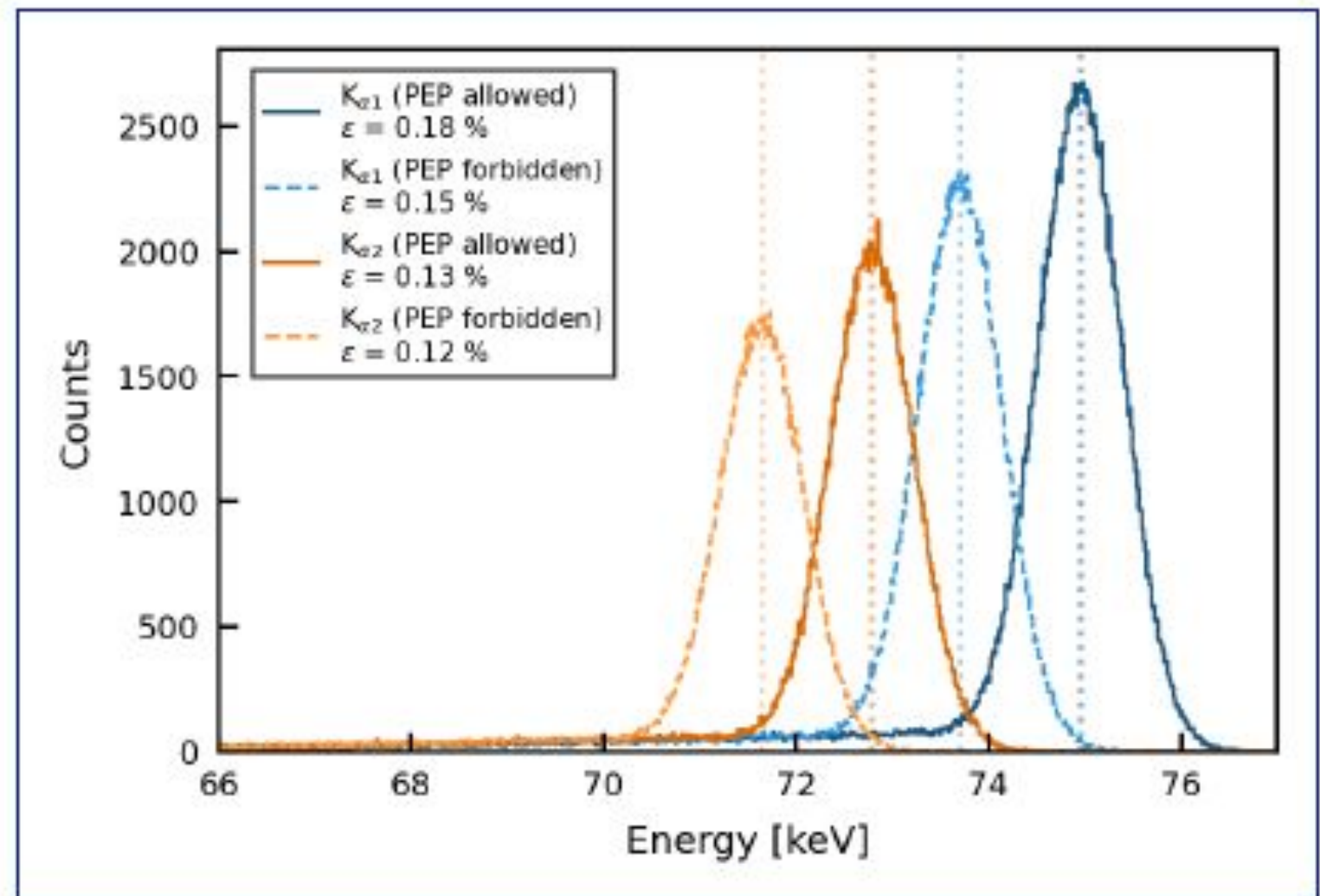
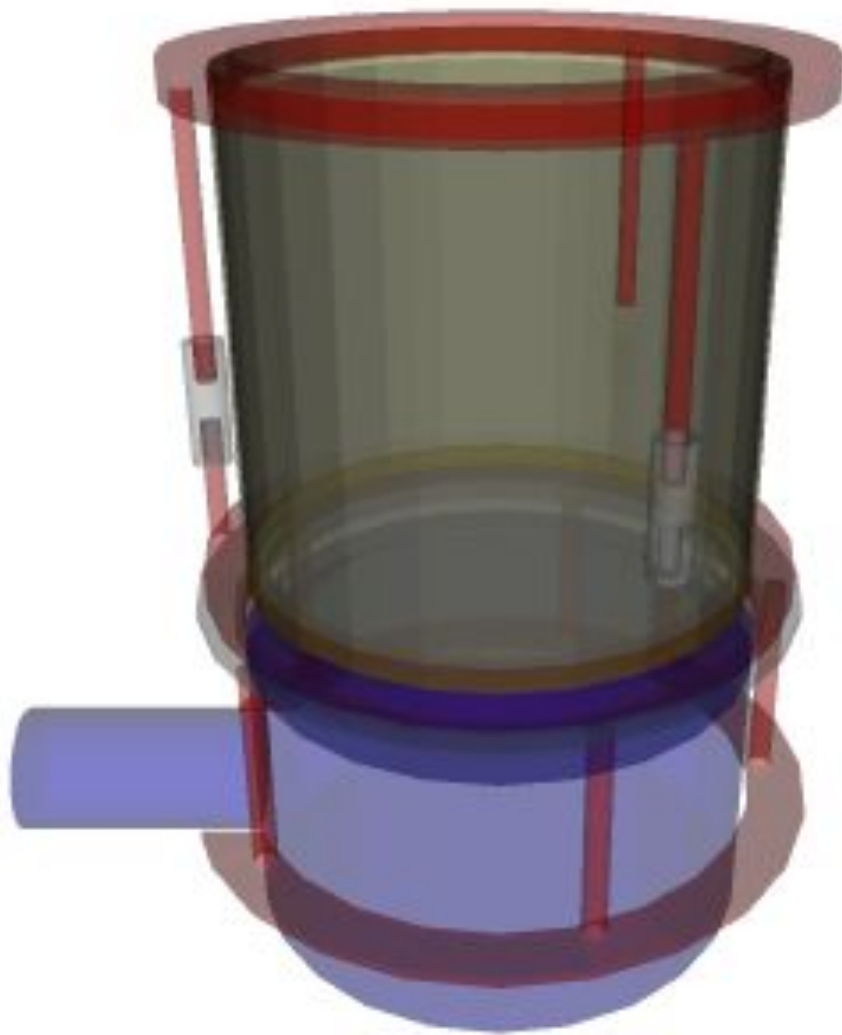
# Detection efficiency simulation

Impact Thickness (Cylindrical Geometry D)



# Detection efficiency simulation

## Detection Efficiency Simulations Full Setup



# simulations of power dissipation

- Challenge: Power dissipation from current will result in heat-up

- Assuming homogeneous conductivity:

$$P = R \cdot I^2 = \frac{\rho \cdot l}{A} \cdot I^2$$

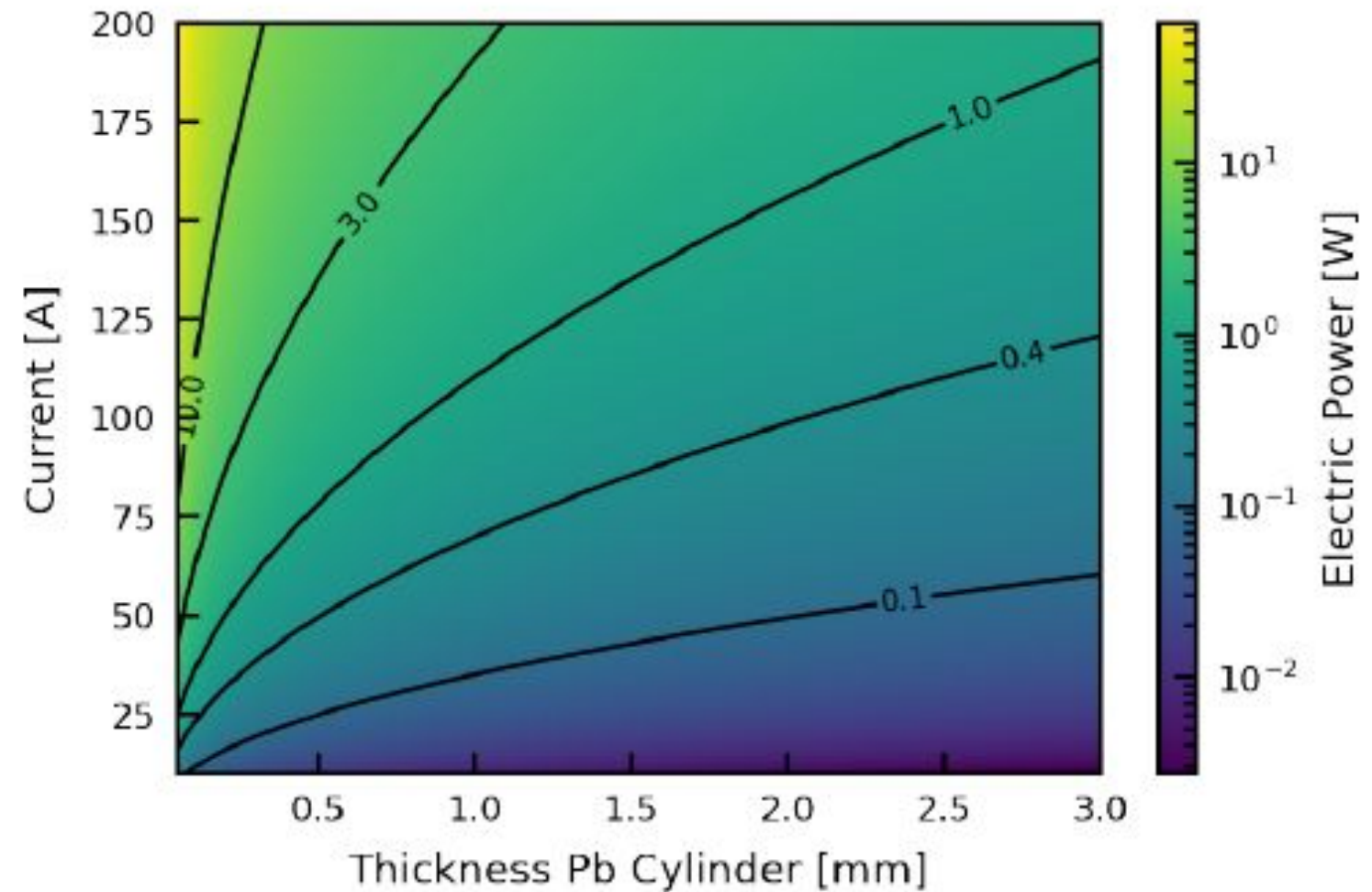
$$\rho_{Pb}(T = 20^\circ C) = 2.2 \cdot 10^{-7} \Omega m^*$$

- For cylindrical geometry D:

$$l = 0.15 m$$

$$A \approx 2 \pi \cdot r_{inner} \cdot d \\ \approx 0.4 m \cdot d$$

for current along cylinder axis,  
results in previous meeting for  
assumption of circular current



with  $I = 400 A$ , 4 months data taking **expected improvement**

w.r. to *Found.Phys.* 42 (2012) 1015-1030

on  $\beta^2/2$  of a **factor about  $10^2$**

**target cooling system “VIP-like” (chiller) needed to counteract heating.**



## ***VIP-2 Closed Systems - new paper published***

- For a generic NCQG model deviations from the PEP in the commutation/anti-commutation relations can be parametrized as:

$$a_i a_j^\dagger - q(E) a_j^\dagger a_i = \delta_{ij}$$

-  $E$  = energy level difference, i.e. the PEP violating X-ray line energy.  $q$  is related to the PEP violation probability by:

$$q(E) = -1 + 2\delta^2(E)$$

- phenomenological method [Chin.Phys. C42 (2018) no.9, 094001] includes, through an analytic expansion, the infrared limit for several different UV-complete quantum field theories:

$$M_k : \quad \delta^2(E) = \frac{E^k}{\Lambda^k} + O(E^{k+1})$$

## VIP-2 Closed Systems - new analysis finalized

- constraints on the PEP violation prob. traduce into constraints on  $\Lambda$  specific for each  $M_k$  parametrization.

-  $k = 1$  corresponds to  $k$ -Poincaré. Different quantization procedures lead to different predictions:

- Arzano-Marcianò procedure - PEP violation is suppressed with a probability proportional to  $\delta^2 = E / \Lambda$
- Freidel-Kowalski-Glikman-Nowak procedure - PEP violation is missing.

So experimental investigation of statistics violations provides important down-top indications on the “right” quantization procedure: **the AM  $k$ -Poincaré field’s quantization model is ruled out.**

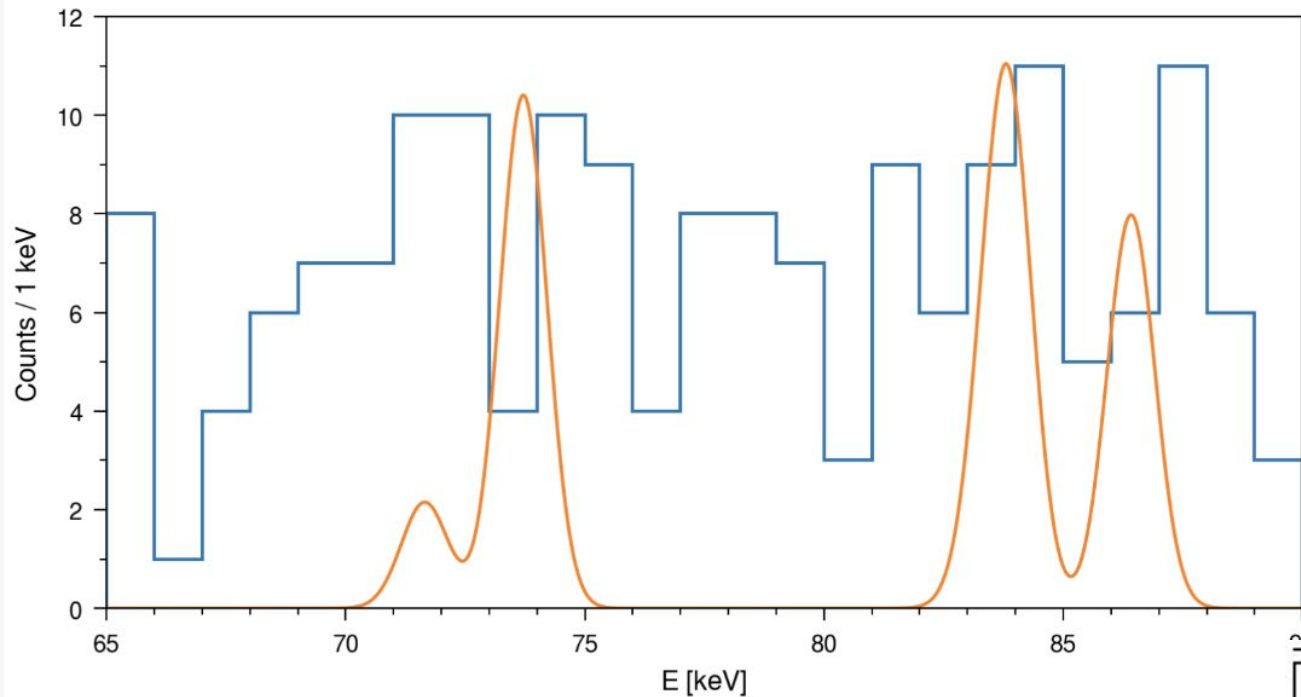
-  $k = 2$  corresponds to  $\theta$ -Poincaré: excluded up to  $\Lambda > 1.6 \cdot 10^{-1}$  Planck scales

-  $k = 3$  corresponds to “triply special relativity” model by Kowalski-Glikman–Smolin (KS). First measurement ever, excluded up to  $\Lambda > 5.6 \cdot 10^{-9}$  Planck scales -> experimental guidance towards future developments of the model with two invariant energy scales accounting for the deformation of the (non-commutative) space-time symmetries.

# VIP-2 Closed Systems - ongoing analyses

## - The normalised signal shape for the $M_3$ parametrization:

**Figure 1.** The figure shows the measured X-ray spectrum corresponding to an acquisition time of  $\Delta t \approx 6.1 \cdot 10^6$  s in the region of interest. For a comparison, the expected signal distribution (with arbitrary normalization) is also shown in orange for the  $A_3$  analysis and the  $M_3$  parametrization.



- The sensitivity on  $\Lambda$  increases with  $E$   
 -> the analysis is repeated by searching for PEP violation signal in  $K\alpha$ ,  $K\beta$  and  $K\alpha + K\beta$  transitions.

Universe 2023, 9(7), 321

$A_i, M_k$	$\bar{S}$	lower limit on $\Lambda$ in unit of Planck scale
$A_1, k = 1$	11.4913	$3.1 \cdot 10^{21}$
$A_1, k = 2$	11.3776	$1.4 \cdot 10^{-1}$
$A_1, k = 3$	11.2610	$4.9 \cdot 10^{-9}$
$A_2, k = 1$	15.1408	$2.8 \cdot 10^{21}$
$A_2, k = 2$	15.1640	$1.4 \cdot 10^{-1}$
$A_2, k = 3$	15.1859	$5.1 \cdot 10^{-9}$
$A_3, k = 1$	18.7270	$4.2 \cdot 10^{21}$
$A_3, k = 2$	19.1847	$1.6 \cdot 10^{-1}$
$A_3, k = 3$	19.5993	$5.6 \cdot 10^{-9}$

## ***VIP-2 Closed Systems - new analysis finalized***

-  **$k = 3$**  corresponds to “triply special relativity” model, by Kowalski-Glikman–Smolin (KS).

The KS framework introduces an additional infrared scale, related to the cosmological constant, and plays the role of an IR regulator.

A quantum field theory endowed with the algebra of symmetries discussed in the KS framework might in principle provide IR/UV mixing.

The development of the field theoretic approach requires deepening the Hopf algebra structure of the new symmetries proposed in the KS model. Since this step is still missing at the theoretical level, our phenomenological analysis may be considered as a guidance for the theory that must be still developed for  $k=3$

Indeed, a possible interplay between the UV energy scale  $\kappa$  and the IR energy scale  $R^{-1}$  related to the cosmological constant by  $\Lambda = R^{-2}$  may induce PEP violations at orders  $k=1$ ,  $k=2$  and  $k=3$

Requesting consistency for  $k=1$  and  $k=2$  with the current experimental bounds then provides strong limits on higher order corrections that can be allowed.

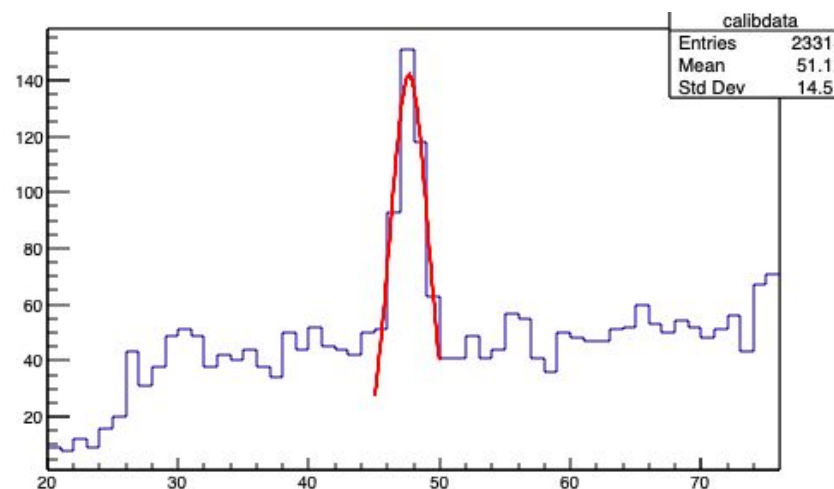
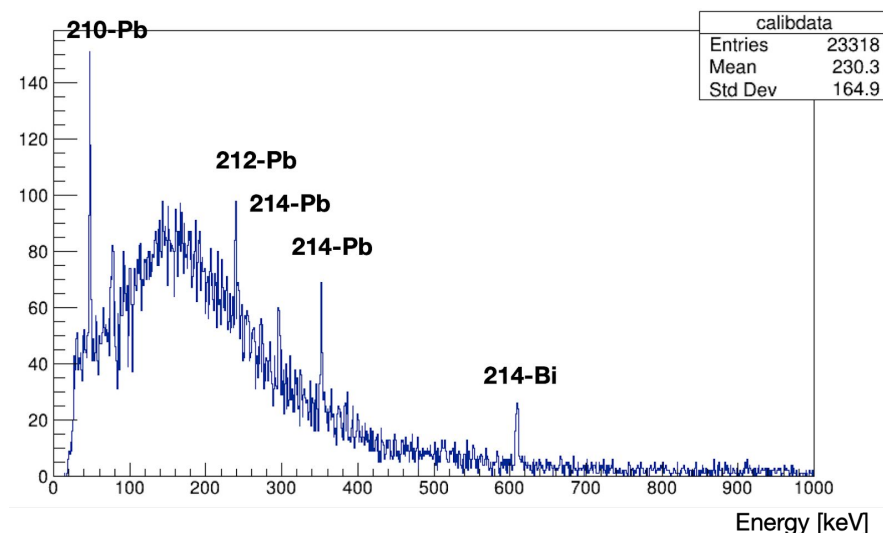


# ***BEGe detector activity 2023-now***

- In order to improve on QG limits → improve on efficiency → use Ge as active material.
- Difficulty: HPGe below 20 keV high background due to electronic noise,
- solution BEGe + Pulse Shape analysis: rejection of electronic noise, disentangle multi vs single hits events (photons from Ge vs photons from outside)

Data from the first run (July-September 2021) analyzed (October 2021 - February 2022):

- preliminary pulse shape discrimination alg. realized
- data calibrated, lower E threshold and resolution determined



sigma @ 50 keV: ~1.5 keV

- the system spectroscopic response, revealed an intrinsic lower energy threshold of about 20 keV, due to electronic noise at low-voltages and an intrinsic noise of the digitizer at 4 mV.

# BEGe detector - improved setup

goal of the experiment is to reach a lower energy threshold of at least 6-7 keV, corresponding to 4-5 mV:

- Flash-ADC-Computer USB connection replaced with optical fibre interface, to reduce electronic noise at low voltages,
- introduced a wide band low noise amplifier (gain of a factor 10 in tension). An extremely-low noise power supply was realized for the digitizer and for the amplifier.

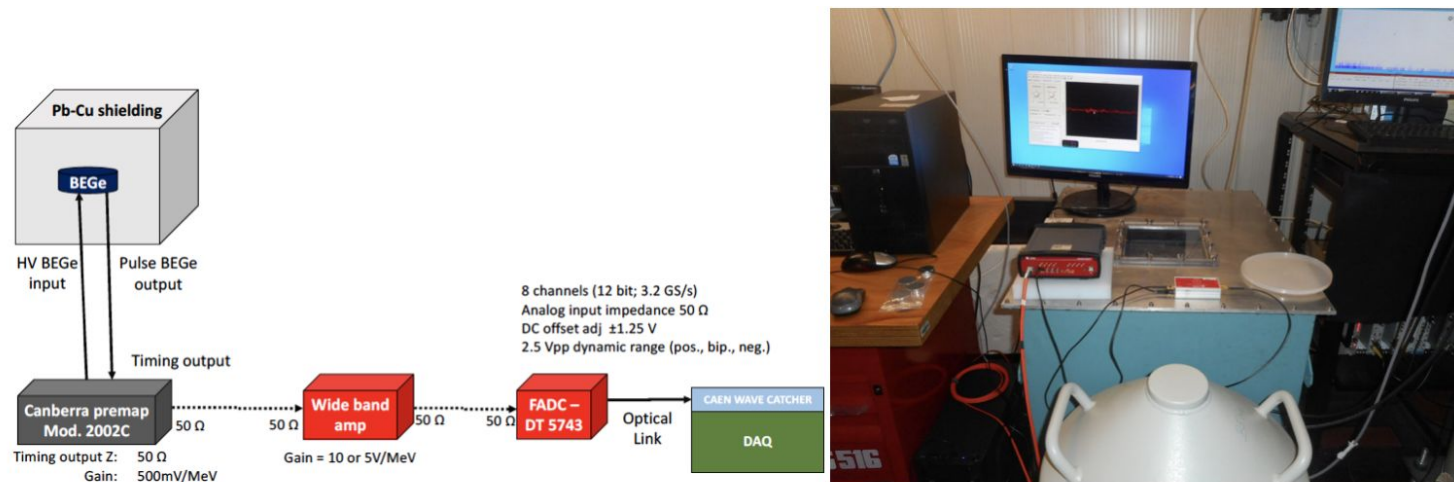


Figure 15. Block diagram of the upgraded BEGe system presently in data taking (left), with amplifier on loan. Picture of the upgraded setup on the right.

## New data taking: February-October 2022 -

(signal shape is changed due to the shaping time introduced by the amplifier). The peak-to-peak noise is now reduced to the level of about 0.5 mV, thus demonstrating the potentiality of the new setup to disentangle signals of 4-5 mV amplitude.

## New data acquisition restarted 3 Feb 2023 - Ongoing

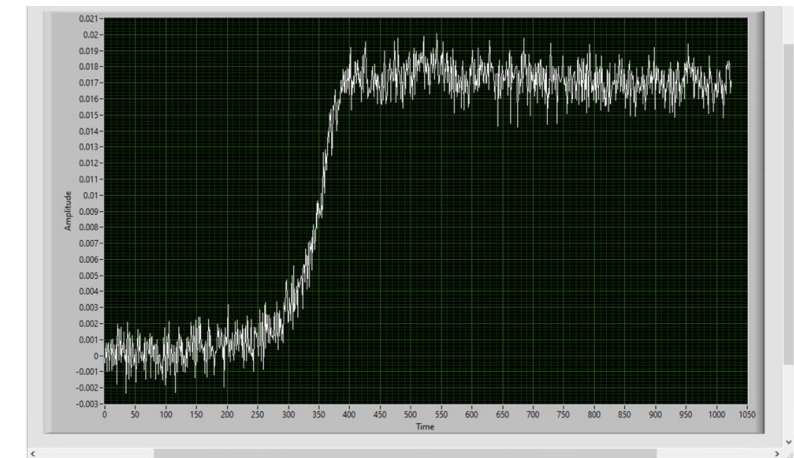


Figure 14: event corresponding to the July-September 2021 data set, showing the intrinsic noise of the digitizer at 4 mV.



Figure 16: the figure shows a typical event corresponding to the data set collected in 2022.

## Guadagno con BEGe

gram/mol			
	72.59	207.2	
numero di atomi in 200 g di Ge		in 22300 g di Pb	rapporto
	1.65918E+24	6.48121E+25	39.06266892
efficienza guadagno		1.86E+04	
il limite scala come la radice del rapporto :			21.79338349
il limite scala linearmente con il rapporto fra le energi			7.071792453
			3.081734035



# Quantum Gravity and the Fate of PEP

- PEP is a direct implication of the Spin Statistics theorem (SST)

One of the key ingredients of SST is Lorentz invariance

➡ PEP is ultimately connected to the fate of the spacetime symmetry

- NCQG models, i.e.  $[x^i, x^j] = i\tilde{\theta}^{ij}/\Lambda_{\text{NC}}$ , invoke **deformations of the Poincaré symmetry**

Relevance of non-commutative geometry in Physics

String theory: NCG is a necessary ingredient for the stability of the theory and to recover the standard model of particle physics (*Seiberg and Witten*)

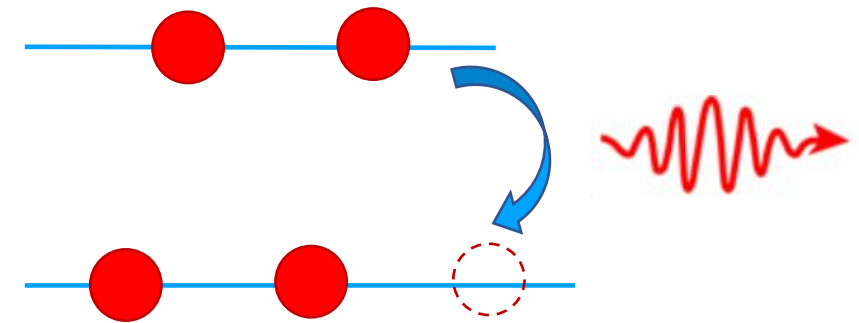
Loop quantum gravity: NCG possibly emerges at mesoscopic scale as a residual property of the discreteness of space at Planckian scales (*Camelia, Marcianò, Cianfrani*)

# *PEPV Transition Amplitude calculation under finalization*

On a phenomenological ground PEPV transitions depend on:

a)  $\Lambda_{NC}$   $\leftrightarrow$  Number of PEP violating transitions

b)  $\tilde{\theta}_{ij}$   $\leftrightarrow$  Angular distribution of the emitted radiation



$$\Gamma_{PEPV} \approx \frac{\Gamma_{rr}}{\Lambda_{NC}^2} \vec{\theta} \cdot (\vec{k} - \vec{p}_i) \times \vec{\gamma} \langle p \rangle_{1S}$$

$$\left[ \begin{array}{l} \Gamma_{rr}: \text{standard radiative recombination rate} \\ \vec{\theta} = (\tilde{\theta}_{23}, \tilde{\theta}_{31}, \tilde{\theta}_{12}) \end{array} \right.$$

**We can get information on the commutation rules of the space coordinates and therefore on the background field underlying noncommutativity**